Late Artinskian–Early Kungurian (Early Permian) warming and maximum marine flooding in the East Gondwana interior rift, Timor and Western Australia, and comparisons across East Gondwana

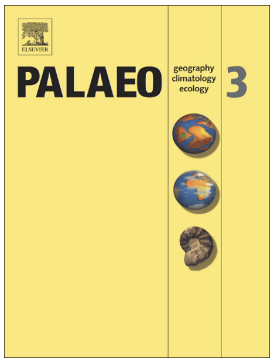

David W. Haig, Arthur J. Mory, Eujay McCartain, John Backhouse, Eckart Håkansson, Andrej Ernst, Robert S. Nicoll, Guang R. Shi, Jennifer C. Bevan, Vladimir I. Davydov, Aaron W. Hunter, Myra Keep, Sarah K. Martin, Daniel Peyrot, Olga Kossavaya, Zelia Dos Santos

PII: S0031-0182(16)30799-4
DOI: doi: 10.1016/j.palaeo.2016.11.051
Reference: PALAEO 8086

To appear in: *Palaeogeography, Palaeoclimatology, Palaeoecology*

Received date: 8 July 2016
Revised date: 23 November 2016
Accepted date: 29 November 2016

Please cite this article as: David W. Haig, Arthur J. Mory, Eujay McCartain, John Backhouse, Eckart Håkansson, Andrej Ernst, Robert S. Nicoll, Guang R. Shi, Jennifer C. Bevan, Vladimir I. Davydov, Aaron W. Hunter, Myra Keep, Sarah K. Martin, Daniel Peyrot, Olga Kossavaya, Zelia Dos Santos , Late Artinskian–Early Kungurian (Early Permian) warming and maximum marine flooding in the East Gondwana interior rift, Timor and Western Australia, and comparisons across East Gondwana. The address for the corresponding author was captured as affiliation for all authors. Please check if appropriate. Palaeo(2016), doi: 10.1016/j.palaeo.2016.11.051

Late Artinskian–Early Kungurian (Early Permian) warming and maximum marine flooding in the East Gondwana interior rift, Timor and Western Australia, and comparisons across East Gondwana

David W. Haig[a,b*], Arthur J. Mory[b,c], Eujay McCartain[b], John Backhouse[b], Eckart Håkansson[a,b], Andrej Ernst[d], Robert S. Nicoll[e], Guang R. Shi[f], Jennifer C. Bevan[b], Vladimir I. Davydov[g], Aaron W. Hunter[b,h,i], Myra Keep[b], Sarah K. Martin[c,j], Daniel Peyrot[a,b], Olga Kossavaya[k], Zelia Dos Santos[l]

[a] Centre for Energy Geoscience, School of Earth and Environment (M004), The University of Western Australia, 35 Stirling Highway, Crawley, WA 6009, Australia

[b] School of Earth and Environment (M004), The University of Western Australia, 35 Stirling Highway, Crawley, WA 6009, Australia

[c] Geological Survey of Western Australia, Department of Mines and Petroleum, 100 Plain St, East Perth, WA 6004, Australia

[d] Institut für Geologie, Universität Hamburg, Bundesstrasse 55, D-20146 Hamburg, Germany

[e] Geoscience Australia, GPO Box 378, Canberra, ACT 2609, Australia

[f] School of Life and Environmental Sciences, Deakin University, 221 Burwood Highway, Burwood, Victoria 3125, Australia

[g] Permian Research Institute, Boise State University, 1910 University Drive, Boise, ID, USA

[h] Department of Applied Geology, Curtin University, GPO Box U1987, Perth WA 6845, Australia

[i] Department of Earth Sciences, University of Cambridge, Downing Street, Cambridge CB2 3EQ UK

[j] Western Australian Museum, 49 Kew Street, Welshpool, WA 6106, Australia,

[k] All Russian Geological Research Institute, Stredny pr., 74, St. Petersburg, 199106, Russia

[l]TIMOR GAP E.P., Level 3, Timor Plaza, Suite 301–314, Rua Presidente Nicolao Lobato, Comoro, P.O. Box No. 003, Dili, Timor-Leste

* Corresponding author.

E-mail address: david.haig@uwa.edu.au

Keywords:

East Gondwana rift; Maubisse Group; Cribas Group; Noonkanbah Formation; Byro Group; Carynginia Formation; Permian climate

ABSTRACT

Substantial new information is presented on upper Artinskian–Kungurian deposits in Timor-Leste and in the Canning, Southern Carnarvon and northern Perth basins of Western Australia. These basins, situated between about 35°S and 55°S palaeolatitude, formed part of the East Gondwana interior rift, a precursor to the rift that 100 my later formed the Indian Ocean in this region. Timor lay near the main axis of the East Gondwana interior rift, whereas the Western Australian basins were marginal splays from the rift axis. The main depocentres developed as a result of faulting that was initiated during the Late Pennsylvanian. Detailed lithostratigraphic and biostratigraphic analyses have been made on the newly recognized Bua-bai limestone and the type Cribas Group in Timor, the Noonkanbah Formation in the Canning Basin, the Byro Group in the Merlinleigh Sub-basin of the Southern Carnarvon Basin, and the Carynginia Formation in the northern Perth Basin. In Timor the succession, which is highly disrupted by faulting, was deposited under open-marine conditions probably in a shelf–basin setting. Restricted, very shallow-water seas flooded the Canning Basin and the Merlinleigh–Byro–Irwin sub-basins of the Southern Carnarvon and northern Perth basins and had highly variable oxygen levels and salinities typical of estuarine environments.

A similar pattern of warming and bathymetric change is recognized in all studied basins. During the early part of the late Artinskian cool conditions prevailed, with water temperatures 0–4°C forming sea ice in the Merlinleigh–Byro–Irwin rift. Rapid warming during the latter part of the late Artinskian was accompanied by maximum marine flooding close to the Artinskian–Kungurian boundary. Climatic and bathymetric conditions then allowed carbonate mounds, with larger fusulines and a variety of algae, to develop in the northern part of the rift system, and

Tubiphytes, conodonts, and brachiopods with Tethyan affinities to migrate into the marginal-rift basins despite the generally adverse water quality at these depositional sites.

Comparison between the stratigraphic record from the East Gondwana interior rift and coeval records from Lhasa and Sibumasu indicate a similar pattern of climate change during the Carboniferous to end Cisuralian. Similar trends probably are present in Eastern Australia although there is confusion over the correlation of some units.

1. Introduction

Phanerozoic rift basins through the interiors of ancient continents provide outstanding archives of past life and the environmental factors that influenced these records. Among the most important factors affecting the water quality and sedimentation patterns in the seas flooding these rifts were temperature and degrees of aridity and humidity in the hinterland. These factors, which interacted with eustasy and tectonic subsidence, determined the amount of precipitation, freshwater runoff and siliciclastic-sediment influx into the interior seas, turbidity, evaporation from surface waters, salinities and water stratification, and ultimately the biota.

The Early Permian (Cisuralian) was an interval of significant climate change (Schmitz and Davydov, 2012) and in east Gondwana includes evidence for melting of large continental ice sheets (Crowell and Frakes, 1971a,b; Isbell et al., 2003; Frank et al., 2015). An almost complete stratigraphic record of this interval exists in basins that formed along the East Gondwana interior rift (Fig. 1; Harrowfield et al., 2005), originally called the “Westralian Geosyncline” by Teichert (1939) and the “Western Australian Trough” by Wopfner (1999). This interior Gondwanan record is accessible along the western passive margin of the Australian continent that resulted from much later (Middle Jurassic–Early Cretaceous) episodes of rifting leading to the opening of the Indian Ocean (Heine and Müller, 2005). The margin and its precursor Gondwanan deposits were later modified in the north by late Miocene collision with Asia (Keep and Haig, 2010; Haig, 2012).

The most accessible Cisuralian records from the East Gondwana interior rift include outcrops in Timor (Charlton et al., 2002) and in the Canning, Southern Carnarvon and northern Perth basins of Western Australia (Fig. 2; Mory, 2010; Hocking et al., 1987; Playford et al., 1976). The Timor sections have been dislocated during the chaotic late Miocene collision (Hamilton, 1979) but contain facies that accumulated in more open parts of the rift system closer to its main axis and also closer to the Paleotethys Ocean than the other basins. The Western Australian basins to the south of Timor were marginal splays off the main rift (Fig. 2) and have undergone very little deformation. Permian deposits closer to the edge of the present-day

passive margin (and presumably also closer to the main axis of the Permian rift) are covered by thick Mesozoic and Cenozoic strata and are rarely reached in petroleum exploration drilling. Recent seismic profiling on the North West Shelf of Western Australia suggests significant topographic relief developed in the rift system with steep slopes and possible reef or mound development on shelf breaks (MacNeill and Marshall, 2015). Although rock records from these environments are presently out of reach, equivalent facies seem to be represented in Timor where the Permian strata were folded, faulted and uplifted on to land during the late Neogene collision.

Although the Cisuralian climate record in parts of the East Gondwana interior rift has long been subject of discussion (e.g. Maitland, 1912; Clapp, 1925; David and Sussmilch, 1931, 1933; Teichert, 1941, 1948; Clarke et al., 1951; Guppy et al., 1958; Lowenstam, 1964; Condon, 1967; Crowe and Towner, 1976a,b; Dickins 1978, 1993, 1996; Forman and Wales, 1981; Hocking et al., 1987; Redfern, 1991; Kennard et al., 1994; Archbold and Shi, 1995, 1996; Lindsay, 1997; Archbold, 1998a,b, 2000; Nicoll and Metcalfe, 1998; Eyles & Eyles, 2000; Eyles et al., 2001; Eyles et al., 2002, 2003, 2006; Dixon and Haig, 2004; Lever, 2004a,b; Torsvik and Cocks, 2004; Gorter et al., 2008; Korte et al., 2008; Mory et al., 2008; Frank et al., 2012; Al-Hinaai and Redfern, 2015; Taboada et al., 2015), few studies have attempted to examine in detail the influence of climate along a north to south transect in the rift. Recent such analyses by us have suggested the following: (1) a global warm spike during the latest Gzhelian (latest Carboniferous) may have initiated rapid melting of ice sheets that resulted in the deposition of thick glacially-influenced successions of the lowest Permian in the Perth, Southern Carnarvon and Canning basins and reefs in Timor (Davydov et al. 2013, 2014); and (2) widespread carbonate marine deposition took place during the late Sakmarian to early Artinskian, extending from Timor in the north to the northern Perth Basin in the south, indicating further warming of climate from the earlier glacial phase but suggesting only a very gradual gradient in north–south temperature along the examined length of the rift (Haig et al., 2014).

In the present paper, based on new data and a review of published information, we investigate the late Artinskian to Kungurian interval represented in marine strata of the interior rift and suggest warming from initial cold conditions to a warm peak close to the Artinskian–Kungurian boundary. We show that this was co-incident with Early Permian maximum marine flooding in the rift basins, and led to warm–temperate conditions during the rest of the Permian in lowland parts of East Gondwana. The results of the study raise questions concerning: (1) relationships between climatic changes, marine flooding in the rift basins, and tectonic

subsidence; and (2) relationships between climatic changes and different rates of biotic change among different plant and animal groups.

2. Material and Methods

The new material for this study (see 7. Appendix 1) was collected during extensive fieldwork in Timor-Leste and in the Canning, Southern Carnarvon and Perth basins. Borehole sections in the Western Australian basins were also examined. Friable mudstones were disaggregated for skeletal microfossil content, and some were digested in HF for palynomorphs, using standard techniques. Carbonate rocks were slabbed, etched in 2% HCl for 4 minutes, flooded with acetone when dry and overlain by acetate film to produce peels for microfacies analysis. Selected thin sections were made or examined from previous studies. Some of the carbonates were digested in acetic acid for the extraction of conodonts. All material is archived in collections of the University of Western Australia, the Geological Survey of Western Australia and Geoscience Australia.

3. East Gondwana interior rift

3.1. Geological setting

3.1.1 Timor Gondwanan Megasequence

Within the geological chaos of Timor, a suite of uppermost Carboniferous to Middle Jurassic sedimentary units is recognized as having Gondwana affinity and is designated the "Gondwana Megasequence" (Harris et al., 1998, 2000; Haig et al., 2007; Haig and Bandini, 2013; Tate et al., 2015). This was deposited near the axis of the East Gondwana interior rift adjacent the Bonaparte Basin of northwest Australia as indicated, for example, by the palaeomagnetic evidence of Chamalaun (1977), the terrestrial plant microfossil evidence of McCartain et al. (2006), and the zircon provenance studies of Spencer et al. (2015). Although various opinions have been published on the composition of the megasequence, our recent studies can link each of the adjacent lithostratigraphic groups listed in Fig. 3, either by boundary contacts visible in the field or by the presence of clasts derived from an adjacent unit. At this stage in our development of a stratigraphic framework for Timor we prefer to recognize broad "groups" rather than "formations", particularly as boundaries are mostly faulted and coherent sections are limited in stratigraphic and lateral extent.

At present we interpret all the Permian carbonate deposits as part of the Maubisse Group and the siliciclastic/volcaniclastic units, including neritic and bathyal facies, as part of the Cribas Group. Haig et al. (2014) showed that the type section of the Maubisse limestone, as designated by Audley-Charles (1968), was about 190 m thick, bounded by siliciclastic or volcaniclastic

units, probably of broad lenticular architecture, and upper Sakmarian–lower Artinskian. There is no continuous limestone succession in the Permian of Timor, contrary to the suggestions made in the summary charts of Charlton et al. (2002).

The thicknesses of the Kulau and Maubisse limestones can be measured in continuous sections (Davydov et al., 2013; Haig et al., 2014); however, the younger limestone units (Fig. 3) seem much thinner and are present in a melange of highly deformed ductile mudstone which has dislocated the stratigraphy. However a broad geographic trend in limestone outcrops can be discerned from our fieldwork in Timor-Leste: the main exposures of Kulau and Maubisse limestone are in a southern belt, whereas younger Permian limestones, including the Bua-bai limestone discussed in this paper, are present in a northern belt (Fig. 4). The tectonic significance of this is at present uncertain.

Volcaniclastic–siliciclastic sandstone and mudstone successions placed in the Permian were referred to as the "Série de Cribas" by Gageonnet and Lemoine (1958) and subdivided into the "Série de Cribas inférieure (renamed the "Atahoc Formation" by Audley-Charles, 1968) and the overlying "Série de Cribas supérieure" (renamed the Cribas Formation by Audley-Charles, 1968). The contact between these units was placed "arbitrarily at the top of an amygdaloidal basalt that locally forms a good marker-horizon" (Audley-Charles 1968, p. 6) but there is no great difference between rock types on either side of the contact at the type locality or in the sections studied by Bird and Cook (1991) in West Timor. The latter authors noted the lowest stratigraphic occurrence of the bivalve *Atomodesma exerata* Beyrich in red limestones at the boundary between the formations and recorded its presence at levels higher in the Cribas Formation. Gageonnet and Lemoine (1958) considered their broad Cribas Series to be basinal flysch facies.

The prolific Permian fossil assemblages from Timor (e.g. Somohole, Bitauni, Basleo and Amarassi, following Haniel, 1915, in West Timor), sometimes referred to as stages, are now known to contain stratigraphically mixed assemblages derived from geologically confused areas (Charlton et al., 2002). These names cannot be used as stratigraphic terms.

3.1.2 West Australian basins

In Western Australia the Permian is best known in marginal rift basins. By contrast, basins along the axis of the East Gondwana interior rift are covered by thick Mesozoic–Cenozoic successions where the Permian has rarely been penetrated by petroleum exploration drilling. The major depocentres in which the Permian is at least moderately well known are the Petrel Sub-basin (Bonaparte Basin), Fitzroy Trough – Gregory Sub-basin (Canning Basin), Merlinleigh–Byro

sub-basins (Southern Carnarvon Basin) and Coolcalalaya Sub-basin – Irwin Terrace (northern Perth Basin) (Figs 1, 2). Both the Southern Bonaparte and Canning basins are northwesterly trending fault-bound grabens flanked by Precambrian basement and Lower Paleozoic strata at relatively shallow depths, with the Permian onlapping older strata. In the Canning Basin (see 3.3) the main Permian depocentre abuts the Broome–Crossland Platform to the south along the Fenton Fault System, and the Lennard Shelf to the north along the Pinnacle Fault System. By comparison, the Permian depocentres of the north-northwesterly to north trending Southern Carnarvon and Perth basins (see 3.4 and 3.5 respectively) are half grabens, loosely differentiated by the Wandagee and Darling fault systems along their western and eastern margins, respectively.

In the Merlinleigh Sub-basin of the Southern Carnarvon Basin (Fig. 2; section 3.4) the Permian onlaps across older strata and on to Precambrian basement to the east and is faulted against older Paleozoic strata to the west. There is no record of the Permian west of this sub-basin on the Gascoyne Platform (section 3.4), where thermal maturity data from the Silurian indicates that if Permian sediment had been deposited there it did not reach any great thickness (Mory et al., 1998). The Byro Sub-basin at the southernmost end of the Southern Carnarvon Basin shows similar structural relationships, but is faulted against a Precambrian inlier along its northwestern margin; its relationship with the Coolcalalaya Sub-basin of the Perth Basin to the southwest is unclear due to a lack of outcrop and paucity of sub-surface data. The Perth Basin is faulted against the West Australian Craton to the east along the 940 km-long Darling Fault System (Fig. 2; section 3.5), with the thickest Permian sections east of the Urella Fault and the Northampton Inlier, in the north. South of that inlier the Permian thins both to the south and west; another thick half graben lies offshore from the Turtle Dove Ridge but the Permian has been intersected in very few wells due to the thickness of the overlying Mesozoic.

Of the main depocentres, the Petrel Sub-basin contains the thickest Permian section, estimated at 20 km from seismic data, but its age is poorly constrained and Mory and Haines (2013, p. 10) deemed the thickness anomalous. The Artinskian–Kungurian in the Bonaparte Basin is not considered further by us due to the lack of outcrop, and the paucity of cored intervals. In the Canning Basin the maximum thickness of the Permian is 2400 m based on drilling (Mory, 2010), compared to about 5000 m in the Southern Carnarvon Basin based on seismic profiles and drilling (Mory and Backhouse, 1997) and possibly 4000 m in the northernmost Perth Basin (Mory and Iasky, 1996).

Whereas topography in the Canning, Southern Carnarvon and Perth basins may have been uneven during early stages of basin infill, by the Sakmarian and through the remainder of the Cisuralian very low-gradient depositional surfaces were present, as evidenced by flat-lying seismic horizons and laterally extensive facies that are mainly very shallow marine or deltaic (Haig, 2004; Mory and Haig, 2011). In the Permian depocenters on the North West Shelf, largely hidden by younger cover but closer to the main rift axis, and in Timor much more prominent topographic shelf-basin relief may have been present (MacNeill and Marshall, 2015; section 3.2).

Upper Artinskian–Kungurian marine deposits are widely distributed in the Canning, Southern Carnarvon and northern Perth basins, although with variable thicknesses (Fig. 2b). The studied units are correlated to the Geological Time Scale (www.stratigraphy.org) in Fig. 5, based on arguments presented in 3.3–3.5.

3.2. Timor

3.2.1 Bua-bai limestone

Gageonnet and Lemoine (1958, photograph 15) illustrated a grainstone containing fusulinids as well as abundant bryozoan and crinoidal debris and rare *Tubiphytes* from an unspecified locality south of Vemasse. During fieldwork in 2013–2015 to relocate this rock unit, small outcrops of fusulinid limestone were found in the vicinity of Bua-bai on the western side of the Vemasse River (Fig. 4A). The Bua-bai limestone is present as isolated small blocks at two localities (1 and 3, Figs. 4A, 6A, B) and as scree in the riverbed (locality 2, Fig. 4A). It is placed within the Maubisse Group, characterized by shallow-water carbonates of Permian age, but as a younger formation than the Maubisse limestone (Haig et al., 2014). A friable unit, probably composed of highly deformed mudstone or muddy fine sandstone that is poorly exposed, surrounds the limestone blocks. Although we cannot be certain that this is the site of Gageonnet and Lemoine's material, the microfacies seem similar.

Because of the limited exposure and dislocated nature of the blocks, no section that provides meaningful information on a stratigraphic succession can be measured. Our analysis of the limestone is based on multiple samples collected to represent the variety of limestone types found at the sites (Table 1; section 7, Appendices 1, 2). Locality 1 is taken as the type area of the Bua-bai limestone, and includes floatstone, packstone, and grainstone/rudstone (Table 1; Fig. 6). The main grain constituents are bryozoans (40%, average of 10 samples), crinoids (38%), foraminifera (13%) and *Tubiphytes* (5%). The bryozoans include a diverse assemblage including

cystoporids, trepostomatids, fenestrids and cryptostomids (partly identified in section 7, Appendix 4). The foraminifera (section 7, Appendix 3) are dominated by the fusulinid *Praeskinnerella* (Fig. 7B–E) and calcivertellids. Also present in the limestone at the type locality are brachiopods (including pseudopunctate and punctate shell types), and rare to very rare bioclasts such as bivalve fragments with prismatic microstructure, , small nodular solenoporacean algae encrusting on bryozoa, dasycladacean algae, echinoid spines, gastropods, ostracods, recrystallized fragments that may include phylloid algae, trilobite carapace fragments, and tuberitinids. Non-skeletal algae are inferred from cement- or sediment-filled large central cavities in delicate trepostomes (Fig. 8G, H). and in calcivertellid foraminifera; these presumably encrusted on the cylindrical stems of a plant-like algal thallus. Scree from the riverbed at locality 2 includes microfacies similar to the type locality.

Locality 3 includes a large block of mostly floatstone (Fig. 6B) that is difficult to sample because of the massive nature of the rock and its smooth surfaces. Large skeletons are present, including probable chambered sponges, solitary rugose corals possessing numerous septa, *Tubiphytes*, planispiral nautiloids or ammonoids, and gastropods.

Limestone outcrop at locality 1 and scree at locality 2 contain abundant *Praeskinnerella*. At this stage of our study, the variability of the *Praeskinnerella* morphotypes is difficult to assess because the tests have no preferred orientation within the rock, perhaps due to bioturbation, and only a few sections close to a centred axial plane are present in the numerous acetate peels. Orientated thin sections have still to be made. *Praeskinnerella* in the Bua-bai limestone seems to be a new species with the closest known representatives of the genus from within the Sakmarian–Artinskian (see discussion in section 7, Appendix 5). At locality 1, *Praeskinnerella* is associated with very rare primitive *Abadehella* Okimura and Ishii (Fig. 7A) comparable to forms recently illustrated by Lucas et al. (2015), as *Abadehella* n. sp., from zone 8B of the Robledo Mountains Formation, New Mexico, considered as early Leonardian (late Artinskian according to these authors and Henderson et al., 2012). They also reported that "similar primitive *Abadehella*" have been found in the Zottachkopf Formation, probably middle to upper Artinskian, of the Carnic Alps (Europe). These are the oldest known records of *Abadehella*. A late Artinskian or early Kungurian age is consistent with the presence of possible *Toriyamaia* sp. (Fig. 7L), possible *Boultonia* sp. (Fig. 7F,G), and *Nankinella* sp. (Fig. 7H–J) that are present with *Praeskinnerella* at locality 1.

Representatives of *Praeskinnerella*, similar to morphotypes at locality 1, are abundant in some of the boulders in the river (locality 2) where they are associated with very rare

Monodiexodina wanneri (Schubert) (Fig. 7K). Ueno (2006) reviewed the distribution of *Monodiexodina* and concluded that *M. wanneri* ranged from the upper Yakhtashian to the Bolorian (i.e. late Artinskian to early Kungurian according to Henderson et al., 2012). At locality 3, fusulinids are extremely rare but include an elongate form that may be *M. wanneri*.

When viewed against the known record of larger Fusulinata from Timor (Table 2), the assemblages found in the Bua-bai limestone are clearly younger than the *Eoparafusulina*-dominated assemblages Schubert (1915) and Thompson (1949) described from West Timor. These may be the same age as the late Sakmarian–early Artinskian Maubisse limestone of Timor-Leste that lacks larger Fusulinata (Haig et al., 2014) and the Kalatash- and Havan-type faunas recorded widely from the Perigondwanan region by Leven (1993) and Leven and Gorgij (2007, 2011a,b). The Bua-bai assemblage lacks *Parafusulina* that is present in assemblages recorded near Mt Aubean in Timor-Leste (Table 2) that also contain *Lantschichites weberi* (Schubert) considered late Capitanian (Table 2). Because the Timor locality probably lies close to the southern limit of the distribution of larger Fusulinata (see section 3.6) and has a very low diversity assemblage, the absence of *Misellina*, the first appearance of which marks the Bolorian (= early Kungurian according to Henderson et al., 2012), may not be biostratigraphically significant.

Among the abundant bryozoans found in the Bua-bai limestone (section 7, Appendix 4), tentative correlations can be made to faunas known from the Canning Basin in Western Australia (see section 3.3) and from Perigondwanan localities in West Papua, northwest Thailand, and Oman. *Streblotrypa* (*Streblotrypa*) *elegans* Sakagami is known from the Lower Permian (?late Artinskian) of Thailand, and from the Aseelah Unit, Saal Formation of eastern Oman; *Streblotrypa* (*Streblascopora*) *irianica* Sakagami is known from the Middle Permian of West Papua, and from the Aseelah Unit, Saal Formation of eastern Oman; *Ascopora asiatica* Sakagami is known from the Lower Permian (?late Artinskian) of Thailand; *Dyscritella tenuirama* Crockford, originally described from the Noonkanbah Formation of the Canning Basin (3.3), is also known in the Lower Permian of Thailand (Sakagami, 1968) and Bolivia (Sakagami, 1995); and *Liguloclema meridianus* (Etheridge), originally described from the Noonkanbah Formation (3.3), has also been recorded from the Lower Permian (?Artinskian-Kungurian) of Thailand (Sakagami, 1968, 1995; Ernst et al., 2008; Ernst and Gorgij, 2013).The foraminiferal and bryozoan faunas known from the Bua-bai limestone do not provide a means for precise correlation to the International Chronostratigraphic Chart based on standard zonations (GTS v2015-1 at www.stratigraphy.org). However, they do suggest a broad upper Artinskian-lower Kungurian correlation, probably within the upper Artinskian. Based on criteria

listed on Table 1 and section 7, Appendix 2, and comparisons with modern carbonate facies, the depositional environment is interpreted as a bryozoan-crinoidal carbonate mound situated at < 30 m water depth; from the limited outcrop thickness and exposure, this facies probably was of limited areal extent.

3.2.2 Cribas Group

The type section of the Cribas Formation, as defined by Audley-Charles (1968) is along the Sumasse River north of the village of Cribas (Fig. 4B). It consists of discontinuous outcrop in cliffs along the river but, as explained below, forms part of a structurally incoherent section. It was mapped by Audley-Charles (1968) as part of the Cribas Anticline, following earlier work by Grunau (1957) and Gageonnet and Lemoine (1958). Audley-Charles (1968) renamed Gageonnet and Lemoine's (1958) "Série de Cribas inférieure (Permien inférieur)" as the Atahoc Formation, and their "Série de Cribas supérieure (Permien)" as the Cribas Formation. Although he described the type section of the Cribas Formation along the Susmasse River north of Cribas, he did not designate a particular type section for the Atahoc Formation, but noted sections along the Sumasse River and two rivers immediately to the east, as well as cliffs north of Cribas as within the type area. The formations were not based strictly on lithostratigraphic criteria but on ammonoids, brachiopods and trilobites of Early Permian age in the "Série de Cribas inférieure" (Atahoc Fromation), and mainly bivalves (*Atomodesma* and *Merismopteria*) of undifferentiated Permian age (tentatively "Late Permian" according to Audley-Charles, 1968) in the "Série de Cribas supérieure" (Cribas Formation). In recent mapping of the region, Tate et al. (2015) combined both formations as the Cribas Formation based on the similarity in rock types, and showed it to be in thrust repetition with undifferentiated Triassic strata. We agree that the formations of Audley-Charles (1968) should be assembled as one unit, characterized mainly by siliciclastic/volcaniclastic lithofacies, but designated as the Cribas Group rather than as a formation. Differentiation of formations within the Cribas Group and the carbonate-dominated Maubisse Group await a greater understanding of the chronostratigraphic and facies relationships of the Permian units assigned to these units (see 3.1.1 and 3.2.1).

Because Audley-Charles (1968) selected the Sumasse River section as type for the Cribas Formation as well as one of the type localities for the Atahoc Formation, we confine our discussion of the Cribas Group to outcrops along this river. Stratigraphic work here has shown that the section is much more complex than previously mapped with the Lower Triassic Niof Group present at C667 (Fig. 4B) and in river cliffs about 1 km south of C502f (Fig. 4B) and a Middle Triassic (Ladinian) outcrop of the Babulu Group at C663 (Fig. 4B). Confirmed Permian

outcrops are present, from north to south along the river, at localities M558, C665, M559, C666, C501, C502, C502f (Figs. 4B, 6; section 7, Appendices 1, 6). The outcrop pattern was originally interpreted as a broad anticline with axis trending approximately east–west between localities M559 and C665 (Fig. 4B) but only a small part of the Permian seems represented here and the lack of outcrop coherency makes this structural interpretation difficult to accept. Bedding orientations along the river (Fig. 4B) do not suggest a simple anticline and the repetition of Triassic outcrop indicates fault-controlled repetition. Exposures in the rivers immediately east of the Sumasse River, described by Gageonnet and Lemoine (1958), are not as structurally deformed as those in Audley-Charles's (1968) type section of the Cribas Formation and form part of a local anticlinal structure. More detailed mapping supported by biostratigraphy is required to establish the structural complexity of the Cribas region.

From the lower part of the Cribas Group, above a 100 m-thick unit of unfossiliferous quartz sandstone, Grunau (1956) reported ammonoids, identified by A.K. Miller and W.M. Furnish of the University of Iowa, as *Stacheoceras* sp. (possibly S. *timorense* Haniel) and a primitive large *Metalegoceras* sp. from a slightly higher stratigraphic level for which a Sakmarian age was suggested. The relationship of *Stacheoceras* sp. to *S. timorense* requires re-evaluation as *S. timorense* is now regarded as Wordian (Leonova, 2011, table 2-2-3). Audley-Charles (1968, fig. 2) showed these ammonoids lie at a level that is probably slightly below that of the localities we examined in the Sumasse River (see Gageonnet and Lemoine, 1958, figs. 3, 4).

At several localities in the Sumasse River near the boundary of the "Série de Cribas inférieure" and "Série de Cribas superieure" mapped by Gageonnet and Lemoine (1958, fig. 4) we recovered Permian microfossil assemblages that provide significant new age information (section 7, Appendix 8). C666 yielded very rare conodonts including *Mesogondolella* sp. cf. *M. intermedia* (Igo) and *Vjalovognathus australis* (Nicoll and Metcalfe) illustrated in Fig. 9A, B. The C666 morphotype designated as *Mesogondolella* sp. cf. *M. intermedia* probably belongs within the middle to upper Artinskian (see discussion in section 7, Appendix 7). *Vjalovognathus australis* is endemic to eastern Gondwana and is known from the Callytharra Formation in the Southern Carnarvon Basin (Nicoll and Metcalfe 1998). The ammonoid evidence for the Callytharra Formation indicates an age from late Sakmarian to early Artinskian (Haig et al., 2014).

The accompanying foraminiferal assemblage in C666 (section 7, Appendix 8) includes *Cornuspira* sp. known from the Noonkanbah Formation (see 3.3) and Bulgadoo Shale (see 3.4)

and *Hedraites plummerae* also found in the Bua-bai limestone (3.2.1). Also present are *Calcitornella* sp., *Trepeilopsis australiensis* Crespin, and *Syzrania* sp. that were described previously from the East Gondwana rift in the lower Callytharra Formation of the Southern Carnarvon Basin (probably upper Sakmarian; Dixon and Haig, 2004; Haig et al., 2014). The limestone at C666 also contains abundant echinodermal debris including crinoid, asterozoan and echinoid plates and *Cidaris*- and *Diadema*-like echinoid spines. Also present are ostracods, gastropods, atomodesmatinid bivalve shell fragments, brachiopod debris, and bryozoans (section 7, Appendix 9). A similar nearby limestone was sampled at M559, where the foraminiferal assemblage is dominated by Miliolata and includes rare *Hemigordius ovatus* Grozdilova, originally described from the Saranian and Filippovian of the Urals (Grozdilova, 1956; lower to middle Kungurian according to Henderson et al., 2012) but recorded by Filimonova (2010, table 2) from as low as Asselian in Central Iran.

Based on these observations, the age of locality C666, positioned just below where Gageonnet and Lemoine (1958) placed the Cribas Series "inférieure" and "superieure" boundary, lies within the Artinskian–Kungurian interval. It probably lies within the middle to late Artinskian, based on the transitional position of *M.* sp. cf. *M. intermedia* between *M. bisselli* and *M. intermedia*. This determination is consistent with other fossils identified from the sample. M559 is probably of similar age.

Elsewhere along the Sumasse River, locality C665 includes a wackestone containing shell debris possibly derived from the bivalve *Atomodesma*, and very rare nodosariid foraminifera including probable *Nodosaria raggatti* Crespin. Dark grey mudstone from M558 contains a poorly preserved foraminiferal assemblage that includes *Howchinella striatosulcata* Crespin, *Nodosaria raggatti* Crespin, *Nodosaria spiculata* Crespin, and *Pseudonodosaria* sp. known also from the Noonkanbah and Bulgadoo formations, and considered to be of latest Artinskian or early Kungurian age (see 3.3 and 3.4). At locality C501 a thick red mudstone bed lies above a succession of thin interbeds of greenish-grey fine sandstone and mudstone. Mudstone samples contain organic-cemented agglutinated foraminifera (including *Hyperammina*?, *Ammodiscus, Glomospira, Hormosina*; Fig. 9C) as well as representatives of the Nodosariata (including *Syzrania, Nodosaria, Pseudonodosaria, Pyramidulina, Laevidentalina*). The presence of *Nodosaria, Pseudonodosaria* and *Pyramidulina* suggest an age no older than late Artinskian (see discussion in 3.3.2). The specimens of *Syzrania* are similar to *Syzrania* sp. from the late Sakmarian–early Artinskian Callytharra Formation in the Southern Carnarvon Basin (Dixon and Haig, 2004) and morphologically close to, although slightly larger than, *S. pulchra* Kireyeva

from the Lower Permian Copper Sandstone Formation of the Donets Basin in the Ukraine (Kireyeva, 1958). Locality C501 is probably upper Artinskian or Kungurian.

The precise age of locality C502a-e is uncertain. The thick-bedded sandstone at this locality includes a low-diversity fragmentary fossil assemblage (mainly bryozoans) of undifferentiated Permian age. Locality C502f includes a red-brown mudstone (Fig. 9D) with atomodesmatinid bivalve fragments and rare indeterminable nodosariid foraminifera.

The conodonts and foraminifera collected from most of these localities suggest these strata belong within the Artinskian–Kungurian interval. Localities C666 and M559 probably belong to the middle or upper Artinskian whereas outcrops at M558 and M501 are probably uppermost Artinskian or Kungurian. The reconstructed succession, therefore, is in part coeval with the Buabai limestone (3.2.1) but is a very different facies. Grunau (1956) characterized the Cribas deposits as typical geosynclinal facies and Gageonnet and Lemoine (1958) and Audley-Charles (1968) suggested that the deposits in the Cribas area represented "flysch" but could not place the depositional environment in terms of its palaeobathymetry. Unfortunately a coherent stratigraphic succession for facies analysis is not present in the Sumasse River and aspects including understanding changes in water depth and temperature are poorly understood.

The older successions exposed at localities M559 and C666 include beds of red limestone (Fig. 6C) that contain shallow-water foraminifera (e.g. *Calcitornella* sp., *Hedraites plummerae*, *Trepeilopsis australiensis*) which probably lived attached to non-skeletal algae in the upper photic zone (see discussion in Dixon and Haig, 2004). These and some of the echinodermal, bryozoan and brachiopod debris probably have been transported from their life environments, perhaps downslope into deeper water. A three-metre thick sandstone bed at M559 shows swaley cross-bedding (Fig. 6F) indicative of deposition above storm wave base in relatively shallow water (see discussion of this bed form by Dumas and Arnott, 2006). The depositional settings of the middle to upper Artinskian at M559 and C666 may have been in the neritic zone.

The mudstone-dominated successions at M558 and M501 include relatively thin sandstone beds with sharp bases that in places display transitions from massive sandstone to ripple-laminated sandstone. These features are interpreted to have been produced by density currents in a relatively deep-water setting. In the mudstone deposits of M558 and M501, the absence of agglutinated foraminiferal species typical of coeval shallow-marine mudstone facies in the Western Australian basins (see 3.3–3.5), and the presence of *Glomospira* morphotypes (Fig. 9C, nos. 2–5) very similar to modern *Glomospira charoides* (Jones and Parker), suggest a deep-marine depositional environment. The modern species is known mostly from bathyal to abyssal

environments (Kaminski and Gradstein, 2012) and has an upper water-depth range of about 100 m (Pflum and Frerichs, 1976).

Abundant bivalve debris (very thin-shelled with prismatic calcite microstructure) forms almost the entire biogenic grain assemblage in some mudstone beds at M588, C665 and C502f (Fig. 9D), and in parts of the latter bed forms a laminated coquina. At M559 and C666, similar shell material is rare. This debris seems to be from the very thin-shelled byssate-attached *Atomodesma exerata*, known in monospecific shell accumulations from widespread localities in Timor (Audley-Charles, 1968; Bird and Cook, 1991). In a general review of the habitat of *Atomodesma*, Kauffman and Runnegar (1975) suggested that it was mainly an "inner sublittoral" dweller attached on relatively firm substrates. However the Timor examples and those from similar facies in the Central Arc Terranes of New Zealand (Campbell, 2000) apparently were adapted to life on deeper water mud in low-oxygen environments unsuitable for other shelled metazoan groups or may have been epi-planktonic attached to floating seaweed that sunk to the seafloor, for example, in storms (but see the discussion of possible epi-planktonic Mesozoic bivalves by Damborenea et al., 2013).

The deep-water *Glomospira* foraminiferal assemblage associated with probable *Atomodesma exerata* in the uppermost Artinskian or Kungurian at M558 and the shallower-water foraminiferal assemblage in the red limestone beds of the middle or upper Artinskian at M559 and C666 perhaps indicate an increase in depositional water depths during the latest Artinskian–Kungurian. However, this interpretation needs to be tested in the more coherent sections in rivers east of the Sumasse River.

3.3. Canning Basin: Noonkanbah Formation

The Noonkanbah Formation (Guppy et al., 1958; Dent, 2016) includes the upper Artinskian to Kungurian, although the precise limits of its stratigraphic range are uncertain. The formation is dominated by shale containing a few widely separated thin to medium sandstone beds. Some of these beds are fossiliferous and some grade to thin shelly packstone (see lithofacies listed on Table 3). No distinct cyclic pattern in sedimentation is recognized, although the basal mudstone beds above the Poole Sandstone were deposited during marine flooding and the transition to sandstones in the overlying Lightjack Formation forms part of a progradational depositional trend. The upper age limit for the Noonkanbah Formation is constrained by the presence of the Roadian ammonoid *Daubichites* about 60 m above the base of the Lightjack Formation (Glenister et al., 1993) and IDTIMS dates of 268.1–270.1 Ma for ash beds within this formation (Mory et al., 2012; Laurie et al., 2016). The age of the base of the Noonkanbah Formation is

limited by the presence in the basal Poole Sandstone (Nura Nura Member) of *Parametalegoceras striatum* (Teichert), *Metalegoceras* (*Artimetalegoceras*) *clarkei* (Miller) and *Thalassoceras wadei* Miller that are considered late Sakmarian (Glenister et al., 1993; Boiko et al., 2008; Leonova, 2011).

For this study, an outcrop section of 640 m was logged and sampled in an area with generally poor exposure at Liveringa Ridge (Figs. 10, 11; section 7, Appendices 10, 11). Guppy et al. (1958) measured a thickness of 683 m at this locality. We did not undertake detailed sampling in the Bruten Yard area (Fig. 10), where Guppy et al. (1958) designated a 406 m thick type section, because the exposure of friable beds there is poorer than at Liveringa Ridge. A borehole (BHP PND-1) 16 km east of Bruten Yard, continuously cored through the Noonkanbah Formation, was also sampled (Figs. 10, 12; section 7, Appendices 12–14). In these sections most of the formation consists of friable mudstone (lithofacies 1, Table 3). The rare packstones (lithofacies 6–7; Table 3, Fig.13) are generally accumulations of skeletal debris that form irregular layers (usually ca. 10–20 cm thick) within slightly thicker (usually <0.5 m) quartz sandstone units (lithofacies 3–5; Table 4). The packstone layers commonly include large clasts (up to ca. 5 cm long) of sandstone. The suite of lithofacies 4–7 (Table 3) probably represents tempestite deposits that accumulated above a very shallow storm-wave base in the interior sea (following Haig, 2003, 2004). Collectively, the lithofacies suggest significant, although variable, inflow of mud-laden freshwater into the shallow sea during deposition of the formation and a humid rather than arid hinterland.

Biostratigraphic distributions showing changes in skeletal composition and diversity (section 7, Appendices 10–13) suggest that the level of maximum marine flooding during Noonkanbah Formation deposition is represented somewhere within the interval 170–350 m above base in the Liveringa outcrop section, and between about 150 m and 260 m below surface in BHP PND-1. Within these intervals, precise determination of the maximum flooding level would require metre-scale analysis of foraminiferal distributions such as made by Haig (2003) for the Quinnanie Shale in the Southern Carnarvon Basin. Similar analysis of the abundance of acanthomorph and polygonomorph (spinose) acritarchs would complement the foraminiferal analysis, as they usually are more abundant in deeper more open-marine facies. In the limited number of samples processed for palynomorphs, the abundance and average size of these acritarchs is variable (section 7, Appendix 14). The mudstone at 175.8 m, where the highest abundance of acritarchs is recorded, was deposited under significantly more marine conditions than at other levels sampled for palynomorphs (section 7, Appendix 14). Bathymetry probably was at its greatest for the Cisuralian in the Canning Basin during the Noonkanbah Formation

maximum flooding interval based on dominance of mudstone rather than sandstone facies, the diversity of the fossil assemblages and the distribution of foraminifera viewed against the palaeobathymetric model of Haig (2003).

Fossil species from the Noonkanbah Formation are listed in section 7, Appendix 15, and in the palynomorph distribution chart (section 7, Appendix 14).The stratigraphic distributions of many of the fossil groups within the formation are not rigorously recorded, but from the distribution charts presented here (section 7, Appendices 10–14) some significant conclusions may be drawn from the observed patterns. The land flora, as represented in the spore-pollen assemblages in BHP PND-1 (section 7, Appendix 14), shows little change throughout the Noonkanbah Formation (see similarities between adjacent samples, Table 4). By comparison, grouping the miospores according to their known or inferred botanical affinities (section 7, Appendix 14) in the succession (Fig. 14) reveals: 1) pollen grains related to glossopterids and other seed ferns are more abundant in the upper part of the succession, and 2) the abundance patterns of gymnosperm pollen and lycophyte spores show an opposite relationship, with highest abundances of the former (at 175.8m and 233.30m) corresponding to lowest numbers of the latter. These trends may be related to changes in temperature and humidity or to changes in proximity to vegetation source areas. However, palynological analyses of a larger number of samples in more sections are required before a sound hypothesis explaining the microfloral distribution patterns can be made. The mud facies faunas are represented mainly by foraminifera (section 7, Appendices 11, 13) which, apart from a significant change in the Nodosariata (Foraminifera) discussed in 3.3.2, show changes in similarity and diversity (Table 4). These variations in part suggest salinity fluctuations with low-diversity organic-cemented agglutinated assemblages reflecting estuarine conditions (following Haig, 2003, 2004) and higher diversity assemblages including Nodosariata and Miliolata representing deeper more open-marine conditions. However, as there are only moderate levels of similarity (43% and 20% for total assemblage and 56% and 25% for organic-cemented siliceous agglutinated foraminifera; Table 4) between the intervals with greatest diversity, more complex factors must have influenced the variability in foraminiferal assemblages. Brachiopods and bryozoans are the main components of the very shallow-water sand faunas. Based on the distributions of brachiopod species charted by Thomas (1954), species composition changes significantly from bed to bed up-section in the formation (section 7, Appendix 16; Table 4). This suggests that shallow-marine sand habitats were developed for only short time intervals in the basin and accommodated successive migrations of sand-dwelling species; each migration-wave adapting to slightly different water quality (perhaps in temperature or turbidity).

Fossil groups reported here for the first time from the Noonkanbah Formation include *Tubiphytes* (Fig. 13B) of uncertain biotic affinity but probably algae (see Vachard and Moix, 2011; Senowbari-Daryan, 2013) encrusting on brachiopod shell fragments in the sand facies, and holothurian spicules common at some levels in the mud facies.

Within the Noonkanbah Formation, conodonts, and foraminifera particularly from within the maximum marine-flooding interval, offer the best means for age correlation. Zonation based on spore-pollen distributions may be used for regional correlation across variable facies. The biostratigraphic correlations, at least on a local and regional scale, can be tested against sequence-stratigraphic comparisons thereby providing insights into eustasy as well as regional and local tectonic events (section 3.6).

At Liveringa Ridge, the conodont *Mesogondolella idahoensis* is present about 230 m above base of the formation, with a related form at ca. 315 m; and *Vjalovognathus shindyensis* is present over a broader range from about 150 m to 315 m. Nicoll and Metcalfe (1998) noted that this material was fragmentary and poorly preserved and suggested an early Kungurian age for the association of *M. idahoensis* and *V. shindyensis*. However, caution is required with the determination as the morphology of gondolellid conodonts may be greatly influenced by environmental factors (Mei and Henderson, 2002; Henderson and Mei, 2007) and stratigraphic ranges of morphotypes may vary at different localities.

Among the foraminifera there is a major taxonomic change within the Nodosariata that should be recognizable in a global context for similar mud facies. In the Liveringa outcrop section, an assemblage of Nodosariata at 2 m above the base of the Noonkanbah Formation is dominated by *Protonodosaria tereta* with a simple rounded aperture (Fig. 15A, B). *Protonodosaria* is not recorded higher in the succession here or in BHP PND-1 but dominates assemblages in older Permian units in the Southern Carnarvon and Perth basins (Crespin, 1958; Foster et al., 1985; Palmieri, 1993; Dixon and Haig, 2004). *Nodosaria* with radiate rather than simple aperture but with variable morphotypes some trending toward *Pseudonodosaria* first appear at 186 m above base in the Liveringa outcrop section and upward from 253.5 m in BHP PND-1. This change from *Protonodosaria*-dominated assemblages to *Nodosaria-Pseudonodosaria* assemblages (Fig. 15C-M) represents a significant step in the evolution of the Nodosariata. In mud facies, similar morphotypes of the *Nodosaria* to *Pseudonodosaria* cline are present in all subsequent geological systems from the Triassic to Neogene, suggesting great conservatism after an abrupt initial appearance. The incoming of the *Nodosaria-Pseudonodosaria* assemblages in the Canning Basin seems to be coincident with maximum

flooding in the Noonkanbah sequence. In carbonate facies outside of the East Gondwana interior rift, recognition of this transition is confused because most records of the Nodosariata are from thin sections where apertural details are difficult to interpret.

On the basis of thin sections, Filimonova (2015) recorded *Pseudonodosaria* (= *Rectoglandulina*) from the lowest Kungurian, *Megousia aagardi-Aphanaia lima* Zone, developed in microbial limestone facies in the Kolyma–Omolon region of northeastern Siberia. This was at a slightly lower level than the Kungurian records of the genus by Karavaeva and Nestell (2007) from the same region. These investigations in the Kolyma–Omolon region did not extend down into the Artinskian, apparently because of change of facies from limestone to underlying mudstone. Working in friable mudstone in the Lower Permian of northern and central Siberia, Gerke (1961) described species of *Protonodosaria* and rare *Pseudonodosaria* (= *Rectoglandulina*) with preservation similar to those from the Noonkanbah Formation. *Protonodosaria proceraformis* (Gerke), which is very similar to *P. tereta* (Crespin) from the basal Noonkanbah Formation, ranges from the base of the Lower Kozchevniki Formation (upper Artinskian) in the Nordvik district to beds containing a microfauna transitional from the underlying assemblage of agglutinated foraminifera to the overlying assemblage of smooth *Frondicularia*. The latter is Ufimian (= Kungurian) in age. According to Gerke (1961) *Pseudonodosaria borealis*, which Palmieri et al. (1994) regarded as synonymous with the Australian *P. sercoldensis*, makes a very rare first appearance within the assemblage of agglutinated foraminifera in the Nordvik region. Collectively the Siberian distributions suggest that the last appearance of *Protonodosaria proceraformis* and the first appearance of *Pseudonodosaria* were close to the Artinskian–Kungurian boundary.

Precise zonal boundaries for basinal and inter-regional correlation are difficult to ascertain using the palynomorph assemblage in the Noonkanbah Formation because of the rarity of spore-pollen zonal index forms such as *Praecolpatites sinuosus* (section 7, Appendix 14). The upper part of the formation, above 175.8 m in BHP PND-1, belongs to the *P. sinuosus* Zone based on presence of the nominate species at frequencies <2% of the spore-pollen count. The lower part of the formation, below about 272 m in BHP PND-1, belongs within the *Microbaculispora trisina* Zone but the boundary with the overlying *P. sinuosus* Zone within the interval 175.8–272 m is indeterminable.

The above evidence suggests that the maximum marine-flooding interval within the Noonkanbah Formation lies close to the Artinskian–Kungurian boundary. More precise correlations may be possible when greater knowledge is obtained about the distributions of some

of the fossil groups in sections elsewhere in East Gondwana particularly those more proximal to the Mesotethyan Ocean.

3.4. Southern Carnarvon Basin: Byro Group

Shale to quartz-sandstone cyclicity at varying scales characterises the Byro Group (Figs. 16, 17). Changes in the ratio of shale to sandstone in the succession were used to recognize eight formations within the Byro Group (Condon, 1967; Hocking et al., 1987). The underlying Billidee Formation forms part of a retrogradational depositional trend that commences in the uppermost Moogooloo Sandstone beneath the Billidee Formation (Mory and Haig, 2011, figs. 37–39) and continues into the Coyrie Formation (Fig. 17). This is distinct from the progradational depositional trend through most of the Moogooloo Sandstone. For this reason, and because it shows an alternation of shale and sandstone units, we place the Billidee Formation within the Byro Group rather than in the underlying Wooramel Group where it was previously included (e.g. Hocking et al., 1987; Mory and Backhouse, 1997; Iasky et al., 1998; and Mory and Haig, 2011).

The basic depositional cycle in the Byro Group is represented by a shallowing-upward parasequence as illustrated in Fig. 18. Parasequence sets that display retrogradational and then progradational trends are used to identify the five major cycles (numbered I to V) shown on Fig. 17. Within the major cycles, levels that represent maximum marine flooding consist of dark grey shale (e.g. Fig. 18B) in most cases containing scattered calcareous mudstone nodules that formed under slow sedimentation early in diagenesis of the seafloor sediment. These thick shale units include high-frequency metre-scale cycles that are not reflected in the physical sedimentology but are apparent in foraminiferal distributions (Haig, 2003). Maximum flooding for the entire Cisuralian succession in the Southern Carnarvon Basin was in cycle II, within the upper part of the Bulgadoo Shale (Figs. 17, 18B). The shale here has the highest total-organic content found within this facies in the basin (Mory and Haig, 2011) and also has a diverse fauna with pelagic as well as benthic components (section 7, Appendices 17–19). An abundant Nodosariata-Miliolata foraminiferal assemblage is present in the upper Bulgadoo Shale but is sparse in maximum-flooding levels of the other cycles. The assemblage in the Bulgadoo Shale includes many dwarf morphotypes that indicate low dissolved-oxygen levels in almost stagnant bottom waters.

Many of the parasequences shoal upwards into hummocky and swaley cross-bedded sandstone facies (Fig. 18B, D, E) as described by Moore and Hocking (1983). In some parasequences, the upper parts of these sand facies are reworked by intense large-scale

bioturbation including *Skolithos* burrows (Fig. 18C). This ichnofacies is distinct from a deeper-water *Zoophycos* facies found in fine sandstone deposited just below storm-wave base (Fig. 18F). No tidal-facies indicators have been observed in sandstone beds at the top of the parasequences. In a major review of hummocky and swaley cross bedding, Dumas and Arnott (2006) noted records in a variety of wave-fetch limited environments (including lakes) as well as open-marine settings and in water depths as shallow as the surf-zone. They found a common feature was the occurrence of these bed forms between storm-wave and fairweather-wave base. Under the shallow interior-sea conditions envisaged by Haig (2003, 2004), a limited wave-fetch area would have resulted in a very shallow wave base.

Dropstones, including boulders up to 1 m in maximum diameter, of white quartzite, stromatolitic limestone/dolomite and granitoid, collectively derived from Proterozoic units that outcrop east of the basin, are present in the Billidee and lower Coyrie formations of Cycle I (Hocking et al., 1987; observations by AJM, DWH, and EH for the present study). These occur as isolated clasts in mudstone or very fine sandstone (Fig. 19D–F), or as scattered small concentrations of clasts in some areas. The latter pattern suggests that the dropstones were ice-rafted rather than carried in the roots of floating trees (following criteria listed by Bennett et al., 1996). Diamictite, as found in the Lyons Group at the base of the Permian succession in the Southern Carnarvon Basin, is absent. The dropstones were probably emplaced by seasonal sea ice (with a thickness up to 125 cm, following modern analogues cited by Dionne, 1993) in the interior sea. Gravel (including boulders to 1 m diameter), reworked from older diamictites and accumulating along the shoreline, was incorporated into ice that developed during winter and released from floating ice during spring and summer warming (see Dionne, 1993, for modern examples). Physical sedimentological features suggesting cold-water conditions are present only in the lower section of Cycle I.

Skwarko (1993b) listed the faunal content known at that time from formations of the Byro Group, but subsequent work means that care should be taken in interpretations made from these lists, particularly in terms of faunal diversity, stratigraphic continuity of distributions through the formation, and formation assignments in areas of very poor outcrop particularly in those areas remote from type sections. The lithostratigraphy for some boreholes is also difficult to interpret (see discussion in section 7, Appendices 1, 18, 19); unfortunately there has been no stratigraphic drilling in the type areas of any formation. Considering the entire thickness of the Byro Group, relatively few beds contain a macrofauna. Updated species lists for Cycles I to III (–IV) are provided here for the Foraminifera (section 7, Appendix 19), Brachiopoda (section 7, Appendix 20), crinoids and corals (section 7, Appendix 21). Note that the published records of

cycles III and IV are difficult to separate because cycle IV includes the upper part of the Wandagee Formation. The palynomorph records of Powis (1981) are used here to gauge the similarity of adjacent cycles (see below). These were taken from intermittent cores in Kennedy Range 1 that penetrated almost the entire Byro Group with the interpreted formation subdivision (Lehmann, 1967) consistent with that known from the outcrop sections.

Foraminifera dominate the mud-facies fauna of the Byro Group with organic-cemented siliceous agglutinated types most diverse and abundant (Astrorhizata in section 7, Appendix 19). Although assemblages of these agglutinated species varied due to water depths and water quality (see Haig's, 2003, analysis of faunas from the Quinnanie Shale), when agglutinated species inventories from cycles I to III are compared, there seems only moderate change in composition through the succession (similarities 51–62%; Table 5). The Nodosariata and Miliolata are confined mainly to the deeper, more open-marine mud facies. Cycle II includes the incoming of the *Nodosaria-Pseudonodosaria* foraminiferal assemblage that replaces a *Protonodosaria* assemblage rare in Cycle I (see section 7, Appendix 19), similar to the transition found in the Noonkanbah Formation (3.3.2).

The sand facies is fossiliferous in only a few beds within each formation of the Byro Group. For example, most of the macrofauna of the Wandagee Formation (which contains the most diverse sand-facies fauna of any formation in the Byro Group, according to Skwarko, 1993) is present in sandstone at the top of three or four parasequences low in the formation. Published detailed stratigraphic distribution charts of the macrofauna are lacking for the Byro Group, although various groups have been charted collectively at formation level (e.g. Skwarko, 1993).

The brachiopod assemblages of the Byro Group (section 7, Appendix 20) show significant change from cycle to cycle (faunal similarities, 9–14%), similar to bed-to-bed changes described in section 3.3 for the Noonkanbah Formation in the Canning Basin. Our field observations suggest that within a formation, there are frequent changes in the composition of conspicuous brachiopod assemblages in the sandstone beds and the faunas rarely repeat up-section. Crinoid and coral assemblages in the sand facies show a similar pattern (Table 5).

Because the terrestrial spore-pollen record from the Byro Group is mainly from borehole sections, some of which have uncertain lithostratigraphic correlations, it is difficult to compile a distribution chart comparing the taxonomic composition of each depositional cycle. Based on the distributions charted by Powis (1981) for Kennedy Range 1, the spore-pollen assemblages from cycles II to V show only moderate change (40–53% similarity between adjacent cycles;

Table 5). In this well, a series of samples taken by Powis (1981) from the cycle I interval were barren of palynomorphs, and preservation in the rest of the section was variable. More subsurface sections, particularly in the type areas of formations are required before the distribution patterns of palynomorphs can be fully understood.

Known ammonoid species in the Byro Group are listed on Fig. 17. Cycle I (Billidee, Coyrie and Mallens formations) belongs to the upper Artinskian ammonoid *Neocrimites fredericksi-Medlicottia orbignyana* Zone (Leonova, 2011). Cycle V contains the ammonoid *Daubichites* Popow indicative of the Roadian (Leonova, 2011; and see discussion on the locality of *Daubichites* in the Bryo Group by Archbold, 1998a,b, 1999). Precise chronostratigraphic positions of cycles II to IV are uncertain within the upper Artinskian to Roadian. Cycle II, which includes the maximum marine flooding level for the entire Byro Group succession (see above), is probably close to the Artinskian–Kungurian boundary. *Pseudoshistoceras simile* Teichert is known from the Coyrie Formation and the Bulgadoo Shale (in cycles I and II of the Byro Group; Fig. 17). This species is an advanced metalegoceratid, derived from *Metalegoceras* Schindewolf during the middle Artinskian (Boiko et al., 2008). The Western Australia records of *P. simile* indicate a stratigraphic position within the Baigendzhinian Substage of the upper Artinskian (Leonova, 2011). Cycle II probably overlaps the Artinskian–Kungurian boundary. This is supported by the incoming of the *Nodosaria-Pseudonodosaria* foraminiferal assemblage in this cycle probably coeval with a similar maximum marine flooding interval containing this assemblage in the Noonkanbah Formation of the Canning Basin (section 3.3). Cycles III and IV, between the last appearance of *P. simile* in cycle II and the first appearance of *Daubichites* in cycle V, are probably Kungurian.

Nicoll and Metcalfe (1998) recorded the conodont *Vjalovognathus shindyensis* from the Coyrie Formation (cycle I). However the two localities where this species was found have very poor outcrop in faulted successions remote from the type area of the formation and the lithostratigraphic designation is therefore uncertain. A sample from the type locality of the Coyrie Formation yielded only a single indeterminate specimen of *Hindeodus* Rexroad and Furnish. Doubt remains as to whether the muddy nodular limestones containing *V. shindyensis* lie in the upper Coyrie Formation or in the Bulgadoo Shale (cycle II). They are consistent with a position near the Artinskian–Kungurian boundary (see 3.3).

Warming through cycles I and II of the Byro Group is indicated by (1) the disappearance of dropstones above the lower Coyrie Formation; (2) the very rare appearance of conodonts either in the upper Coyrie Formation or the Bulgadoo Shale; (3) the appearance in cycle II formations of brachiopods with “Tethyan” warm-water affinity (e.g. *Demonedys*,

Fredericksia(?), *Tornquistia*, *Quinquenella*, *Retimarginifera*, *Spiriferella*, and *Spiroelytha*), some of which persisted through cycles III and IV (Archbold and Shi, 1995); and (4) the diversification of the stemless crinoid *Calceolispongia* in Cycles II and III (Teichert, 1991). This suggests that by the latest Artinskian–earliest Kungurian relatively warm sea conditions were present in the Southern Carnarvon Basin, compared to earlier in the late Artinskian, and may have persisted through the Kungurian. This is a trend that appears similar to that in the Noonkanbah Formation in the Canning Basin (3.3). Within the Byro Group, the high frequency of hummocky and swaley cross-bedding in quartz sandstone at the top of parasequences (Moore and Hocking, 1983), particularly in cycles II–IV, suggests periods of more intense storm-wave activity than in the Canning Basin to the north, or the Perth Basin to the south where coeval formations (vis. Noonkanbah and Carynginia formations; see 3.3 and 3.5) include fewer beds of this facies with a relatively greater mudstone or muddy fine sandstone component. Perhaps during cycles II–IV, the Southern Carnarvon Basin was situated in a cyclonic belt or a mid-latitude winter storm-tract (see modelling by PSUCLIM, 1999).

3.5. Northern Perth Basin

3.5.1 Carynginia Formation

The Carynginia Formation consists of mudstone with interbedded quartz sandstone showing hummocky cross stratification in some beds (Clarke et al., 1951; Playford et al., 1976; Le Blanc Smith and Mory, 1995). All outcrops of the formation, including those in the type area, lie on the Irwin Terrace that is at the southern end of a marginal-rift basin (Figs. 1, 16A) which also includes, from north to south, the Merlinleigh and Byro sub-basins attributed to the Southern Carnarvon Basin, and the Coolcalalaya Sub-basin north of the Irwin Terrace, attributed to the Perth Basin. In subsurface the formation extends west from the Irwin Terrace across the northern part of the Perth Basin (Figs. 20–22).

At the type outcrop area in the Irwin River region (Figs. 1, 20), the Carynginia Formation overlies the Irwin River Coal Measures with a disconformable contact well exposed in the South Branch of the river (Fig. 23A). Here very thin, discontinuous lenses of quartz granules and small pebbles lie along a marine-flooding erosion surface. In the mudstone-dominated parasequence at the base of the formation, organic-cemented siliceous agglutinated foraminifera are common and are the only marine fossils found at this level. They include a few species of very large tubular forms (several millimetres long; section 7, Appendix 22) perhaps adapted for infaunal life within mud and very cold-water temperatures (see below). In the lower 20 m of the formation exposed in the South and North Branches of the Irwin River, a progradational

depositional trend is apparent (Figs 21, 23B), with the proportion of sandstone progressively increasing in ascending parasequences. This lower part of the Carynginia Formation contains scattered dropstones (some about 1 m in size; Fig. 23D). Most of the dropstones are granitic and derived from Archean units that are exposed on the eastern side of the Darling Fault a few kilometres east of the Carynginia Formation outcrops (Fig. 19). In higher sections of the formation in the Irwin River area, mudstone-dominated parasequences lack dropstones. In one of these in the northern branch of the river, a stem from a *Glossopteris* tree with attached fructification and leaf (Fig. 23C) was found in a thin sandstone bed. According to Playford et al. (1976), no shell macrofossils have been found in confirmed outcrops of the Carynginia Formation in the Irwin River area or in boreholes on the Irwin Terrace and none were found during this study. In the IRCH 1 bore section (at locality 2 on the Irwin Terrace; Fig. 20B), a 92 m section of the Carynginia Formation was continuously cored. The lower 60 m of the formation in this well contains scattered dropstones, and mudstones within the section include sparse organic-cemented siliceous agglutinated foraminifera as the only evidence of a shelly marine fauna. On the Irwin Terrace, the Carynginia Formation becomes sandier to the south of the type area (Playford, 1959; Le Blanc Smith and Mory, 1995).

Because of the lack of a marine fauna containing age-diagnostic species, stratigraphic correlation of the Carynginia Formation with units in contiguous sub-basins to the north, forming the marginal-rift system, relies on (1) broad sequence-stratigraphic comparisons, (2) climatostratigraphic considerations, and (3) palynostratigaphy. The marine flooding that terminated deposition of the Irwin River Coal Measures and initiated marine sedimentation of the Carynginia Formation corresponds to the major marine flooding level in the uppermost Moogooloo Sandstone of the Merlinleigh Sub-basin that led to deposition of the Byro Group (section 3.3). The presence of dropstones in the lower Carynginia Formation on the Irwin Terrace is similar to their occurrence in the Billidee and lower Coyrie Formations in the Merlinleigh Sub-basin and both indicate a cold interval with sea ice (see 3.3; and also Clarke et al., 1951, for the Carynginia Formation occurrences). In a sample collected during this study 40 cm above the base of the Carynginia Formation in the South Branch of the Irwin River, a spore-pollen assemblage (section 7, Appendix 23) suggests a position somewhere below the *Praecolpatites sinuosus* spore-pollen zone (as defined by Backhouse, 1991; Mory and Backhouse, 1997). Backhouse (1993) suggested that the section in IRCH 1 from 25.3 m to 87 m belongs to the lower *P. sinuosus* Zone, with the marker species (*P. sinuosus*) present only in the basal sample studied in this well, but this needs review. The zone is represented in the Byro Group in the Merlinleigh Sub-basin (section 3.3) and in the Noonkanbah Formation of the

Canning Basin (section 3.2), but the marker species is often very rare or absent (see Appendix 14 for the Noonkanbah Formation distribution of the species). A review by Mory and Backhouse (1997) suggested that the Carynginia Formation ranges from the upper *Microbaculispora trisina* Zone to within the *M. villosa* spore-pollen zone and is equivalent to the Byro Group and lower Kennedy Group (i.e. cycles I–V) of the Merlinleigh Sub-basin.

West of the Irwin Terrace, the northern Perth Basin extends to the present ocean–continent boundary (that resulted from Early Cretaceous rifting), and presumably near the main axis of East Gondwana interior rift. Marine Permian, including the Carynginia Formation is known from the northern Perth Basin as far south as about 30°S present-day latitude (Fig. 20). In Woodada Deep 1 (locality 1 on Fig. 20; Fig. 22), the formation is 289 m thick, and is divided into a lower mud-dominated unit, a middle sand-dominated section, and an upper mud-dominated unit. Sparse organic-cemented siliceous agglutinated foraminifera have been found in core 4 of the lower unit and in the lower part of the upper unit (core 3). However a more diverse foraminiferal assemblage is present higher in the upper unit (in cores 1 and 2; see section 7, Appendix 13). Besides siliceous agglutinated species this fauna includes calcareous foraminifera such as a nodosariid with radiate aperture placed in *Pseudonodosaria* sp. (Fig. 24I) and miliolids including a morphotype tentatively identified as *Hemigordius* sp. (Fig. 24G) as well as indeterminate calcivertellines encrusting on quartz grains (Fig. 24E). These suggest that the upper mudstone unit of the Carynginia Formation in this well was deposited under more open-marine deeper-water conditions than the lower mudstone unit at this locality. The presence of *Pseudonodosaria* indicates a stratigraphic level equivalent to or higher than the Bulgadoo Shale (maximum marine-flooding level in the Merlinleigh Sub-basin, section 3.3).

In the upper part of the Carynginia Formation in BMR 10 stratigraphic hole, 16 km east of Woodada Deep 1, several brachiopods and a conulariid were found in carbonaceous mudstone suggesting an age-correlation to the lower part of the Byro Group in the Merlinleigh Sub-basin (MacTavish, 1965).

In the sections on the Irwin Terrace as well as to the west in the northern Perth Basin, the meagre fossil assemblages found in the Carynginia Formation suggest very restricted marine conditions, but with maximum marine flooding in the upper part of the formation and an increase in water temperature from very cold with sea ice during deposition of the lower part of the formation to warmer conditions, free of sea ice, during deposition of the upper section. The warmer interval probably was during the time represented by the *P. sinuosus* Zone (i.e. latest Artinskian to Kungurian).

3.5.2 Mingenew Formation

Small outcrops of fossiliferous ferruginous sandstone are present over isolated areas near the western faulted boundary of the Irwin Terrace. Stratigraphic relationships between the Mingenew Formation and other Permian formations on the Terrace are uncertain because of faulting and poor outcrop. In contrast to the Carynginia Formation, large shell fossils are common and diverse in some beds of the Mingenew Formation (Playford et al., 1976; Skwarko, 1993). Brachiopods, bivalves and gastropods are present, preserved as internal and external moulds, as well as moulds of *Glossopteris* leaves. On the basis of the brachiopods, Archbold (1998a,b) correlated the Mingenew Formation with the Coyrie Formation in the Merlinleigh Sub-basin and with the Madeline Formation (considered part of the Coyrie Formation; Hocking et al., 1980) in the Byro Sub-basin. He also considered it equivalent to the lower Carynginia Formation, but apparently without direct evidence. In his stage correlations, this level was regarded as belonging to the Sargin part of the Baigendzhinian Sub-stage of the Upper Artinskian (uppermost Artinskian according to Henderson et al., 2012). Elsewhere in the northern Perth Basin, abundant shelly faunas are known only from the upper Sakmarian Fossil Cliff Member of the Holmwood Shale and the upper Middle Permian (probably Capitanian) Beekeeper Formation known only from subsurface, but not from the Irwin Terrace. In terms of palaeogeography, it is difficult to reconcile the abundance of robust shelly material in sandstones of the Mingenew Formation with the lack of macrofauna in sandstones at the top of shoaling upward parasequences in the supposedly coeval Carynginia Formation.

3.6 East Gondwana Rift Synthesis

In basins adjacent to the axis of the interior rift system, upper Artinskian–Kungurian sections are best known from the structurally complex Timor orogen in the northern part of the rift (see 3.2), and poorly known further south only in subsurface wells in, for example, the western part of the northern Perth Basin (see 3.5.1). Despite the structurally disjointed sections, the depositional models suggested by Bird and Cook (1991, figs. 5, 8) for the Cribas Group exposed in West Timor, may apply to most of the marine axial basins in the northern part of the rift system. Here, small carbonate banks were present in bypass zones on a delta-dominated shelf adjacent to a deeper basin that was probably fault-generated. Basinal deposition took place mainly from density currents transporting sediment derived from the shelf. In the western part of the northern Perth Basin, about 2000 km south of Timor, the meagre marine fauna known from the Carynginia Formation (see 3.5.1) suggests marginal-marine conditions. In the southern Perth Basin the entire Permian is non-marine (Playford et al., 1976; Le Blanc Smith and Kristensen,

1998). This suggests that marine bathmetry decreased from north to south along the axis of the East Gondwana interior rift.

The best-understood upper Artinskian–Kungurian sections are in the marginal rift basins,which splayed off the axial rift system, in onshore Western Australia. Here marine conditions were very different from those in basins adjacent the main rift axis of the East Gondwana interior rift. The stratigraphic records in the marginal basins (see sections 3.3–3.5) indicate a wet climate with great influxes of fresh water laden with fine-grained sediment. There was significant high-frequency variability in environmental conditions such as in salinity, turbidity, dissolved-oxygen levels, and water depth. The sea-floor gradient was very gentle with no shelf–basin topography and the overall bathymetry was very shallow. Because of limited wave-fetch, a very shallow wave base determined the position of the sand-mud interface. These conditions inhibited extensive carbonate-bank development irrespective of water temperature and also may have prevented the migration into the basin of many species with limited tolerance to such environmental variability. Haig (2003, 2004) noted that the marine conditions in the interior seas that flooded the marginal basins were estuarine-like and suggested that the Baltic Sea and estuaries in southwest Western Australia provided modern analogues for these environments. Organic-cemented siliceous agglutinated foraminifera are the most persistent and abundant marine fossil shells found in the marginal basins. These foraminifera are particularly characteristic of modern estuaries with variable, but generally low, salinity and some, including species of *Ammobaculites* and *Trochammina*, show remarkable resemblance to modern species (Haig, 2004; Ostrognay and Haig, 2014).

The differences between the more open-marine basins along the northern axis of the rift system (such as in Timor) and the marginal rift basins with estuarine-like variability should be central in any discussion of the biogeographic affinities of the biota (Table 6). The absence of particular fossil groups from the marginal rift basins may be due to the peculiar conditions here and may have no palaeoclimate significance. For example, Dickins (1993) pointed out the absence of colonial corals, which he regarded as warm-water indicators. The meagre coral fauna of the marginal rift basins (see 3.3, 3.4) consists only of small solitary rugose types and a few tabulate corals. These probably represent the few species able to tolerate the variable marine conditions and the ephemeral mobile sandy substrates of the shallow interior seas during the late Artinskian– Kungurian. They were either adapted for sticking in soft sand (e.g. the conical-shaped rugose corals) or anchoring on to other skeletal objects or to intraclasts (e.g. the tabulate corals). Similarly, the foraminiferal assemblage contains no specific warm-water indicators. Tetrataxaceans, endothyraceans, pseudoammodiscids and lasiodiscids, of Tethyan affinity, have

not been recognized although these are present in older units in the marginal rift basins, including *Tetrataxis* in the Calytrix Member of the Grant Formation (Canning Basin) that is no younger than late Sakmarian (Taboada et al., 2015) and *Tetrataxis*, *Endothyra*, *Pseudoammodiscus,* and *Monotaxinoides* from upper Sakmarian–lower Artinskian limestones known from the Canning and Southern Carnarvon Basins (Haig et al., 2014). The absence of these foraminifera and of larger fusulines from the upper Artinskian–Kungurian is probably related to water quality such as influx of mud-laden freshwater, turbidity, and fluctuating salinity.

The stratigraphic record for the marginal rift basins documented in sections 3.3–3.5 and summarized in Table 7, suggests that (1) maximum marine flooding in these basins (Fig. 25) for the Artinskian–Kungurian interval (and for the entire Cisuralian) was close to the Artinskian–Kungurian boundary, and (2) water temperatures increased from very cold (< 4°C with sea-ice in the south) at the beginning of the late Artinskian to at least warm-temperate during the latest Artinskian and early Kungurian. Although common in Eastern Australia, Glendonites have not been observed in the Western Australian Permian (Gorter, 2002), suggesting that water temperatures may have remained above 0°C (following Carr et al., 1989; Swainson and Hammond, 2001; Selleck et al., 2007). In contrast to the lower Byro Group in the Southern Carnarvon Basin (see 3.4) and the lower Carynginia Formation (see 3.5) in the northern Perth Basin, dropstones have not been recorded in the coeval lower part of the Noonkanbah Formation (see 3.3) in the Canning Basin, and none have been recorded from Timor successions. This suggests that there may have been a contemporaneous south to north increase in temperature similar to the ~10°C gradient during the late Sakmarian–early Artinskian from 35°S to 55°S palaeolatitude (as discussed by Haig et al., 2014).

The Bua-bai limestone in Timor was deposited probably close to 35°S palaeolatitude (Fig. 1) during the latest Artinskian on an open-marine shelf near the rift axis (see 3.2.1). Although it contains common larger fusulines and a variety of algae (including dasycladaceans), the fusuline assemblage is of low diversity and the dasycladacean and solenacean algae are very rare (see section 7, Appendix 2, 3). Bryozoans and crinoids are the dominant biogenic elements in the limestone. This suggests that Timor was positioned near the southern limits of the distributions of larger fusulines, dasycladaceans and solenaceans in a warm-temperate sub-tropical belt.

In the Canning Basin, within the maximum marine-flooding interval of latest Artinskian–early Kungurian age, temperate to warm-temperate biotic indicators are present. These include *Tubiphytes*, conodonts, and certain brachiopod, bryozoan and crinoid species known from more

tropical regions. Although it was most common in warm water, *Tubiphytes* ranged rarely into cooler environments (Hüneke et al., 2001, fig. 8). The low abundance and stunted growth of *Tubiphytes* (Fig. 13B) in the very limited packstones of the Noonkanbah Formation probably reflect local environmental restrictions on carbonate-facies development and should not be taken as significant for climate interpretation, other than indicating temperate or warm conditions. A few beds in the middle part of the Noonkanbah Formation, (e.g. within the 150–350 m above base interval in the Liveringa outcrop section; Fig. 11), contain the most prolific and diverse, although rare with few species, conodont assemblages known from the Australian Cisuralian (Nicoll and Metcalfe, 1998). According to Nicoll and Metcalfe (2001, p. 65) the fauna belongs to a "Tethyan Gondwanaland conodont province" characterized by the endemic *Vjalovognathus* and a few associated *Hindeodus* and *Mesogondolella* that migrated into the interior rift basins during times of "climate amelioration". The brachiopod fauna of the Noonkanbah Formation includes species of *Kiagsiella*, *Retimarginifera* and *Costiferina* identified by Archbold and Shi (1995, p. 208) as being evidence of a "warmer" water Tethyan or Asian influence. However, they also identified "cold or cool" genera in the Noonkanbah Formation. The stratigraphic distributions of brachiopod species, under modern taxonomy, have not been charted in the Noonkanbah Formation so faunal trends cannot be defined at present. Although the distributions of bryozoan species through the Noonkanbah Formation were not outlined in detail, Crockford (1957) described many species (section 7, Appendix 15) and noted some similarities to comparable types in Timor, the Sakmarian and "Artinskian" of the Urals and the "Artinskian" of Vancouver Island. These species are currently under revision by AE and EH. Despite the shallow-water variable environments that existed in the interior sea during deposition of the Noonkanbah Formation (see 3.3.1), the fauna includes some species that are also known in the peri-Gondwana region, more proximal to Mesotethys than the Noonkanbah localities, where they lived in more open-marine facies of both heterozoan and photozoan aspect. These include *Eridopora permiana*, *Dyscritella tenuirama*, *Hinganella bella*, *Liguloclema meridianus*, *Mackinneyella obesa*, *Minilya princeps*, *Streblotrypa* (*Streblascopora*) *marmionensis* and *Timanotrypa australis* (see Ernst et al., 2008; Ernst, 2016). These suggest a warm-water influence in the Noonkanbah fauna. Of these species, *D. tenuirama* and *L. meridianus* are also present in the Bua-bai Limestone of Timor (3.2.1).

Within the Southern Carnarvon Basin, late Artinskian warming is supported by brachiopod distributions discussed by Archbold and Shi (1995). They identified within the cycle II formations, *Demonedys*, *Fredericksia*(?), *Tornquistia*, *Quinquenella*, *Retimarginifera*, *Spiriferella*, and *Spiroelytha* of "Tethyan" warm-water affinity. Some of these genera persisted

through cycles III and IV. This suggests that by the latest Artinskian–earliest Kungurian warm to warm-temperate sea conditions were present in the Southern Carnarvon Basin and at least temperate conditions persisted through the Kungurian. Warming is also suggested by diversification of the stemless crinoid *Calceolispongia* in Cycles II and III (Teichert 1991).

Korte et al. (2008) and Mii et al. (2013) reviewed stable isotope records from the Noonkanbah Formation (Canning Basin) and the Byro Group (Southern Carnarvon Basin) with most determinations based on brachiopod shells that were not precisely positioned in terms of their positions within formations and age. These results are confusing and contrary to the sedimentological and biostratigraphic evidence presented here. For example, Korte et al. (2008) reported an increase in δ18O ‰ (V-PDB) from the upper Artinskian though Kungurian suggesting a decrease in sea-surface temperature, although they acknowledged a variety of water-quality and preservational factors may have influenced the data. Mii et al. (2012) also qualified their conclusions but suggested either a cool climate or relatively high sea-water salinity for deposition of the Noonkanbah Formation and Byro Group. These records are considered unreliable and future stable-isotope work must be accompanied by detailed sedimentological and biostratigraphic documentation and facies analysis.

4. Comparison of East Gondwana palaeoclimate trends

Mississippian to Cisuralian climate records for the East Gondwana interior rift, Lhasa and Sibumasu (Fig. 26; section 7, Appendix 24) show similar patterns that support the Early Permian reconstruction of East Gondwana shown in Figs. 1 and 26. In each region, the Mississippian is represented by warm-water facies, a major depositional hiatus is present through much of the Pennsylvanian and this is followed by lowest Permian units containing diamictites and dropstones. Warming took place during the later Early Permian. Because of structural complications and low resolution chronostratigraphy, published documentation of the stratigraphic successions in Lhasa and Sibumasu are difficult to interpret in terms of changes in palaeobathmetry. At present, sequences and intervals of maximum marine flooding cannot be compared between the regions. Known marine faunas of the Artinskian-Kungurian in Lhasa and Sibumasu (Appendix 24) are typical of open-marine axial rift-basins and differ markedly from the faunas of the more restricted-marine marginal-rift basins in Western Australia.

The climate record for the Permian in eastern Australia (Fielding et al., 2008; Frank et al., 2015) is confused. This is because: (1) new CA-IDTIMS dating has substantially revised the ages of many units in the Bowen Basin formerly placed in the Guadalupian and Lopingian and now considered Lopingian (Metcalfe et al., 2015, Nicoll et al., 2015; Laurie et al., 2016); and (2)

controversy exists as to the identification and age of some of the Cisuralian marine units in this basin (Waterhouse and Shi, 2013; Frank et al., 2015. Warming close to the Artinskian–Kungurian boundary similar to that observed by us in the East Gondwana interior rift was indicated by stratigaphic and oxygen-isotope studies in the Sydney Basin (Waterhouse and Shi, 2010, 2013; Mii et al., 2012).

From the Mostyndale Mudstone Member at the base of the Cattle Creek Formation in the Bowen Basin, Palmieri (1994, pl. 14) illustrated an assemblage of nodosariid foraminifera that seems very close to the assemblage recorded here (Fig. 15) in the maximum marine flooding interval of latest Artinskian–early Kungurian age within the Western Australian marginal rift basins. Palmieri's (1994) identification of *Protonodosaria* in the Mostyndale fauna is based on specimens in which apertures seem poorly preserved. Because of test shape these are considered here to be part of the *Nodosaria–Pseudonodosaria* plexus that replaces *Protonodosaria* assemblages during the late Artinskian in the Western Australian basins (see sections 3.3 and 3.4). The Mostyndale Mudstone represents marine flooding above the non-marine Reids Dome beds (Draper, 2013). For the Bowen Basin succession, Nicoll et al. (2015) correlated the lower Cattle Creek Formation with the lower part of the Tiverton Formation. The latter contains rare ammonoids that Leonova (2011) regarded as Kungurian. Although cold-water indicators have been recorded in the Cattle Creek Formation, they come from members above the Mostyndale Mudstone (Fielding et al., 2008, fig. 4), and this unit may represent a similar marine flooding and warming episode to that recognized in the uppermost Artinskian–lower Kungurian in the marginal rift basins in Western Australia.

5. Discussion

The opening of the Indian Ocean to form the present-day western continental margin of Australia was by progressive north to south rifting that took place during an interval of 50 my from about 190 Ma (Early Jurassic) in New Guinea, 165 Ma in the Timor region, 155 Ma between Timor and Exmouth Plateau, and 135 Ma south of Exmouth Plateau (Pigram and Panggabean, 1984; Heine and Müller, 2005; Haig and Bandini, 2013). Metcalfe (2006) suggested that Lhasa rifted from Greater India during the Late Jurassic. Based on provenance studies, Zhu et al. (2011) found that zircons from the Permian of Lhasa probably were derived from a Proterozoic orogenic belt in southern Western Australia, but suggested that these were reworked from older sedimentary units in Lhasa after it rifted from the "north-western" Australian margin during the Late Devonian. The Permian climate record in Lhasa does not support this age of rifting.

Similar progressive rifting to that which formed the Indian Ocean may have taken place during the earlier opening of Mesotethys (also called Neotethys), but the age of rifting is uncertain. The opening of Mesotethys has generally been taken as Early or Middle Permian. Based on palaeomagnetic and biostratigraphic observations, Metcalfe (2006) suggested that Sibumasu (part of the Cimmerian continent) rifted from Gondwana during the late Early Permian. Our work in the Eastern Gondwana interior rift indicates that, during the Early Permian, similar climate variation (and concomitant faunal changes) took place both within basins along this rift system as well as those represented in Sibumasu and Lhasa. Environmental differences, for example peculiar conditions in the estuarine-like marginal rift basins in Western Australia, may explain coeval faunal differences between the regions.

A more convincing indicator of the rifting of segments of Cimmeria away from Gondwana to form Mesotethys may be the cessation of subsidence in the Merlinleigh–Irwin marginal-rift basin during the Middle Permian (D to E, Figs. 1, 25) and in the Canning Basin during the Early Triassic. In the former narrow elongate basin, rift-related subsidence was initiated during the Late Pennsylvanian, reconfiguring a much broader previous interior sag, and continued during the Early Permian and Roadian with accumulation of almost 5 km of very shallow-marine sediment (Fig. 26A; Mory and Haig, 2011). No further deposition took place until a veneer of Cretaceous and Cenozoic marine deposits formed on a passive continental margin after the Early Cretaceous opening of the Indian Ocean in this region. In the Canning Basin, Kennard et al. (1994) noted that there was “extension and rapid subsidence” associated with the commencement of the glacially influenced deposition of the Grant Group (during the latest Gzhelian or earliest Asselian; Mory, 2010) and subsidence continued through the Permian. Deposition of the very shallow marine to marginal marine “Late Carboniferous to Permian Megasequence” (as designated by Kennard et al., 1994) ceased during the Early Triassic (Fig. 25B). In the onshore Canning Basin, no further major episodes of subsidence and deposition took place until latest Jurassic and Early Cretaceous marine flooding following continental breakup and Indian Ocean formation. The cessation of subsidence in these marginal rift basins during the Middle Permian and Early Triassic may have been the result of the relaxation of crustal stresses associated with progressive south to north rifting of parts of Cimmeria from the Gondwanan margin. This requires confirmation from, for example, palaeomagnetic studies or comparisons of the terrestrial flora (including spore-pollen assemblages). Marine biogeographic comparisons, often used in past studies, may be misleading unless equivalent environments are compared.

The present study together with our recent studies in the East Gondwana interior rift (Davydov et al., 2013; Haig et al., 2014) have provided us with a much broader view of the relationships between stratigraphic patterns, intracontinental rifting and climate during the Pennsylvanian and Cisuralian in this region, as well as a better understanding of the biotic changes during Cisuralian amelioration of climate following melting of the Pennsylvanian continental ice sheet.

During the Late Pennsylvanian four very significant events took place in East Gondwana:
(1) A depositional hiatus during most of the Pennsylvanian was overlain by glacially-influenced deposits (see section 4). The hiatus is probably represented also in eastern Australia successions (see correlation chart of Fielding et al., 2008, fig. 2; and note that Carboniferous radiometric dates of Roberts et al., 1995, require testing by modern CA-ID TIMS techniques). The hiatus suggests that deposition was interrupted by a widespread continental ice sheet.
(2) Initiation of intracontinental rift-basins both along major rift axes as well as smaller-scale basins splaying from axial rifts. Metcalfe (1996, p. 616, 617) noted examples of this throughout East Gondwana.
(3) Initiation of major rift-related volcanism (e.g. Roever, 1942, and Davydov et al., 2013, in Timor; Reeckmann and Mebberson, 1984, in Canning Basin; Ali et al., 2012 in Himalayan India).
(4) Abrupt warming during the late Gzhelian, global in extent, led to small coral-algal reef buildups in Timor, and to very rapid melting of the ice sheet and deposition of great thicknesses of glacially influenced sediment (deglaciation) during the Asselian and early Sakmarian in the newly created interior rifts (Davydov et al., 2013; and see Ridd, 2009 for description of rifts in Sibumasu).

A relationship between intracontinental rifting and associated volcanism and the abrupt global climate change that resulted in the melting of a large continental ice-sheet (with associated eustatic sea-level variation as well as isostatic uplift of previously covered continental areas) is possible. This needs to be considered through a global overview of Pennsylvanian–Cisuralian events that is beyond the scope of this study.

On the East Gondwanan lowlands, west of the eastern Australian orogenic belt, the continental ice sheet had melted by the late Sakmarian (Haig et al., 2014; and section 4) when warmer and drier conditions in the interior seas allowed the development of carbonate shoals with sheet-like architecture in the marginal-rift basins and larger carbonate mounds in basins along the main rift axis. In both settings the carbonate sediment was dominated by bryozoan and

crinoidal debris. In the marginal rift basins, the carbonate deposits formed at the top of shoaling-upward mud to limestone cycles during early stages of a lower frequency cycle involving early retrogradation followed by longer progradation leading to sand-dominated facies (e.g. the Callytharra–Wooramel cycle in the Merlinleigh Sub-basin; the Poole cycle in the Canning Basin; see Fig. 27).

In the marginal rift basins, the next major low-frequency cycle, of late Artinskian to Roadian age, is the Byro–Kennedy cycle in the Merlinleigh Sub-basin and the Noonkanbah–Lightjack cycle in the Canning Basin (Fig. 26). The late Artinskian to Kungurian parts of this cycle are the subject of this paper. The Kennedy Group (see Lever, 2002, 2004a, 2004b, and Lever and Fanning, 2004) and the Lightjack Formation (Mory, 2010) are of early Middle Permian age and represent the sand-dominated final progradational stage of the broader cycle. In the marginal rift basins we have documented cyclicity at various scales during the late Artinskian–Kungurian, including high frequency metre-scale cycles in a thick mudstone unit, and suggest that at least the broader cycles in this interval can be recognized across basins. A maximum marine-flooding level is present close to the Artinskian–Kungurian boundary and seems to represent maximum flooding for the entire Permian in these basins. This level coincides with a warming peak from cold conditions during the early part of the late Artinskian, and is probably coeval with fusulinid limestone found in Timor as well as the first appearance of atomodesmatinid laminites in deeper water deposits of an axial basin there. The widespread recognition of the cyclicity, and the coincidence of maximum marine flooding with a warming peak suggests that eustatic variation associated with climate change played a major role in the stratigraphic patterns. This was superimposed on what appears to have been fairly uniform subsidence (Fig. 26). Lever (2004a) suggested that cyclicity in the Kennedy Group of early Middle Permian age was controlled by "Milankovitch-scale eustatic changes". However, the available low-resolution chronometry does not allow this to be confirmed in a definitive way for the underlying late Artinskian–Kungurian section.

In the marginal rift basins, significant changes took place in the marine biota during the late Artinskian–Kungurian. There were frequent changes in the very shallow-marine sand-facies fauna, with few species reappearing in later cycles. In the marine mud facies (that accumulated below a shallow wave base) the foraminiferal faunas varied according to high-frequency changes in bathmetry, but many species reappeared when similar conditions returned to the depositional site. One of the most significant evolutionary events apparent in the depositional record here is the development of the foraminiferal Class Nodosariata. Up until the early part of the late Artinskian, nodosariid assemblages were dominated by *Protonodosaria* with simple

rounded apertures. During the latest Artinskian warming, these primitive assemblages were replaced by a plexus of morphotypes belonging to *Nodosaria* and *Pseudonodosaria* exhibiting radiate apertures.

Within the interior seas, because of the low-gradient sea floor and the very shallow wave-base determining the sand-mud interface, a relatively small change in water depth would displace sand-facies faunas over a large area. The marine sand-facies faunal record is dominated by brachiopods, and is generally based on widely separated fossiliferous beds at the top of cycles where normal-marine salinity levels were established. Perhaps the disjunct faunal record in the sand facies can be explained by temperature variations superimposed on water-depth and salinity changes.

Given the cold to warm-temperate transition during the late Artinskian, changes in the terrestrial flora in land areas adjacent to the interior seas should be apparent in the spore-pollen record from the marine mud-facies. The record in the marginal rift basins suggests that no dramatic shifts in terrestrial vegetation took place during the late Artinskian–Kungurian but spore-pollen taxonomy may not fully reflect differences among closely related land-plant species that may be adapted to different climatic conditions.

6. Conclusions

1. Marine upper Artinskian–Kungurian deposits are recognized both in basins close to the axis of the East Gondwana interior rift and in marginal rift basins that splayed from the main rift axis. The major depocentres are in rifts that were initiated during the late Pennsylvanian. Northern basins along the main axis of the rift system have a fully marine upper Artinskian–Kungurian succession, whereas coeval deposits further south in the southern Perth Basin are entirely fluvial.

2. In the northern part of the East Gondwana interior rift in Timor, the Bua-bai limestone was deposited as a small bryozoan-crinoidal mound on a shallow-water shelf during the latest Artinskian. Larger fusulines, together with *Tubiphytes* and rare solenoporacean and dasycladacean algae indicate warm conditions. The diversity of these groups suggests that the depositional site was probably near southern limits of their biogeographic distributions. Disrupted sections make it difficult to assess depositional trends in coeval siliciclastic and volcaniclastic units of the Cribas Group. These indicate a probable increase in water depth close to the Artinskian–Kungurian boundary. Kungurian sandstones display features suggesting deposition from density currents and suggest a shelf-to-basin depositional system.

3. The Canning Basin is a marginal-rift basin in northern Western Australia about 1000 km south of Timor. During the late Artinskian–Kungurian the Noonkanbah Formation was deposited in a very shallow sea with low-gradient sea floor and with variable estuarine-like water conditions. The formation includes the maximum marine flooding interval, close to the Artinskian–Kungurian boundary, for the entire Permian succession in the basin. Rare *Tubiphytes*, conodonts, and brachiopods with Tethyan affinities indicate warm to warm-temperate conditions. Water quality in the interior sea may have influenced the diversity of the biota. A significant change in the foraminiferal Class Nodosariata took place during maximum marine flooding with a modern-type *Nodosaria-Pseudonodosaria* assemblage displacing an older *Protonodosaria* assemblage. Brachiopods of the shallow-water sand facies, found in relatively few beds in the formation, change frequently up section, whereas only moderate change is observed among the Foraminifera of the mud facies. Terrestrial spore-pollen assemblages also show only moderate change up-section.

4. About 1000 km southwest of the Canning Basin, in the Southern Carnarvon Basin, the Merlinleigh and Byro sub-basins form a narrow marginal rift that continues south to the Irwin Terrace in the northern Perth Basin. Late Artinskian–Kungurian deposition (Byro Group) took place in a very shallow sea with very low gradient sea floor and with variable estuarine-like water conditions. In the Merlinleigh and Byro sub-basins, the Byro Group displays distinct cyclicity on various scales. Five major depositional cycles are recognized with maximum marine flooding during cycle 2 (upper Bulgadoo Shale, close to the Artinskian–Kungurian boundary). Distinct warming is indicated by dropstones in the early part of cycle I (early late Artinskian), disappearing later in cycle I, and the influx of brachiopods with Tethyan affinities during cycle II (close to the Artinskian–Kungurian boundary). The changeover in nodosariid assemblages, similar to that recognized in the Canning Basin, takes place between cycles I and II. Marine macrofossil assemblages are known from only a few beds in each formation; foraminifera are persistent in mud facies that accumulated below a shallow wave base. In a comparison of entire fossil assemblages from each major depositional cycle, brachiopods, crinoids and corals of the shallow-water sand facies show low similarity between cycles, foraminifera of the mud facies (below storm-wave base) show only moderate change, and terrestrial spore-pollen show moderate change.

5. In the northern Perth Basin, the Irwin Terrace is contiguous with the Merlinleigh–Byro rift of the Southern Carnarvon Basin. Here the upper Artinskian–Kungurian includes the Caryginia Formation that was deposited under marginal-marine conditions. Warming during the late Artinskian is indicated by the presence of dropstones in the lower part of the formation but none

higher in the formation. In the Dandaragan Trough to the west, closer to the axis of the East Gondwana interior rift, the Carynginia Formation is known only from the subsurface. Based on a study of isolated cores, a more open-marine mud facies is present in the upper part of Carynginia Formation, either upper Artinskian or lower Kungurian, compared with the lower part of the unit (lower part of upper Artinskian).

6. In the East Gondwana interior rift system, within the limits of present knowledge, it appears that similar patterns of warming and bathymetric change took place during the late Artinskian–Kungurian in all basins. During the early late Artinskian cool conditions prevailed, with water temperatures 0–4°C allowing sea ice in the Merlinleigh–Byro–Irwin rift. Rapid warming during the latter part of the late Artinskian was accompanied by maximum marine flooding close to the Artinskian–Kungurian boundary. Climatic and bathymetric conditions then allowed carbonate-mounds with larger fusulines and a variety of algae to develop in the northern part of the rift system, and *Tubiphytes*, conodonts, and brachiopods with Tethyan affinities to migrate into the marginal-rift basins despite the generally adverse water quality at these depositional sites.

7. The widespread recognition of depositional cyclicity in the marginal rift basins, and the coincidence of maximum marine flooding with a warming peak, suggests that eustatic variation associated with climate change played a major role in the stratigraphic patterns. The eustatic responses were superimposed on relatively uniform tectonic subsidence.

8. Across East Gondwana, similar broad patterns of Carboniferous to Cisuralian climate change are recognized between records from the East Gondwana interior rift, Lhasa and Sibumasu. The Eastern Australian record is confused by uncertain stratigraphic relationships there, but probably follows a similar pattern. The eight major conclusions drawn from this study indicate that significant tectonic, climate, and marine-flooding events took place during the late Artinskian–Kungurian in East Gondwana. This record provides a basis for global comparisons that may lead to a better understanding of the Permian climate system.

7. List of Appendices

Data on which this paper is founded are recorded in the following appendices presented in the Supplementary Material attached to the article.

Appendix 1. Studied material and localities.

Appendix 2. Distribution of biogenic grain types found in studied samples of the Bua-bai limestone, Timor-Leste.

Appendix 3. Distribution of Foraminifera found in studied samples of the Bua-bai limestone, Timor-Leste.

Appendix 4. Distribution of Bryozoa found in studied samples of the Bau-bai limestone at the type locality.

Appendix 6. Notes on *Praeskinnerella* from the Bua-bai limestone.

Appendix 5. Description of samples from Permian outcrop along the Sumasse River. (samples listed from north to south as shown in Fig. 4B).

Appendix 7. Notes on *Mesogondolella* from the Cribas Group.

Appendix 8. Distribution of Foraminifera found in studied samples of the Cribas Group in type area. along Sumasse River, Timor-Leste.

Appendix 9. Distribution of biogenic grain types found in studied samples of the Cribas Group in type area along Sumasse River, Timor-Leste.

Appendix 10. Distribution of biogenic grain types found in samples studied from the Liveringa Ridge outcrop section through the Noonkanbah Formation, Canning Basin, Western Australia.

Appendix 11. Distribution of Foraminifera found in samples studied from the Liveringa Ridge outcrop section through the Noonkanbah Formation, Canning Basin, Western Australia.

Appendix 12. Distribution of biogenic grain types found in samples studied from the BHP PND-1 bore-section continuously cored through the Noonkanbah Formation, Canning Basin, Western Australia.

Appendix 13. Distribution of Foraminifera found in samples studied from the BHP PND-1 bore-section continuously cored through the Noonkanbah Formation, Canning Basin, Western Australia.

Appendix 14. Distribution of palynomorphs found in samples studied from the BHP PND-1

bore-section continuously cored through the Noonkanbah Formation, Canning Basin, Western Australia.

Appendix 15. List of marine fossils (excluding palynomorphs) known from the Noonkanbah Formation, Canning Basin, Western Australia (updated from Skwarko, 1993)

Appendix 16. Distribution of brachiopods in sandstone-packstone beds exposed in the type section of the Noonkanbah Formation in the Bruten Yard area, Canning Basin, Western Australia. Species nomenclature follows that originally used by Thomas (1954).

Appendix 17. List of marine fossils (excluding palynomorphs) known from Cycle II (Bulgadoo Shale and Cundlego Formation) in the Byro Group of the Southern Carnarvon Basin, Western Australia; updated from Skwarko (1993). Appendix 18. Distribution of biogenic grain types in studied samples of the Byro Group, Southern Carnarvon Basin, Western Australia.

Appendix 19. Distribution of Foraminifera in studied samples of the Byro Group, Southern Carnarvon Basin, Western Australia.

Appendix 20. Summary distribution of Brachiopoda present in the major sedimentary cycles I, II, III-IV, V of the Byro Group, Southern Carnarvon Basin, Western Australia. Cycles III and IV cannot be separated in the known distribution records which have been updated from Skwarko (1993).

Appendix 21. Summary distribution of crinoids and corals present in the major sedimentary cycles I, II, III-IV, V of the Byro Group, Southern Carnarvon Basin, Western Australia. Cycles III and IV cannot be separated in the known distribution records which have been updated from Skwarko (1993).

Appendix 22. Distribution of Foraminifera and other biogenic grain types in studied samples of the Carynginia Formation, northern Perth Basin.

Appendix 23. Palynomorphs from 40 cm above base (sample 27/7/14-1; Appendices 1, 20) of the Carynginia Formation in an outcrop section in the South Branch of the Irwin River, Irwin Terrace, northern Perth Basin.

Appendix 24. Climate trends across the East Gondwana lowlands during the Mississippian to Cisuralian. Annotations 1–16 related to numbers adjacent columns in Fig. 25.

8. References

Al-Hinaai, J., Redfern, J., 2015. Tectonic and climatic controls on the deposition of the Permo-Carboniferous Grant Group and Reeves Formation in the Fitzroy Trough, Canning Basin, Western Australia. Marine and Petroleum Geology 59, 217–231.

Ali, J.R., Aitchison, J.C., Chik, S.Y.S., Baxter, A.T., Bryan, S.E., 2012. Paleomagnetic data support Early Permian age for the Alor Volcanics in the lower Siang Valley, NE India: Significance for Gondwana-related break-up models. Journal of Asian Earth Sciences 50, 105–115.

Archbold, N.W., 1998a. Correlations of the Western Australian Permian and Permian ocean circulation patterns. Proceedings of the Royal Society of Victoria 110, 85–106.

Archbold, N.W., 1998b. Marine biostratigraphy and correlation of the west Australian Permian basins. In: Purcell, P.G., Purcell, R.R. (Eds.), The sedimentary basins of Western Australia 2. Petroleum Exploration Society of Australia; Western Australian Basins Symposium, Perth, WA, 1998, Proceedings, 141– 151.

Archbold, N.W., 1999. Permian Gondwanan correlations: the significance of the western Australian marine Permian. Journal of African Earth Sciences 29, 63–75.

Archbold, N.W., 2000. Palaeobiogeography of the Australasian Permian. Memoirs of the Association of Australasian Palaeontologists 23, 287–310.

Archbold, N.W., Shi, G.R., 1995. Permian brachiopod faunas of Western Australia: Gondwanan-Asian relationships and Permian climate. Journal of Southeast Asian Earth Sciences 11, 207–215.

Archbold, N.W., Shi, G.R., 1996. Western Pacific Permian marine invertebrate palaeobiogeography: Australian Journal of Earth Sciences 43, 635–641.

Audley-Charles, M.G., 1968. The geology of Portuguese Timor. Geological Society of London, Memoir 4, 1–75.

Backhouse, J., 1991. Permian palynostratigraphy of the Collie Basin, Western Australia. Review of Palaeobotany and Palynology 67, 237–314.

Backhouse, J., 1993. Palynology and correlation of Permian sediments in the Perth, Collie, and Officer Basins, Western Australia. Geological Survey of Western Australia Report 34, 111–128.

Belford, D.J., 1968, Permian Foraminifera from BMR Bores 6, 7, 8, and 9, Western Australia. Australian Bureau of Mineral Resources, Geology and Geophysics, Bulletin 80, 1–13.

Bennett, M.R., Doyle, P., Mather, A.E., 1996. Dropstones: their origin and significance. Palaeogeography, Palaeoclimatology, Palaeoecology 121, 331–339.

Bird, P.R., Cook, S.E., 1991. Permo-Triassic successions of the Kekneno area, West Timor: implications for palaeogeography and basin evolution. Journal of Southeast Asian Earth Sciences 6, 359–371.

Boiko, M.S., Leonova, T.B., Mu Lin, 2008. Phylogeny of the Permian Family Metalegoceratidae (Goniatitida, Ammonoidea). Paleontological Journal 42, 585–595.

Campbell, H.J., 2000. The marine Permian of New Zealand. In: Yin, H., Dickins, J.M., Shi, G.R., Tong, J. (Eds.), Permian-Triassic Evolution of Tethys and Western Circum-Pacific. Elsevier Science B.V., 111–125.

Carr, P.F., Jones, B.G., Middleton, R.G., 1989. Australian Mineralogist 4, 3–12.

Chamalaun, F.H., 1977. Paleomagnetic evidence for the relative positions of Timor and Australia in the Permian. Earth and Planetary Science Letters 34, 107– 112.

Charlton, T.R., Barber, A.J., Harris, R.A., Barkham, S.T., Bird, P.R., Archbold, N.W., Morris, N.J., Nicoll, R.S., Owen, H.G., Owens, R.M., Sorauf, J.E., Taylor, P.D., Webster, G.D., Whittaker, J.E., 2002. The Permian of Timor: stratigraphy, palaeontology and palaeogeography 20, 719–774.

Clapp, F.G., 1925. A few observations on the geology and geography of the Northwest and Desert Basins, Western Australia. Proceedings of the Linnean Society of New South Wales 50, 47–66.

Clarke, E. de C., Prendergast, K.L., Teichert, C., Fairbridge, R.W., 1951. Permian succession and structure in the northern part of the Irwin Basin, Western Australia. Journal of the Royal Society of Western Australia 35, 31–84.

Condon, M.A., 1967. The geology of the Carnarvon Basin, Western Australia. Part 2: Permian stratigraphy. Bureau of Mineral Resources, Geology and Geophysics, Australia, Bulletin 77, 1–191.

Crespin, I., 1958. Permian Foraminifera of Australia. Australian Bulletin of the Bureau of Mineral Resources, Geology and Geophysics, 48, 1–207.

Crockford, J., 1957. Permian Bryozoa from the Fitzroy Basin, Western Australia. Australian Bulletin of the Bureau of Mineral Resources, Geology and Geophysics, 34, 1–136.

Crowe, R.W. A., Towner, R.R., 1976a. Environmental interpretation of the Permian Nura Nura Member of the Poole Sandstone, Noonkanbah sheet area, Canning Basin: a gradation between fluviatile and shallow water marine facies. Western Australia Department of Mines, Annual Report for 1975, 59–62.

Crowe, R.W.A., Towner, R.R., 1976b. Permian Depositional History of the Noonkanbah 1:250,000 Sheet Area. Australian Bureau of Mineral Resources, Geology and Geophysics, Record 1976/24, 1–50.

Crowell, J.C., Frakes, L.A., 1971a. Late Paleozoic glaciation: Part IV, Australia. Geological Society of America Bulletin 82, 2515–2540.

Crowell, J.C., Frakes, L.A., 1971b. Late Palaeozoic glaciation of Australia. Journal of the Geological Society of Australia 17, 115–155.

Damborenea, S.E., Echevarría, J., Ros-Franch, S., 2013. Southern Hemisphere palaeobiogeography of Triassic–Jurassic marine bivalves. Springer, Dordrecht.

David, T.W.E. and Sussmilch, C.A., 1931. Upper Paleozoic glaciations of Australia. Bulletin of the Geological Society of America 42, 481–522.

David, T.W.E., Sussmilch, C.A., 1933. The Carboniferous and Permian periods in Australia. Report of the XVI International Geological Congress, Washington, 1933, 629–644.

Davydov, V.I., Haig, D.W., McCartain, E., 2013. A latest Carboniferous warming spike recorded by a fusulinid-rich bioherm in Timor Leste: Implications for East Gondwana deglaciation. Palaeogeography, Palaeoclimatology, Palaeoecology 376, 22–38.

Davydov, V.I., Haig, D.W., McCartain, E., 2014. Latest Carboniferous (Late Gzhelian) fusulinids from Timor Leste and their paleobiogeographic affinities. Journal of Paleontology 88, 588–605.

Dent, L., 2016. Facies analysis of Lower Permian strata, Canning Basin, Western Australia and implications for CO_2 sequestration. Geological Survey of Western Australia Report 149, 1–104.

Dickins, J.M., 1978. Climate of the Permian in Australia: The invertebrate faunas. Palaeogeography, Palaeoclimatology, Palaeoecology 23, 33–46.

Dickins, J.M., 1993. Palaeoclimate. Bulletin of the Geological Survey of Western Australia 136, 7–9.

Dickins, J.M. 1996. Problems of a late Palaeozoic glaciation in Australia and subsequent climate in the Permian. Palaeogeography, Palaeoclimatology, Palaeoecology 125, 185–197.

Dionne, J-C., 1993. Sediment load of shore ice and ice rafting potential, upper St. Lawrence Estuary, Québec, Canada. Journal of Coastal Research 9, 628–646.

Dixon, M., Haig, D.W., 2004. Foraminifera and their habitats within a cool-water carbonate succession following glaciation, Early Permian (Sakmarian), Western Australia. Journal of Foraminiferal Research 34, 308–324.

Draper, J. J., 2013. 5.8 Bowen Basin. In Jell, P.A. (ed.), Geology of Queensland. Geological Survey of Queensland, Brisbane, 371–384.

Dumas, S., Arnott, R.W.C., 2006. Origin of hummocky and swaley cross-stratification — The controlling influence of unidirectional current strength and aggradation rate. Geology 34, 1073–1076.

Ernst, A., 2016. Bryozoan fauna from the Permian (Artinskian–Kungurian) Zhongba Formation of southwestern Tibet. Palaeontologia Electronica 19.215A, 1–59.

Ernst, A., Weidlich, O., Schäfer, P., 2008. Stenolaemate Bryozoa from the Permian of Oman. Journal of Paleontology 82, 676–716.

Ernst, A., Gorgij, M.N., 2013. Lower Permian bryozoan faunas from Kalmard area, central Iran. Neues Jahrbuch für Geologie und Paläontologie, Abhandlungen 268, 275–324.

Eyles, C.H., Eyles, N., 2000. Subaqueous mas flow origin for Lower Permian diamictites and associated facies of the Grant Group, Barbwire Terrace, Canning Basin, Western Australia. Sedimentology 47, 343–356.

Eyles, N., Eyles, C.H., Apak, N., Carlsen, G.M., 2001. Permian–Carboniferous tectono-stratigraphic evolution and petroleum potential of the northern Canning Basin, Western Australia. The American Association of Petroleum Geologists, Bulletin 85, 989–1006.

Eyles, N., Mory, A.J., Backhouse, J., 2002. Carboniferous–Permian palynostratigraphy of west Australian marine rift basins: resolving tectonic and eustatic controls during Gondwanan glaciations. Palaeogeography, Palaeoclimatology, Palaeoecology 184, 305–319.

Eyles, C.H., Mory, A.J., Eyles, N., 2003. Carboniferous–Permian facies and tectono-stratigraphic succession of the glacially influenced and rifted Carnarvon Basin, Western Australia. Sedimentary Geology 155, 63–86.

Eyles, N., Mory, A.J., Eyles, C.H., 2006. 50-million-year-long record of glacial to postglacial marine environments preserved in a Carboniferous-Lower Permian graben, northern Perth Basin, Western Australia. Journal of Sedimentary Research 76, 618–632.

Fielding, C.R., Frank, T.D., Birgenheier, L.P., Rygel, M.C., Jones, A.T., Roberts, J., 2008. Stratigraphic record and facies associations of the late Paleozoic ice age in eastern Australia (New South Wales and Queensland). The Geological Society of America Special Publication 441, 41–57.

Filimonova, T.V., 2010. Smaller foraminifers of the Lower Permian from Western Tethys. Stratigraphy and Geological Correlation 18, 687–811.

Filimonova, T.V., 2015. New species of the Order Nodosariida from the Kungurian–Ufimian (Permian) of the Kolyma–Omolon region (northeastern Russia). Paleontological Journal 49, 1–9.

Forman, D.J., Wales, D.W., 1981. Geological evolution of the Canning Basin, Western Australia: Bureau of Mineral Resources, Australia, Bulletin 210, 1–91.

Foster, C.B., Palmieri, V., Fleming, P.J.G., 1985. Plant microfossils, Foraminiferida, and Ostracoda, from the Fossil Cliff Formation (Early Permian, Sakmarian), Perth Basin,Western Australia. Special Publication of the South Australian Department of Mines and Energy 5, 61–105.

Frank, T.D., Pritchard, J.M., Fielding, C.R., Mory, A.J., 2012. Cold-water carbonate deposition in a high-latitude, glacially influenced Permian seaway (Southern Carnarvon Basin, Western Australia). Australian Journal of Earth Sciences 59, 479–494.

Frank, T.D., Shultis, A.I., Fielding, C.R., 2015. Acme and demise of the late Palaeozoic ice age: A view from the southeastern margin of Gondwana. Palaeogeography, Palaeoclimatology, Palaeoecology 418, 176–192.

Gageonnet, R., Lemoine, M., 1958. Contribution à la connaissance de la géologie de la province Portugaise de Timor. Estudos, Ensaios e Documentos, Junta de Investigações do Ultramar, 48 pp. 1–138.

Gerke, A.A., 1961. Foraminifery permskikh, triasovykh i leyasovykh otlozheniy neftenosnykh rayonov Severa Tsentral'noy Sibiri. Trudy - Institut Geologii i Mineral'nykh Resursov Mirovogo Okeana, VNII Okeangeologiya, 120, 1–519.

Glenister, B.F., Rogers, F.S., Skwarko, S.K., 1993. Ammonoids. Bulletin of the Geological Survey of Western Australia 136, 54–63.

Gorter, J., 2002. Why are there no Glendonites in the Western Australian Permian. PESA News 55, p. 38.

Gorter, J.D., Poynter, S.E., Bayford, S.W., Caudullo, A., 2008. Glacially influenced petroleum plays in the Kulshill Group (Late Carboniferous Early Permian) of the southeastern Bonaparte Basin, Western Australia. The APPEA Journal 48, 69–113.

Grozdilova, L.P., 1956. Miliolidae of the upper Artinskian (Lower Permian) of the western slope of the Urals [in Russia] All-Union Petroleum Scientific Research Geological Prospecting Institute, Trudy n.s., 8, 521–532.

Grunau, H.R., 1956. Zur Geologie von Portugiesisch-Ost-Timor. Mitteilungen der Naturforschenden Gesellschaft in Bern, Neue Folge, 13, X1–XVIII.

Grunau, H.R., 1957. Neue Daten zur Geologie von Portugiesisch Osttimor. Eclogae Geologicae Helvetiae 50, 70–97.

Guppy, D.J., Lindner, A.W., Rattigan, J.H., Casey, J.N., 1958. The geology of the Fitzroy Basin, Western Australia. Bulletin of the Bureau of Mineral Resources, Geology and Geophysics, Australia, 36, 116 p.

Hagen, D., Kempler, E., 1976. Geology of the Thong Pha Phum area (Kanchanaburi Province, West Thailand). Geologisches Jahrbuch, Reiche B, 21, 53–91.

Haig, D.W., 2003. Palaeobathymetric zonation of foraminifera from lower Permian shale deposits of a high-latitude southern interior sea. Marine Micropaleontology 49, 317–334.

Haig, D.W., 2004. Comparison of foraminifera and habitats from Australian Permian and Cretaceous Interior Seas. Memoirs of the Association of Australasian Palaeontologists 29, 31–46.

Haig, D.W., 2012. Palaeobathymetric gradients across Timor during 5.7–3.3 Ma (latest Miocene–Pliocene) and implications for collision uplift. Palaeogeography, Palaeoclimatology, Palaeoecology 331–332, 50–59.

Haig, D.W., Bandini, A.N., 2013. Middle Jurassic Radiolaria from a siliceous argillite block in a structural melange zone near Viqueque, Timor Leste: Paleogeographic implications. Journal of Asian Earth Sciences 75, 71–81.

Haig, D.W., McCartain, E., Barber, L., Backhouse, J., 2007. Triassic-Lower Jurassic foraminiferal indices for Bahaman-type carbonate bank limestones, Cablac Mountain, East Timor. Journal of Foraminiferal Research 37, 248–264.

Haig, D.W., McCartain, E., Mory, A.J., Borges, G., Davydov, V., Dixon, M., Ernst, A., Groflin, S., Håkansson, E., Keep, M., Dos Santos, Z., Shi, G.R., Soares, J., 2014. Postglacial Early Permian (late Sakmarian–early Artinskian) shallow-marine carbonate deposition along a 2000 km transect from Timor to west Australia. Palaeogeography, Palaeoclimatology, Palaeoecology 409, 180–204.

Hamilton, W., 1979. Tectonics of the Indonesian region. U.S. Geological Survey Professional Paper 1078, 1–335.

Haniel, C.A., 1915. Die Cephalopoden der Dyas von Timor. Paläontologie von Timor 3, 1–153.

Harris, R., Kaiser, J., Hurford, A., Carter, A., 2000. Thermal history of Australian passive margin cover sequences accreted to Timor during Late Neogene arc-continent collision, Indonesia. Journal of Asian Earth Sciences 18, 47–69.

Harris, R.A., Sawyer, R.K., Audley-Charles, M.G., 1998. Collisional melange development: Geological associations of active melange-forming processes with exhumed melange facies in the western Banda orogen, Indonesia. Tectonics 17, 458–479.

Harrowfield, M., Holdgate, G., Wilson, C.J.L., McLoughlin, S., 2005. Tectonic significance of the Lambert graben, East Antarctica: reconstructing the Gondwanan rift. Geology 33, 197–200.

Heine, C., Müller, R.D., 2005. Late Jurassic rifting along the Australian North West Shelf: margin geometry and spreading ridge configuration. Australian Journal of Earth Sciences 52, 27–39.

Henderson, C.M., Davydov, V.I., Wardlaw, B.R., 2012. Chapter 24, The Permian Period. In: Gradstein, F.M., Ogg, J., Schmitz, M., Ogg, G. (Eds.), The Geologic Time Scale 2012. Elsevier, Amsterdam.

Henderson, C.M., Mei, S., 2007. Geographical clines in Permian and lower Triassic gondolellids and its role in taxonomy. Palaeoworld 16, 190–201.

Hocking, R.M., Moore, P.S., Moors, H.T., 1980. Modified stratigraphic nomenclature and concepts in the Palaeozoic sequence of the Carnarvon Basin, W.A. Geological Survey of Western Australia Annual Report 1979, 51–55.

Hocking, R.M., Moors, H.T., Van De Graaff, J.E., 1987. Geology of the Carnarvon Basin, Western Australia. Geological Survey of Western Australia Bulletin 133, 1–289.

Hüneke, H., Joachimski, M., Buggisch, W., Lützner, H., 2001. Marine carbonate facies in response to climate and nutrient level: The Upper Carboniferous and Permian of central Spitsbergen (Svalbard). Facies 45, 93–136.

Iasky, R.P., Mory, A.J., Ghori, K.A.R., Shevchenko, S.I., 1998. Structure and petroleum potential of the southern Merlinleigh Sub-basin, Carnarvon Basin, Western Australia. Geological Survey of Western Australia Report 61, 1–39.

Isbell, J.I., Miller, M.F., Wolfe, K.L., Lenaker, P.A., 2003. Timing of late Paleozoic glaciation in Gondwana: Was glaciation responsible for development of northern hemisphere cyclothems? Geological Society of America Special Paper 370, 5–24.

Kaminski, M.A., Gradstein, F.M., 2012. Atlas of Paleogene Cosmopolitan Deep Water Agglutinated Foraminifera. http://www.nhm2.uio.no/norges/atlas/

Karavaeva, N.I., Nestell, G.P., 2007. Permian foraminifers of the Omolon Massif, northeastern Siberia, Russia. Micropaleontology 53, 161–211.

Kauffmann, E.G., Runnegar, B., 1975. Atomodesma (Bivalvia), and Permian species of the United States. Journal of Paleontology 49, 23–41.

Keane, M., 1999. Sequence stratigraphy, palaeontology and depositional environment of the middle Byro Group: Tools for analysing the evolution of Merlinleigh Sub-basin, Western Australia. University of Western Australia, B.Sc. Honours Thesis, 105 p.

Keep, M., Haig, D.W., 2010. Deformation and exhumation in Timor: Distinct stages of a young orogeny. Tectonophysics 483, 93–111.

Kennard, J.M., Jackson, M.J., Romine, K.K., Shaw, R.D., Southgate, P.N., 1994. Depositional sequences and associated petroleum systems of the Canning Basin, W.A. In: Purcell, P.G., Purcell, R.R. (Eds.), The sedimentary basins of Western Australia. Petroleum Exploration Society of Australia; Western Australian Basins Symposium, Perth, WA, 1994, Proceedings, 657–676.

Kireyeva, G.D., 1958. On the age of the Copper Sandstone Formation of the Donbas and the foraminifera occurring in it [in Russian]. USSR Research Institute for Geological Prospecting (VNIGNI), Trudy VNIGNI, Moscow, 9, 157–176.

Korte, C., Jones, P.J., Brand, U., Mertmann, D., Veizer, J., 2008. Oxygen isotope values from high-latitudes: Clues for Permian sea-surface temperature gradients and Late Palaeozoic deglaciation. Palaeogeography, Palaeoclimatology, Palaeoecology 269, 1–16.

Langhi, L., Borel, G.D., 2005. Influence of the Neotethys rifting on the development of the Dampier Sub-basin (North West Shelf of Australia), highlighted by subsidence modelling. Tectonophysics 397, 93–111.

Laurie, J.R., Bodorkos, S., Nicoll, R.S., Crowley, J.L., Mantle, D., Mory, A.J., Wood, G.R., Backhouse, J., Holmes, E.K., Smith, T.E., Champion, D.C., 2016. Calibrating the Middle and Late Permian palynostratigraphy of Australia to the geologic time scale via U-Pb zircon CA-IDTIMS dating. Australian Journal of Earth Science, doi:10.1080/08120099.2016.1233456

Le Blanc Smith, G., Kristensen, S., 1998. Geology and Permian coal resources of the Vasse River Coalfield, Perth Basin, Western Australia. Geological Survey of Western Australia Record 1998/7, 1–49.

Le Blanc Smith, G., Mory, A.J., 1995. Geology and Permian coal resources of the Irwin Terrace, Perth Basin, Western Australia. Geological Survey of Western Australia Report 44, 1–60.

Lehmann, P.R., 1967. Kennedy Range No. 1 well completion report, West Australian Petroleum Pty. Limited. Geological Survey of Western Australia file W322A1, WAPIMS database (https://wapims.dmp.wa.gov.au/wapims).

Leonova, T.B., 2011. Permian ammonoids: biostratigraphic, biogeographical, and ecological analysis. Paleontological Journal 45, 1206–1312.

Leven, E., 1993. Early Permian fusulinids from the Central Pamir. Rivista Italiana di Paleontologia e Stratigrafia 99, 151–198.

Leven, E.Ja., Gorgij, M.N., 2007. Fusulinids of the Khan formation (Kalmard region, eastern Iran) and some problems of their paleobiogeography. Russian Journal of Earth Sciences 9, ES1004, doi:10.2205/2007ES000219.

Leven, E.Ja., Gorgij, M.N., 2011a. The Kalaktash and Halvan assemblages of Permian fusulinids from the Padeh and Sang-Variz sections (Halvan Mountains, Yazd Province, Central Iran). Stratigraphy and Geological Correlation 19, 141–159.

Leven, E Ja, Gorgij, M.N., M.N., 2011b. Fusulinids and stratigraphy of the Carboniferous and Permian in Iran. Stratigraphy and Geological Correlation 19, 687–776.

Lever, H., 2002. Stratigraphy of the Upper Permian Kennedy Group of the onshore Carnarvon Basin (Merlinleigh Sub-basin), Western Australia. Australian Journal of Earth Sciences 49, 539–550.

Lever, H., 2004a. Climate Changes and Cyclic Sedimentation in the Mid-Late Permian: Kennedy Group, Carnarvon Basin, Western Australia. Gondwana Research, 7, 135–142.

Lever, H., 2004b. Cyclic sedimentation in the shallow marine Upper Permian Kennedy Group, Carnarvon Basin, Werstern Australia. Sedimentary Geology 172, 187–209.

Lever, H., Fanning, C.M., 2004. Alunite alteration of tuffaceous layers and zircon dating, Upper Permian Kennedy Group, Carnarvon Basin, Western Australia. Australian Journal of Earth Sciences 51, 189–203.

Lindsay, J.F., 1997. Permian postglacial environments of the Australian Plate. In: Martini, I. P. (Ed.), Late glacial and postglacial environmental changes: Quaternary, Carboniferous-Permian, and Proterozoic. Oxford University Press, New York, 213–229.

Lowenstam, H.A., 1964. Palaeotemperatures of the Permian and Cretaceous Periods. In A.E.M. Nairn (ed.), Problems in Palaeoclimatology. Interscience, London, 227–248.

Lucas, S.G., Krainer, K., Vachard, D., 2015. The Lower Permian Hueco Group, Robledo Mountains, New Mexico (U.S.A.). New Mexico Museum of Natural History and Science Bulletin 65, 43–95.

MacNeill, M.D., Marshall, N., 2015. A Permian-Early Triassic deep shelf system along the NWS Margin with oil-prone potential. AAPEA Abstract 2209970.

MacTavish, R.A., 1965. Completion report BMR 10 and 10A Beagle Ridge Western Australia. Australian Bureau of Mineral Resources, Geology and Geophysics, Report 80, 1–39.

Maitland, A.G., 1912. Relict of the Permo-Carboniferous ice age in Western Australia: Presidential address. Journal of the Natural History & Science Society of Western Australia, 4, 12–29.

McCartain, E., Backhouse, J., Haig, D., Balme, B., Keep, M., 2006. Gondwana-related Late Permian palynoflora, foraminifers and lithofacies from the Wailuli Valley, Timor Leste. Neues Jahrbuch für Geologie und Paläontologie, Abhandlungen 240, 53–80.

Mei, S., Henderson, C.M., 2002. Comments on some Permian conodont faunas reported from Southeast Asia and adjacent areas and their global correlation. Journal of Asian Earth Sciences 20, 599–608.

Metcalfe, I., 1980. Palaeontology and age of the Panching Limestone, Pahang, West Malayasia. Geology and Palaeontology of Southeast Asia 21, 11–17.

Metcalfe, I., 1984. Stratigraphy, palaeontology and palaeogeography of the Carboniferous of Southeast Asia. Memoires de la Societe Geologique de France 147, 107–118.

Metcalfe, I., 1996. Gondwanaland dispersion, Asian accretion and evolution of eastern Tethys. Australian Journal of Earth Sciences 43, 605–623.

Metcalfe, I., 2006. Palaeozoic and Mesozoic tectonic evolution and palaeogeography of East Asian crustal fragments: The Korean Peninsula in context. Gondwana Research 9, 24–46.

Metcalfe, I., 2013a. Gondwana dispersion and Asian accretion: Tectonic and palaeogeographic evolution of eastern Tethys. Journal of Asian Earth Science 66, 1–31.

Metcalfe, I., 2013b. Tectonic evolution of the Malay Peninsula. Journal of Asian Earth Sciences 76, 195– 213.

Metcalfe, I., Crowley, J.L., Nicoll. R.S., Schmitz, M., 2015. High-precision U-Pb CA-TIMS calibration of Middle Permian to Lower Triassic sequences, mass extinction and extreme climate-change in eastern Australian Gondwana. Gondwana Research 28, 61–81.

Mii, H-s., Shi, G.R., Cheng, C-j., Chen, Y-y., 2012. Permian Gondwanaland paleoenvironment inferred from carbon and oxygen isotope records of brachiopod fossils from Sydney Basin, southeast Australia. Chemical Geology 291, 87–103.

Mii, H-s., Shi, G.R., Wang, C-a., 2013. Late Paleozoic middle-latitude Gondwana environment-stable isotope records from Western Australia. Gondwana Research, 24, 125–138.

Moore, P.S., Denman, P.D., Hocking, R.M., 1980. Sedimentology of the Byro Group (Lower Permian), Carnarvon Basin), Western Australia. Geological Survey of Western Australia Annual Report 1979, 55–64.

Moore, P.S., Hocking, R.M., 1983. Significance of hummocky cross-stratification in the Permian of the Carnarvon Basin, Western Australia. Journal of the Geological Society of Australia 30, 323–331.

Mory, A.J. 2010. A review of mid-Carboniferous to Triassic stratigraphy, Canning Basin, Western Australia. Geological Survey of Western Australia Report 107, 1–130.

Mory, A.J., Backhouse, J., 1997. Permian stratigraphy and palynology of the Carnarvon Basin, Western Australia. Geological Survey of Western Australia Report 51, 1–42.

Mory, A.J., Crowley, J., Nicoll, R.S., Metcalfe, I., Mantle, D., Mundil, R., Backhouse, J., 2012. Wordian (Middle Permian) U-Pb CA-IDTIMS isotopic ages from the Lightjack Formation, Canning Basin,Western Australia. Proceedings of the 34th International Geological Congress 2012. Brisbane, Australian Geosciences Council, p. 3386.

Mory, A.J., Haig, D.W., 2011. Permian–Carboniferous geology of the northern Perth and Southern Carnarvon Basins, Western Australia — a field guide. Geological Survey of Western Australia Record 2011/14, 1–65.

Mory, A.J., Haines, P.W., 2013. A Paleozoic perspective of Western Australia. West Australian Basins Symposium, Perth, WA, 18-21 August 2013, Petroleum Exploration Society of Australia, 25 p.

Mory, A.J., Hocking, R.M., 2011. Permian, Carboniferous and Upper Devonian geology of the northern Canning Basin, Western Australian — a field guide. Geological Survey of Western Australia Record 2011/16, 1–36.

Mory, A.J., Iasky, R.P., 1996. Stratigraphy and structure of the onshore northern Perth Basin, Western Australia. Geological Survey of Western Australia Report 46, 1–101.

Mory, A.J., Nicoll, R.S., Gorter, J.D., 1998. Lower Palaeozoic correlations and thermal maturity, Carnarvon Basin, WA. In: Purcell, P.G., Purcell, R.R. (Eds.), The sedimentary basins of Western Australia 2. Petroleum Exploration Society of Australia; Western Australian Basins Symposium, Perth, WA, 1998, Proceedings, 599–611.

Mory, A.J., Redfern, J., Martin, J.R., 2008. A review of Permian–Carboniferous glacial deposits in Western Australia. Geological Society of America, Special Paper 441, 29–40.

Nicoll, R.S., Metcalfe, I., 1998. Early and Middle Permian conodonts from the Canning and Southern Carnarvon Basins, Western Australia: Their implications for regional

biogeography and palaeoclimatology. Proceedings of the Royal Society of Victoria 110, 419–461.

Nicoll, R.S., Metcalfe, I., 2001. Cambrian to Permian conodont biogeography in East Asia-Australasia. In Metcalfe, I., Faunal and floral migrations and evolution in SE Asia and Australasia, p. 60–71. Lisse, A.A. Balkema/Swets and Zeitlinger.

Nicoll, R., McKellar, Ayaz, S.A., Laurie, J., Esterle, J., Crowley, J., Wood, G., Bodorkos, S., 2015. CA-IDTIMS dating of tuffs, calibration of palynostratigraphy and stratigraphy of the Bowen and Galilee basins. In: Australian Institute of Geoscientists Bowen Basin Symposium 2015, 211–218.

Nogami, Y., 1963. Fusulinids from Portuguese Timor (Palaeontological study of Portuguese Timor, 1)**.** Memoirs of the College of Science, University of Kyoto, Series B, 30, 59–68.

Orchard, M.J., Forster, P.J.L., 1988. Permian conodont biostratigraphy of the Harper Ranch beds, near Kamloops, south-central British Columbia. Geological Survey of Canada Paper 88-8, 1–27.

Ostrognay, D., Haig, D.W., 2012. Foraminifera from microtidal rivers with large seasonal salinity variation, southwest Western Australia. Journal of the Royal Society of Western Australia 95, 137–153.

Palmieri, V., 1988. Globivalvulinid Foraminifera from the Permian of Queensland. Alcheringa 12, 27–47.

Palmieri, V., 1993. Foraminifers. Bulletin of the Geological Survey of Western Australia 136, 30–32.

Palmieri, V., 1994. Permian foraminifera in the Bowen Basin, Queensland. Queensland Geology 6, 1–125.

Palmieri, V., Foster, C.B., Bondareva, E.V., 1994. First record of shared species of Late Permian small foraminiferids in Australia and Russia: time correlation and plate reconstruction. AGSO Journal of Australian Geology and Geophysics 15, 359–365.

Pflum, C.E., Frerichs, W.E., 1976. Gulf of Mexico deep-water foraminifers. Cushman Foundation for Foraminiferal Research, Special Publication 14, 1–125.

Pigram, C.J., Panggabean, H., 1984. Rifting of the northern margin of the Australian continent and the origin of some microcontinents in eastern Indonesia. Tectonophysics 107, 331–353.

Playford, G., 1959. Permian stratigraphy of the Woolaga Creek area, Mingenew District, Western Australia. Journal of the Royal Society of Western Australia 42, 7–32.

Playford, P.E., Cockbain, A.E., Low, G.H., 1976. Geology of the Perth Basin, Western Australia. Geological Survey of Western Australia Bulletin 124, 1–311.

Powis, G.D., 1981. Palynological report on four wells from the Merlinleigh Sub-basin Western Australia. Esso Australia Ltd. Palaeontological Report 1981/23. Geological Survey of Western Australia file G30200A1, WAPIMS database (https://wapims.dmp.wa.gov.au/wapims).

PSUCLIM, 1999. Storm activity in ancient climates. 2, An analysis using climate simulations and sedimentary structures. Journal of Geophysical Research 104 (D22), 27295–27320.

Redfern, J., 1991. Subsurface facies analysis of Permian-Carboniferous glaciogenic sediments, Canning Basin. In: Ulbrich, H., Rocha-Campos, A. (Eds.), Gondwana 7 Proceedings. University of Sao Paulo, Sao Paulo, 349–363.

Reeckmann, S.A., Mebberson, A.J., 1984. Igneous Intrusions in the north-west Canning Basin and their impact on oil exploration. In: Purcell, P.G., Purcell, R.R. (Eds.), The Canning Basin. Geological Society of Australia and Petroleum Exploration Society of Australia Symposium, Perth, WA, 1984, Proceedings, 389–399.

Ridd, M.F., 2009. The Phuket Terrane: A late Palaeozoic rift at the margin of Sibumasu. Journal of Asian Earth Sciences 36, 238–251.

Roberts, J., Claoue-Long, J., Jones, P.J., Foster, C.B., 1995. SHRIMP zircon age control of Gondwanan sequences in Late Carboniferous and Early Permian Australia. In: Dunay, R.E., Hailwood, E.A. (Eds.), Non-biostratigraphical Methods of Dating and Correlation, Geological Society Special Publication 89, 145–174.

Roever, W.P. De, 1942. Olivine-basalts and their alkaline differentiates in the Permian of Timor. In: Brouwer, H.A. (Ed.), Geological Expedition to the Lesser Sunda Islands IV. N.V. Noord-Hollandsche Uitgevers Maatschappij, Amsterdam, 209–289.

Ross, C.A., Ross, J.R., 2003. Fusulinid sequence evolution and sequence extinction in Wolfcampian and Leonardian Series (Lower Permian), Glass Mountains, West Texas. Rivista Italiana di Paleontologia e Stratigrafia 109, 281–306.

Sakagami, S., 1968. Permian Bryozoa from Khao Phrik, near Rat Buri, Thailand. Contributions to the Geology and Palaeontology of Southeast Asia. 43. Geology and Palaeontology of Southeast Asia, 4, 45–66.

Sakagami, S., 1995. Upper Paleozoic bryozoans from the Lake Titicaca region, Bolivia. Pt. 1. Introductory remarks, stratigraphy and systematic paleontology. Pt. 2. Systematic paleontology. Transactions and Proceedings of the Palaeontological Society of Japan, New Series, 180, 226–281.

Schmitz, M.D., Davydov, V.I., 2012. Quantitative radiometric and biostratigraphic calibration of the Pennsylvanian–Early Permian (Cisuralian) time scale and pan-Euramerican chronostratigraphic correlation. Geological Society of America Bulletin 124, 549–577.

Schubert, R., 1915. Die Foraminiferen des jüngeren Paläozoikums von Timor. Paläontologie von Timor II, 49–59.

Selleck, B.W., Carr, P.F., Jones, B.G., 2007. A review and synthesis of glendonites (pseudomorphs after ikaite) with new data: assessing applicability as recorders of ancient coldwater conditions. Journal of Sedimentary Research 77, 980–981.

Senowbari-Daryan, B., 2013. *Tubiphytes* Maslov, 1956 and description of similar organisms from Triassic reefs of the Tethys. Facies 59, 75–112.

Skwarko, S.K., 1993. A list of Permian fossils from the Collie, Perth, Carnarvon, and Canning Basins. Bulletin of the Geological Survey of Western Australia 136, 89–109.

Slater, B.J., McLoughlin, S., Hilton, J., 2015. A high-latitude Gondwanan lagerstätte: The Permian permineralised peat biota of the Prince Charles Mountains, Antarctica. Gondwana Research 27, 1446–1473.

Spencer, C.J., Harris, R.A., Major, J.R., 2015. Provenance of Permian–Triassic Gondwana Sequence units accreted to the Banda Arc in the Timor region: Constraints from zircon U–Pb and Hf isotopes. Gondwana Research, http://dx.doi.org/10.1016/j.gr.2015.10.012.

Spratt, J., Dentith, M.C., Evans, S., Aitken, A.R.A., Lindsay, M., Hollis, J.A., Tyler, I.M., Joly, A., Shragge, J., 2014. A magnetotelluric survey across the Kimberley Craton, northern Western Australia. Geological Survey of Western Australia Report 136, 1–92.

Swainson, I.P., Hammond, R.P., 2001. Ikaite, $CaCO_3 \cdot 6H_2O$: cold comfort for glendonites as paleothermometers. American Minerlaogist 86, 1530–1533.

Taboada, A.C., Mory, A.J., Shi, G-R., Haig, D.W., Pinilla, M.K., 2015. An Early Permian brachiopod-gastropod fauna from the Calytrix Formation, Barbwire Terrace, Canning Basin, Western Australia. Alcheringa 39, 207–223.

Tate, G.W., McQuarrie, N., Hinsbergen, D.J.J. van, Bakker, R.R., Harris, R., Haishui, J., 2015. Australia going down under: Quantifying continental subduction during arc-continent accretion in Timor-Leste. Geosphere doi:10.1130/GES01144.1

Teichert, C. 1939. Recent research in the Permian of Western Australia. The Australian Journal of Science 2, 5–7.

Teichert, C., 1941. Upper Paleozoic of Western Australia: Correlation and paleogeography. Bulletin of the American Association of Petroleum Geologists 25, 371–415.

Teichert, C., 1948. Climates of Australia during the Carboniferous, Permian and Triassic. International Geological Congress, Report of the Eighteenth Session, Great Britain, 1948, Part 1, 206–208.

Teichert, C., 1991. New data on the Permian crinoid family Calceolispongiidae in Western Australia. Journal of the Royal Society of Western Australia 73, 113–121.

Thomas, G.A., 1954. Preliminary report on Permian brachiopod faunas of the Fitzroy Basin. Australian Bureau of Mineral Resources, Geology and Geophysics, Record 1954/9, 1–11.

Thompson, M.L., 1949. The Permian fusulinids of Timor. Journal of Paleontology 23, 182–192.

Torsvik, T.H., Cocks, L.R.M., 2004. Earth geography from 400 to 250 Ma: a palaeomagnetic, faunal and facies review. Journal of the Geological Society 161, 555–572.

Torsvik, T.H.,Van der Voo, R., Preeden, U., Mac Niocaill, C., Steinberger, B., Doubrovine, P.V., Hinsbergen, D.J.J. van, Domeier, M., Caina, C., Tohver, E., Meert, J.G., McCausland, P.J.A., Cocks, R.M., 2012. Phanerozoic polar wander, palaeogeography and dynamics. Earth-Science Reviews 114, 325–368.

Tumanskaya, O.G., 1953. Concerning Upper Permian fusulinids of the southern Ussuri territory. Trudy Vsesoyuznogo Naucho-Issledovatel'skogo Geologicheskogo Instituta (VSEGEI), Moscow.

Ueno, K., 2006. The Permian antitropical fusulinoidean genus Monodiexodina: Distribution, taxonomy, paleobiogeography and paleoecology. Journal of Asian Earth Sciences 26, 380–404.

Vachard, D., Moix, P., 2011. Late Pennsylvanian to Middle Permian revised algal and foraminiferan biostratigraphy and palaeobiogeography of the Lycian Nappes (SW Turkey): Palaeogeographic implications. Revue de Micropaléontologie 54, 141–174.

Waterhouse, J.B., Shi, G.R., 2010. Evolution in a cold climate. Palaeogeography, Palaeoclimatology, Palaeoecology 298, 17–30.

Waterhouse, J.B., Shi, G.R., 2013. Climatic implications from the sequential changes in diversity and biogeographic affinities for brachiopods and bivalves in the Permian of eastern Australia and New Zealand. Gondwana Research 24, 139–147.

Webster, G.D., Lane, G., 2007. New Permian crinoids from the Battleship Wash patch reef in southern Nevada. Journal of Paleontology 81, 951–965.

Wopfner, H., 1999. The Early Permian deglaciation event between East Africa and northwestern Australia. Journal of African Earth Science 29, 77–90.

Wopfner, H., Jin, X.C., 2009. Pangea megasequences of Tethyan Gondwana-margin reflect global changes of climate and tectonism in Late Palaeozoic and Early Triassic times — a review. Palaeoworld 18, 169–192.

Zhu, D-C., Zhao, Z-D., Niu, Y., Dilek, Y., Mo, X-X., 2011. Lhasa terrane in southern Tibet came from Australia. Geology 39, 727–730.

FIGURE CAPTIONS

Fig. 1. East Gondwana during the Artinskian–Kungurian, showing the position of the East Gondwana interior rift; Timor (A) on the eastern side of the main rift axis, and the west Australian marginal rift basins that splay from the main axial rift: (B, Northern Bonaparte Basin; C, Canning Basin; D, Merlinleigh-Byro sub-basins within broader Southern Carnarvon Basin; E, Irwin Sub-basin within broader northern Perth Basin). Continental reconstruction modified from Harrowfield et al. (2005), Metcalfe (2013a, b), and Slater et al. (2015). Ages of cratonic nuclei adjacent to the rift are from Harrowfield et al. (2005) and Spratt et al. (2014). South Pole position at 280 Ma and palaeolatitudes are from Torsvik et al. (2012). Cross-section across the Eastern Gondwana interior rift (EGIR) and the Mesotethyan rift (MR) follows Langhi and Borel (2005).

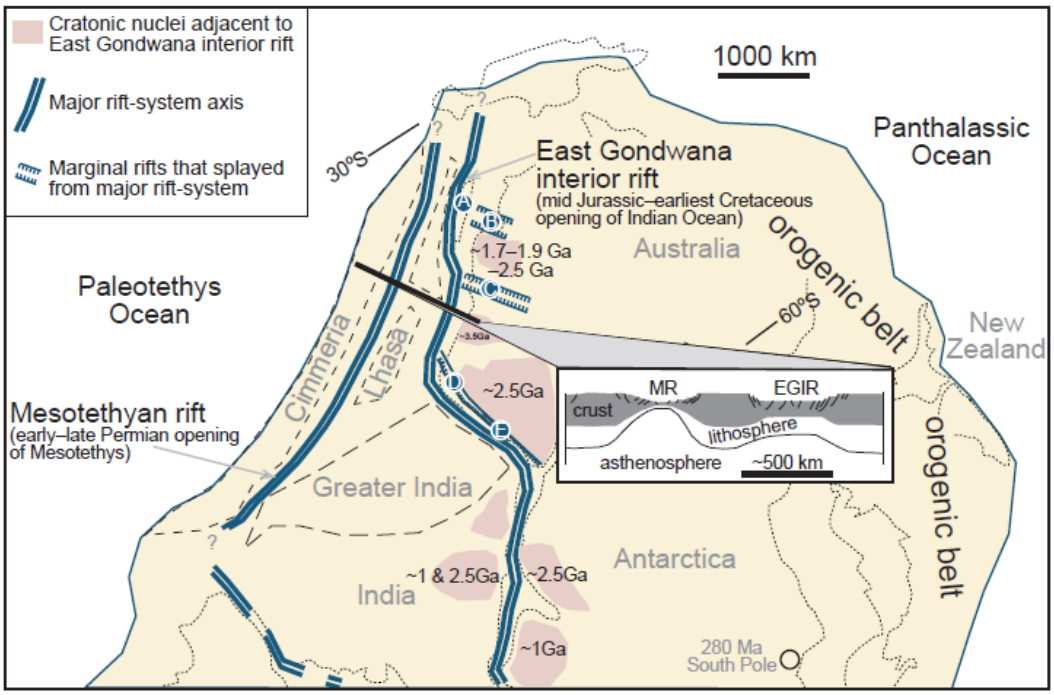

Fig. 2. (a) Basement-terrane map of west Australia showing Paleozoic–Mesozoic depocentres

(compiled by FROGTECH, www.frogtech.com.au). (b) Isopach map for the Artinskian–Kungurian showing major depocentres. Note (1) the Fitzroy Trough is part of the broader Canning Basin; (2) most of the Southern Carnarvon Basin west of the Merlinleigh Sub-basin was a relative high during the Early Permian (underpinned by the Proterozoic Northampton inlier) as suggested by absence of Permian strata and by low thermal maturation levels in older Paleozoic formations in this region (Iasky et al., 1998); (3) the Permian on the North West Shelf (Northern Carnarvon, Roebuck, Browse, and Northern Bonaparte basins) is poorly known due to the great thickness of Mesozoic and Cenozoic cover.

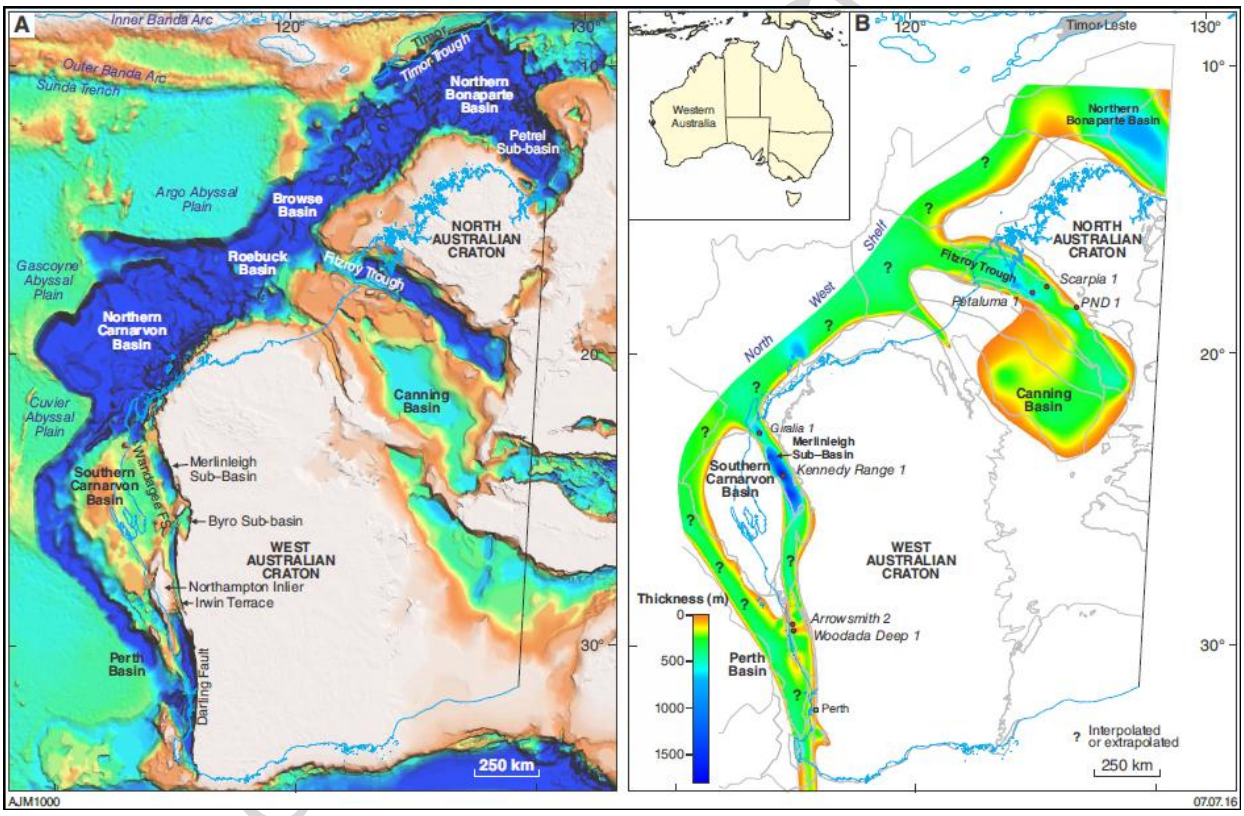

Fig. 3. Reconstructed stratigraphic framework for the Gondwana Megasequence in Timor Leste (modified from Haig and Bandini, 2013). In the left-hand column, C = Carboniferous; P = Permian, with subdivisions, C = Cisuralian, G = Guadalupian, L = Lopingian; Tr = Triassic; J = Jurassic. Estimated thickness of each unit is given in metres.

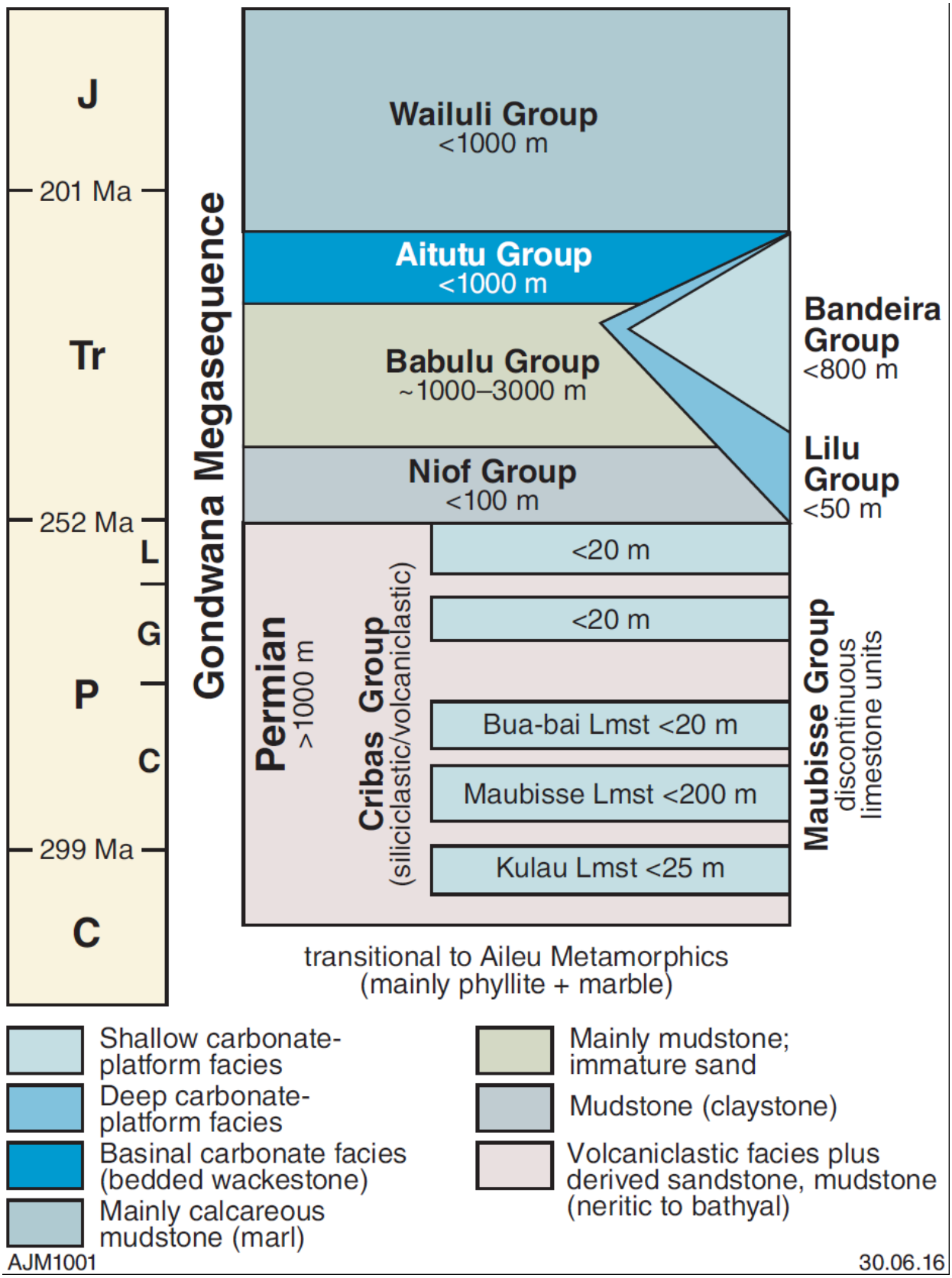

Fig. 4. SRTM image of Timor (compiled from NASA Shuttle Radar Topography Mission images) showing the location of study areas: A, Bua-bai area (see section 3.2.1); C, Cribas area (see section 3.2.2).

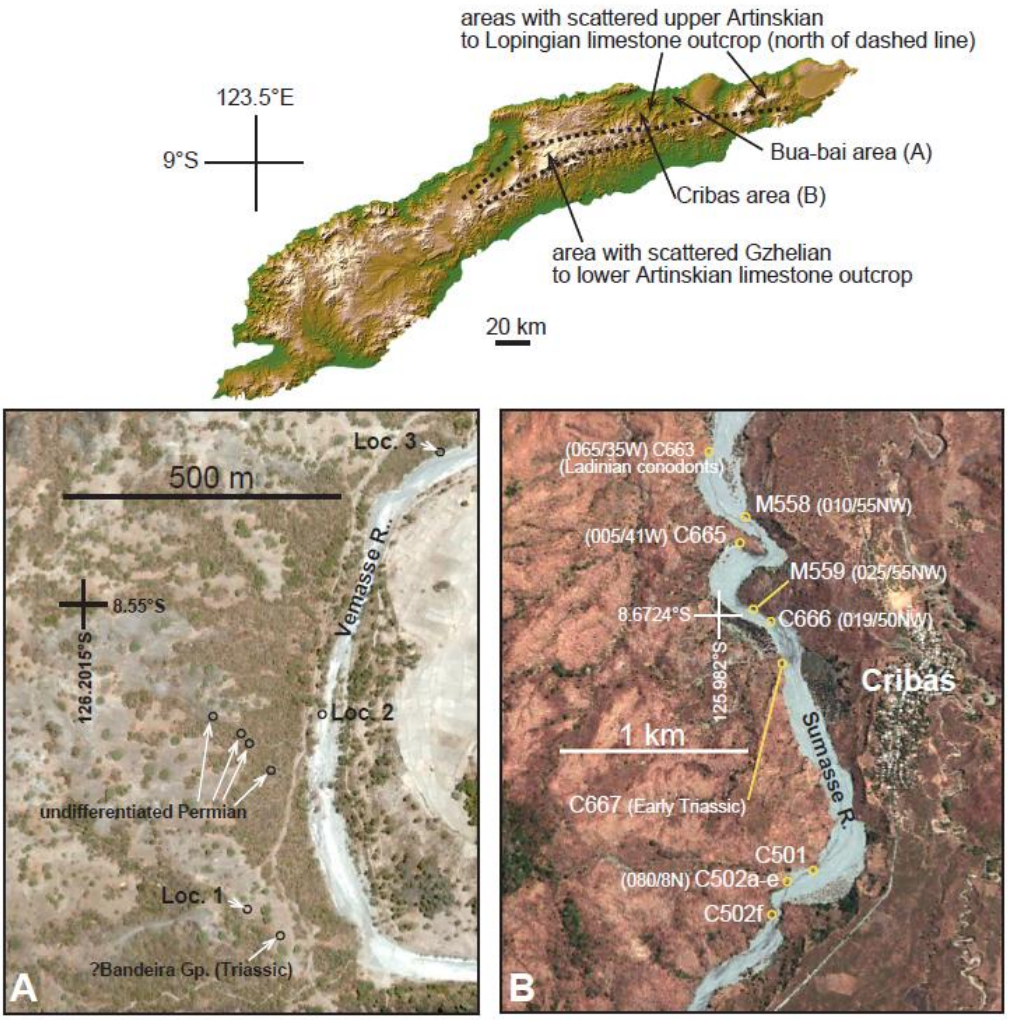

Fig. 5. Chronostratigraphic correlation of units in studied basins of the East Gondwana interior rift. The formations and the placement of formation boundaries within chronostratigraphic levels of uncertainty are discussed in sections 3.2– 3.5.

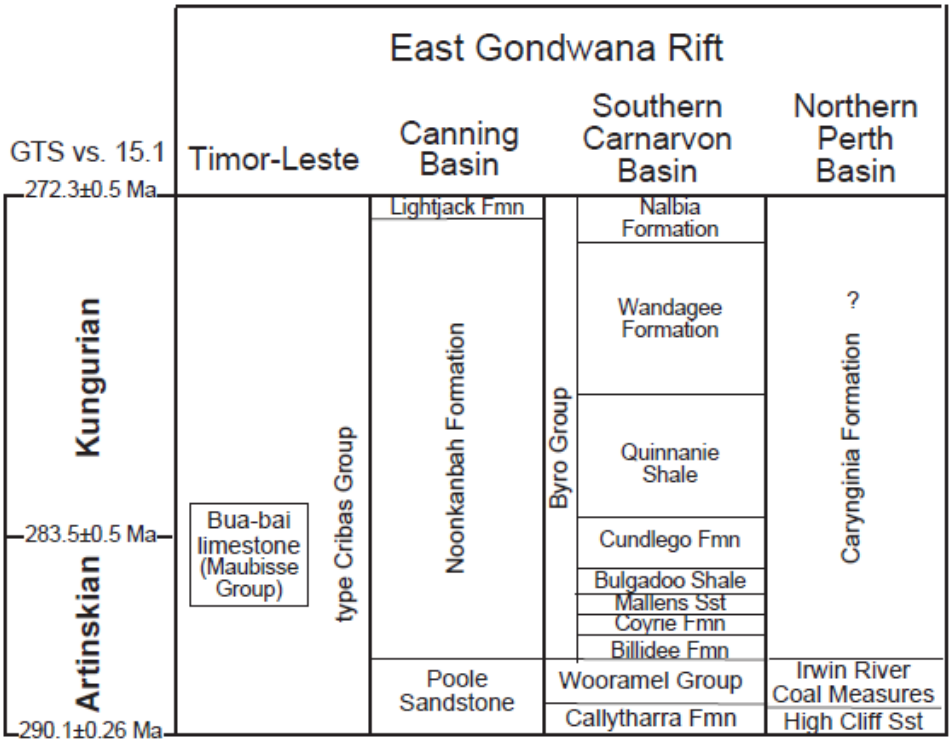

Fig. 6. Representative outcrop of the Artinskian–Kungurian in Timor-Leste. A, Bua-bai limestone at Locality 1 (Fig. 4A); B, Bua-bai limestone represented by red floatstone facies at Locality 3 (Fig. 4A); C, red interbedded indurated and friable mudstone from locality M558 (Fig. 4B) with common *Atomodesma* sp. moulds; D, part of succession exposed at locality M559 passing from sandstone-dominated at base (bottom right hand side of photo) into mudstone-dominated facies; E, sandstone-dominated outcrop from locality M559 (Fig. 4B) with thin to medium bedded sandstone; F, probable swaley cross stratification in sandstone beds from section illustrated in E; G, silt-rich mudstone and interbedded sandstone exposed at locality C501 (Fig. 4B); H, sandstone-dominated section exposed at locality C502a–e (Fig. 4B) which comprises thick sandstone beds interbedded with mudstone. This section displays common soft sediment deformation and bidirectional ripple-crests on bedding planes.

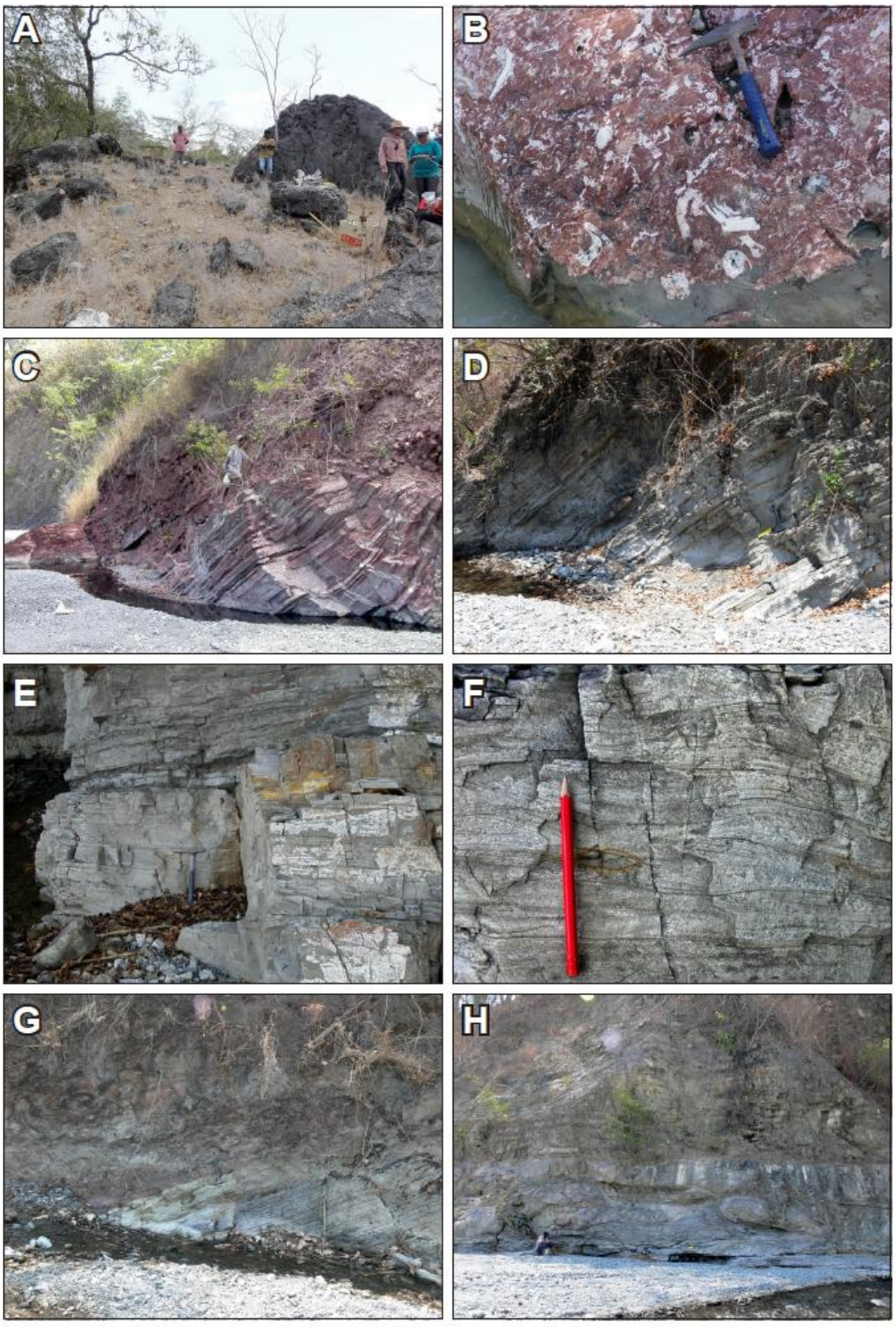

Fig. 7. Important representatives of the Fusulinata (Foraminifera) from the Bua-bai limestone. Bar scales = 1 mm, except for F, G and L = 0.1 mm. Images from acetate peels. A, *Abadehella*

sp., slightly off-centred axial section; B–E, *Praeskinnerella* sp., very slightly oblique to almost centred axial sections; F, G, *Boultonia*? sp., F, off-centred oblique-to-axial section, G, off-centred slightly oblique equatorial section; H– J, *Nankinella*? sp., H, off-centred slightly oblique-to-equatorial section; I, off-centred, oblique-to-axial section; slightly off-centred and slightly oblique axial section; K, *Monodiexodina wanneri* (Schubert), axial section; L, *Toriyamaia*? sp., off-centred, oblique-to-axial section.

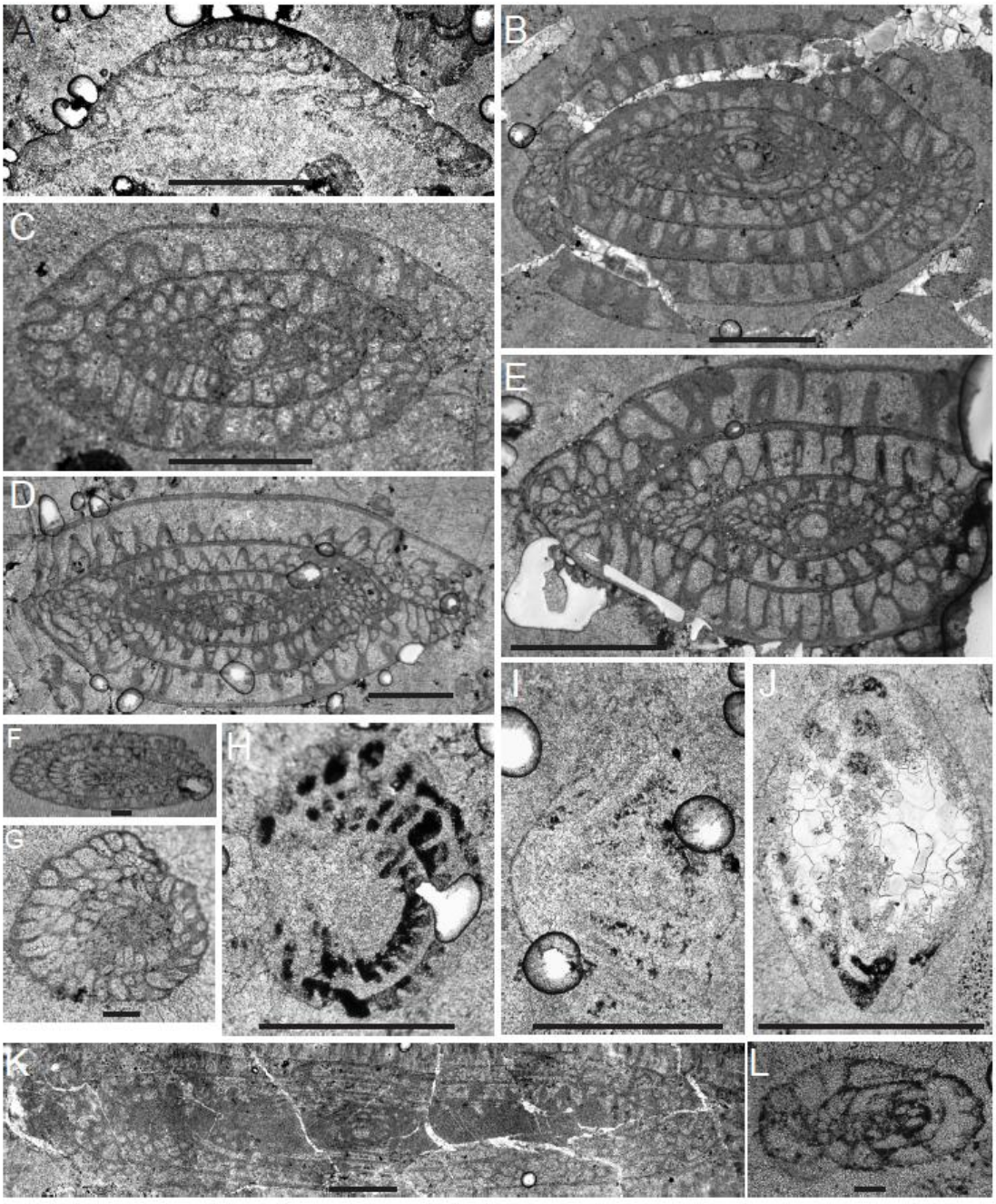

Fig. 8. Bryozoans important for correlation, from the type locality (Loc. 1, fig. 4A) of the Buabai limestone. Images from acetate peels. A: *Ascopora asiatica* Sakagami; B: *Streblotrypa* (*Streblotrypa*) *elegans* Sakagami; C: *S.* (*Streblascopora*) *irianica* Sakagami, tangential section; D: *S.* (*S.*) *irianica*, longitudinal section; E: *Dyscritella* sp. cf. *tenuirama* Crockford; F: *Liguloclema meridianus* (Etheridge); G: tubular trepostome, axial cavity filled with sediment and exterior surface covered with thick radiating, syntaxial cement; H: tubular trepostome, both axial cavity and exterior surface covered with thick radiating, syntaxial cement. Uniform magnification; scale bar = 1 mm.

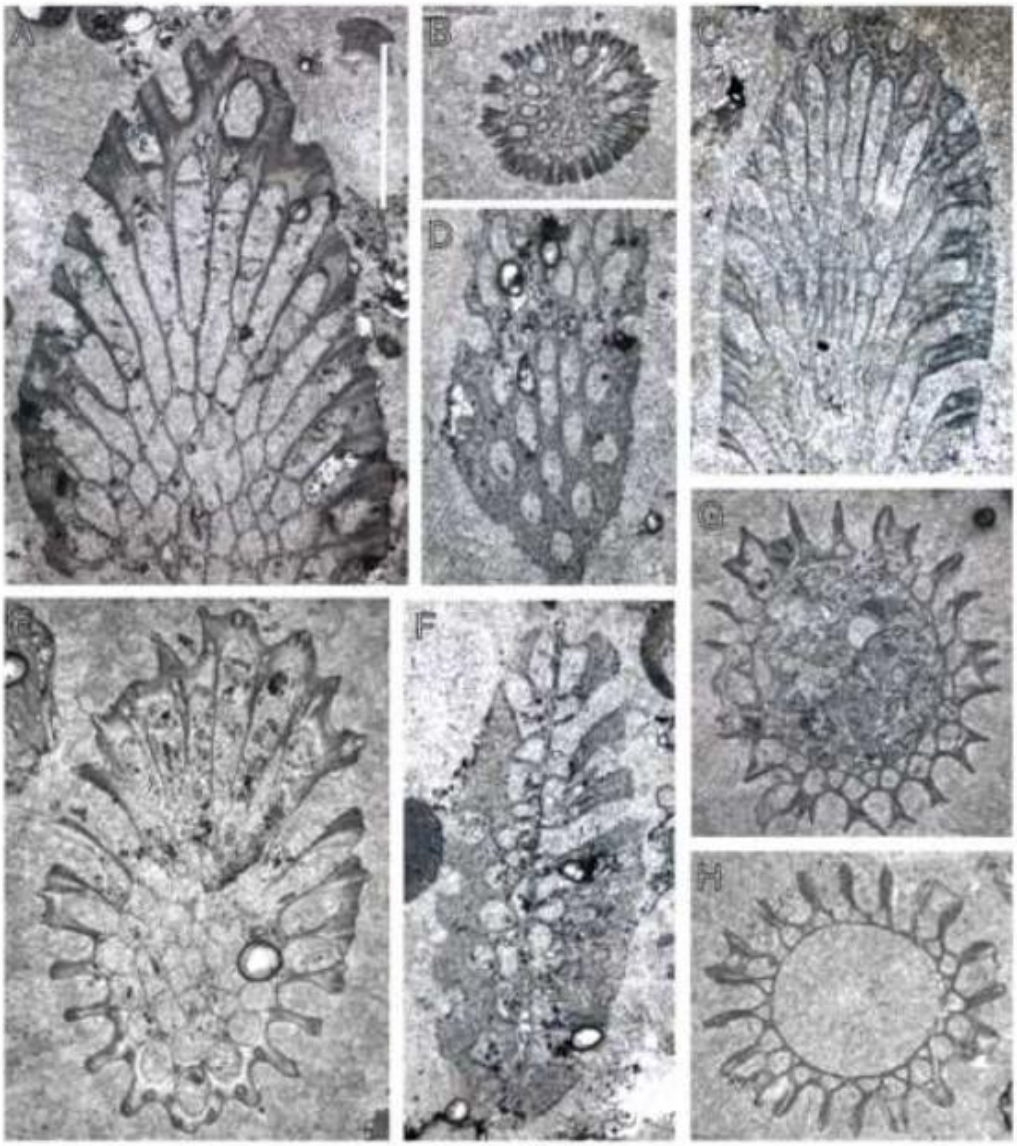

Fig. 9. Selected microfossils from the Cribas Group, Sumasse River. Bar scales in A–C are 0.1 mm; in D, 1 mm. A, B, Conodonts from C666; SEM images; A, *Vjalovognathus australis* Nicoll and Metcalfe, upper and lateral views; B, *Mesogondolella* cf. *intermedia* (Igo), upper, lateral and lower views. C, Foraminifera from C501; reflected light images rendered through multiple focal planes; 1, *Ammobaculites erugatus* Crespin; 2–5, *Glomospira* sp.; 6, 7,

Hormosina sp.; 8, *Laevidentalina* sp.; 9, 10, *Syzrania* sp.; 11, *Nodosaria raggatti* Crespin; 12, *Pseudonodosaria* sp.; 13. *Pyramidulina* sp. D, acetate peel image of mudstone with abundant debris of very thin-shelled atomodesmatinid bivalves displaying prismatic microstructure, from C502f.

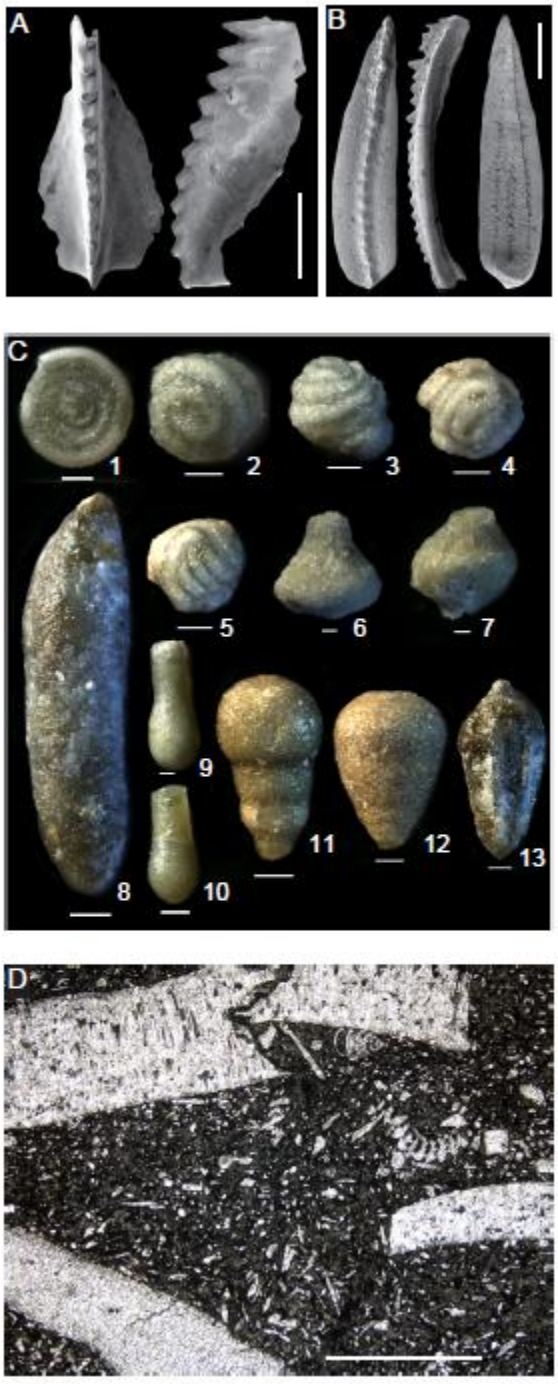

Fig. 10. Outcrop and subsurface distribution of Noonkanbah Formation in Canning Basin (modified from Mory, 2010). The approximate positions of the major fault systems bounding the "Fitzroy Trough" graben (see 3.1.2) are shown. Following conventions used by the Geological Survey of Western Australia, physiographic terms are used to designate structural entities within the basin; these have no palaeogeographic connotations.

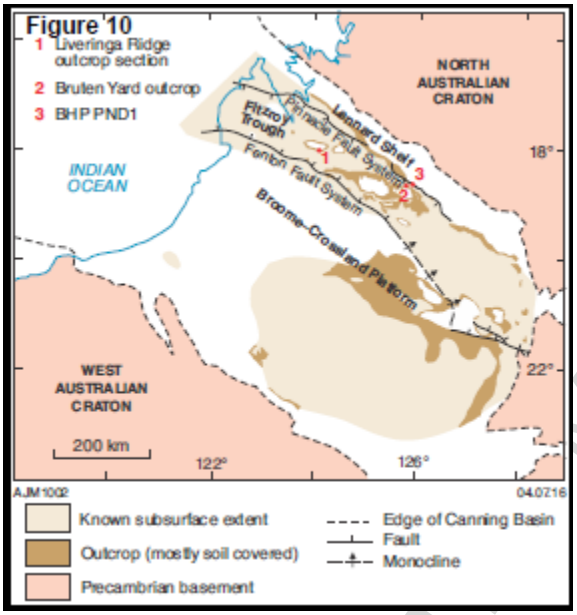

Fig. 11. Summary log of the Noonkanbah Formation in the Liveringa Ridge outcrop section (see locality on Fig. 10). Letters in brackets after species names indicate: A, algae?; Bi, bivalve; C, conodont; F, foraminifer. Numbers in stratigraphic column refer to lithofacies listed in Table 3.

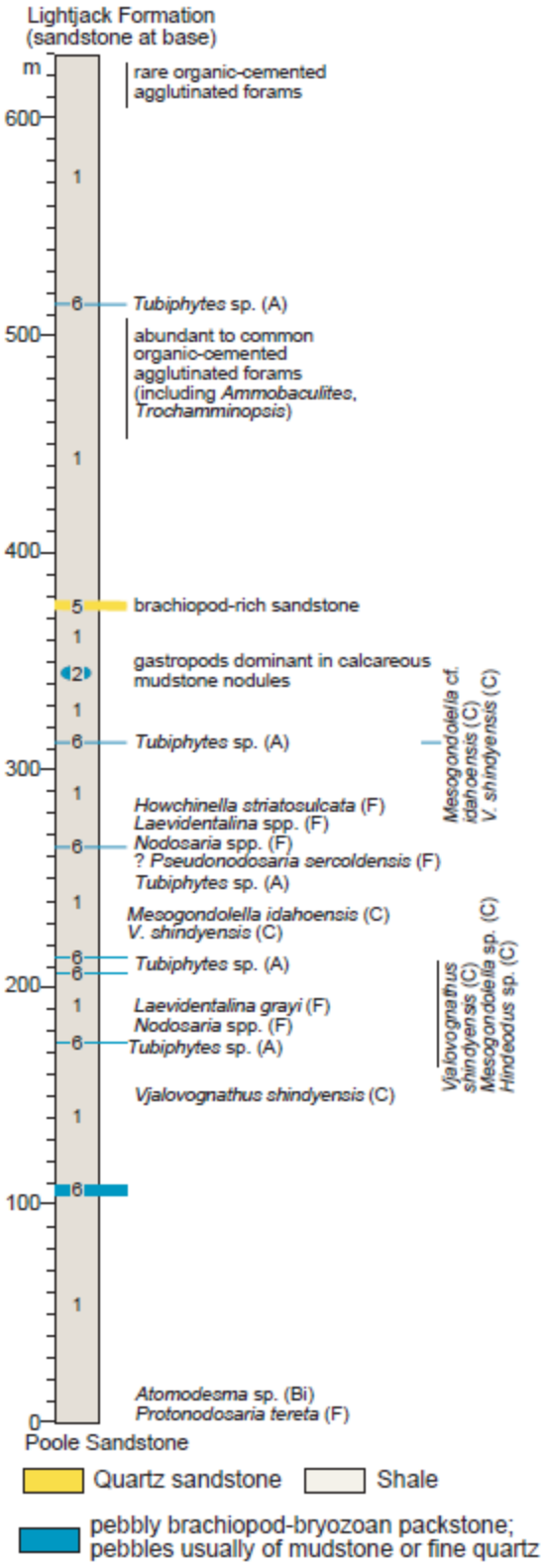

Fig. 12. Summary log of the Noonkanbah Formation in BHP PND-1 boresection (see Fig. 10 for locality). Letters in brackets after species names are as in Fig. 11. Numbers in stratigraphic column refer to lithofacies listed on Table 3.

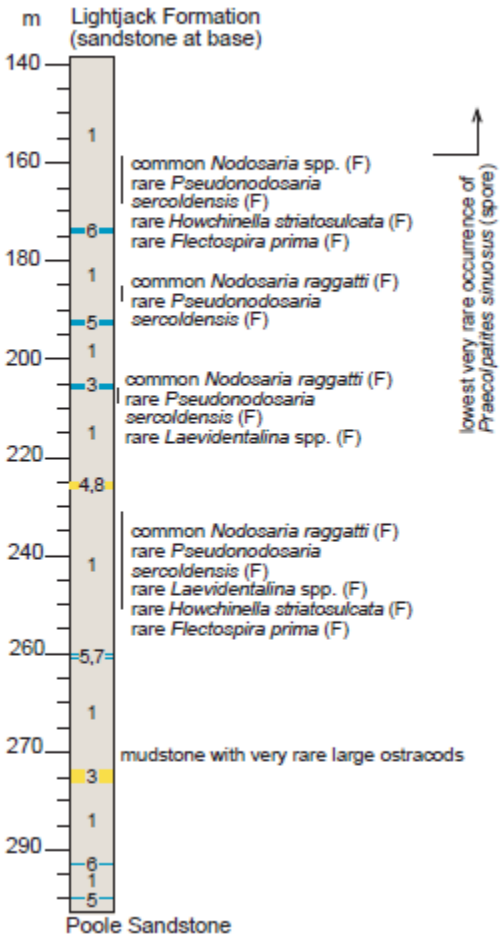

Fig. 13. Microfacies typical of lithofacies 6 and 7 of the Noonkanbah Formation (acetate peels). A, tightly packed brachiopod-bryozoan packstone (lithofacies 6). B *Tubiphytes* sp. encrusted on productid brachiopod shell. C, D, bryozoan-brachiopod packstone (Lithofacies 7). A–C from Liveringa Ridge outcrop section; A, 13-7-08-26 at 173 m; B, 12-7-08-5 at 514 m; C, 13-7-08-

22 at 101 m. D from BHP PND-1, 260.5–260.55 m. Bar scales = 1 mm.

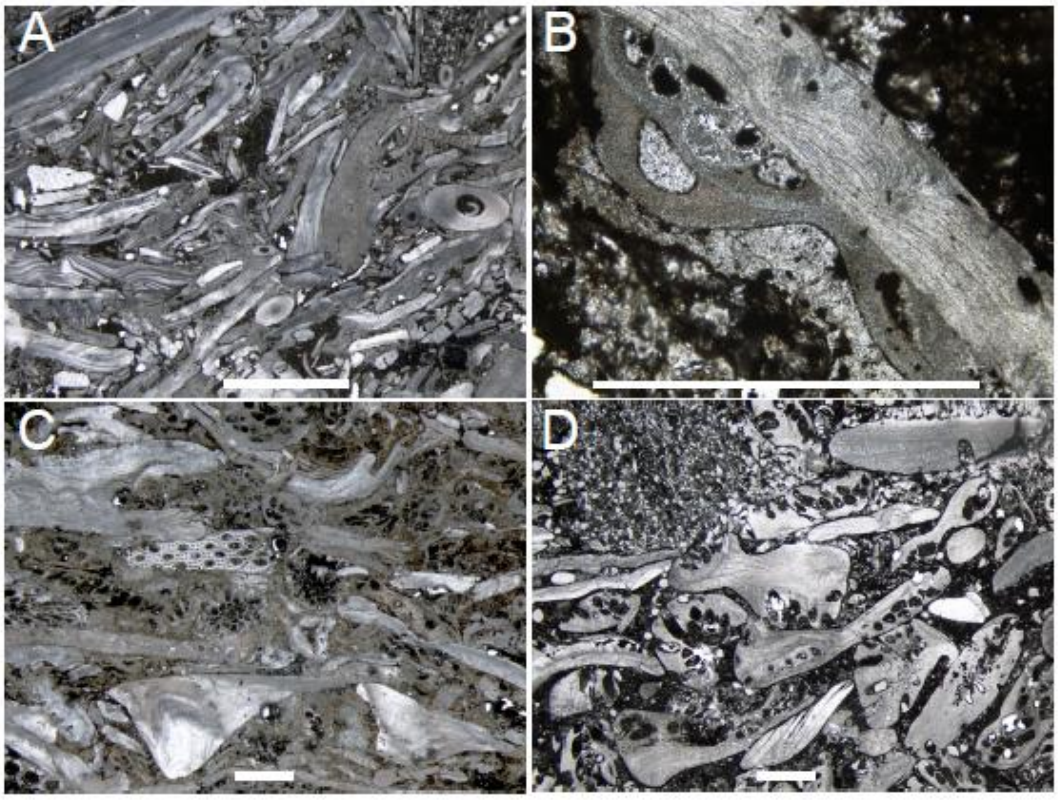

Fig. 14. Changes in the main palynofloral components in BHP PND-1 (Noonkanbah Formation). Attributions of palynomorphs to the palynofloral components are justified in section 7, Appendix 14.

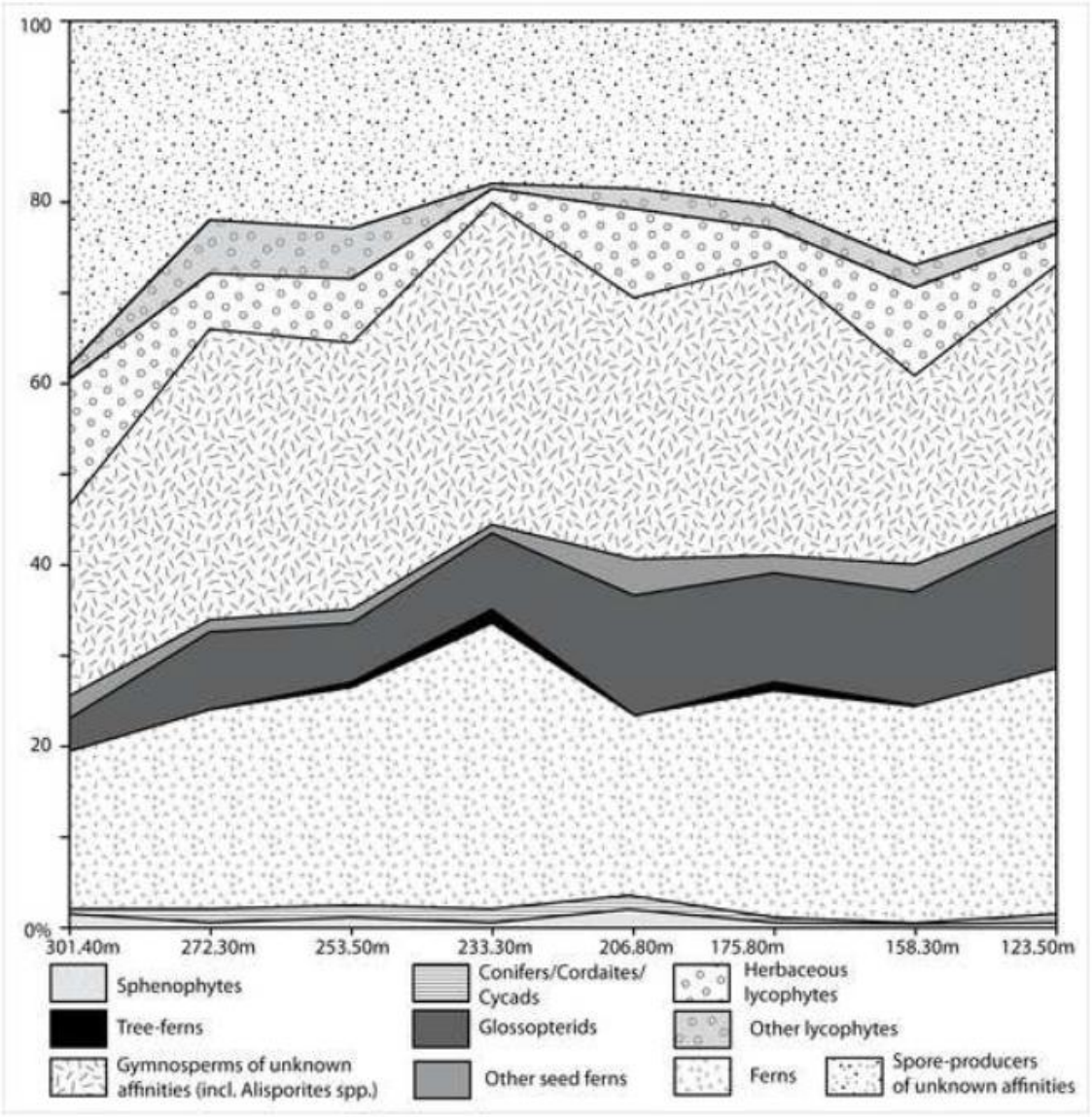

Fig. 15. Foraminifera representative of the change from *Protonodosaria* assemblages to *Nodosaria–Pseudonodosaria* assemblages that occurs within the Noonkanbah Formation. A, B, *Protonodosaria tereta* (Crespin), comparable to *Protonodosaria proceraformis* (Gerke). C–M, morphotypes within the highly variable *Nodosaria–Pseudonodosaria* plexus including C and D closest to the holotype of *Nodosaria raggatti* Crespin, J and K similar to *Nodosaria cuspidatula* Gerke, and L, M closest to the holotype of *Pseudonodosaria serocoldensis* (Crespin) and

synonmous with *Pseudonodosaria borealis* (Gerke) according to Palmieri et al. (1994); N, *Laevidentalina* sp. Specimens A, B from sample 13-7-08-24, 2m above base of Noonkanbah Formation, Liveringa Ridge outcrop section; C–G, I, N, from BHP PND-1 at 243.3 m; H, J–M, from BHP PND-1 at 158.3 m.

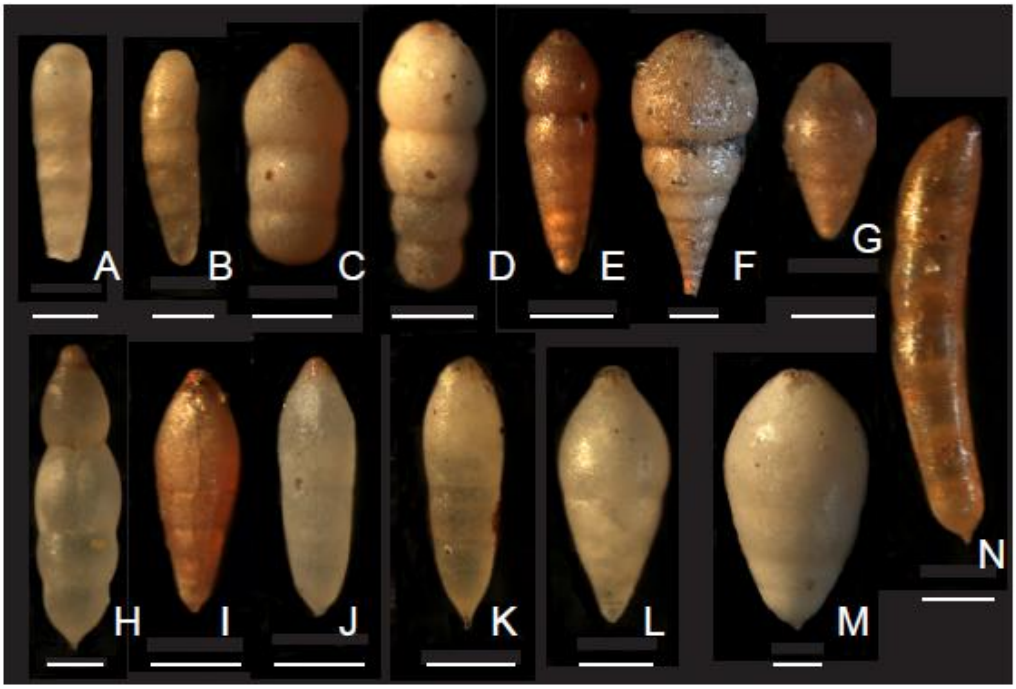

Fig. 16. A) Gravity anomaly image of the northern Perth and South Carnarvon Basins.B) Systematic geological map of the Merlinleigh Sub-Basin (Southern Carnarvon Basin) showing the extent of outcrop of the Byro Group (modified from Moore et al., 1980 and Moore and Hocking, 1983).

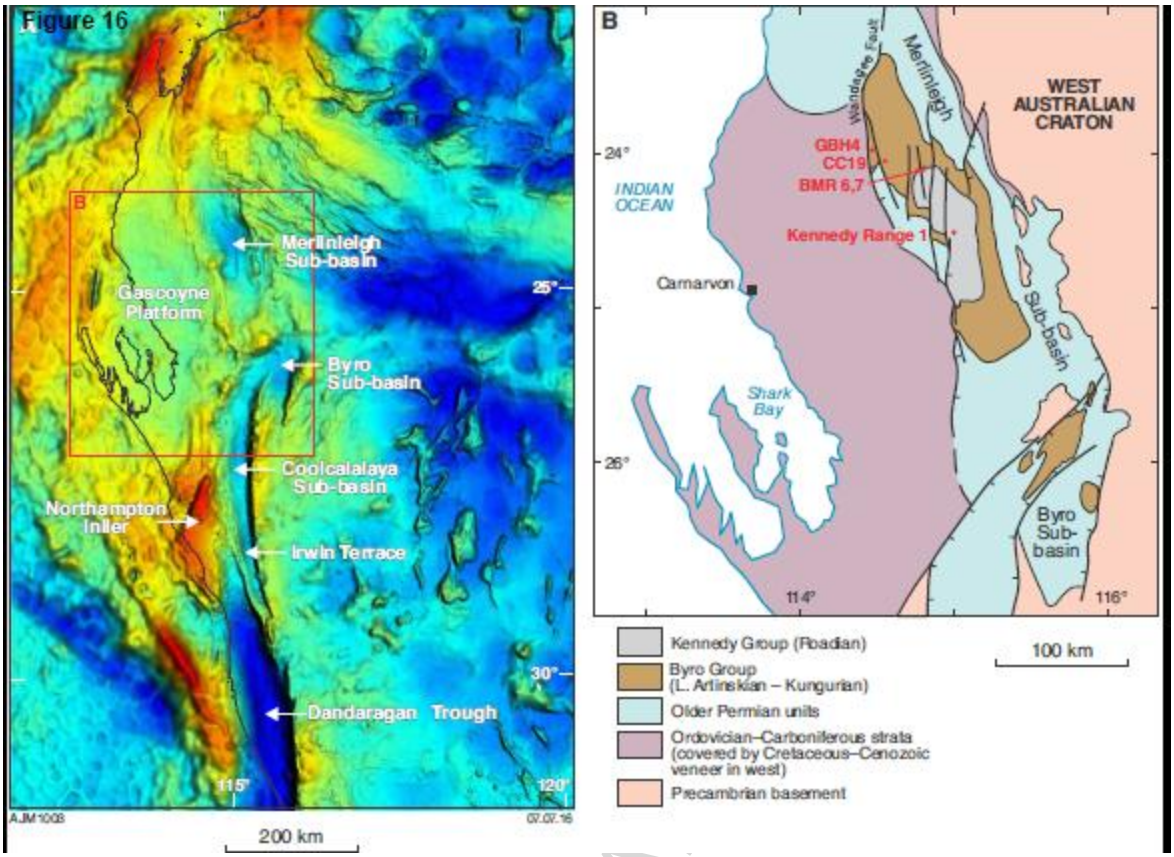

Fig. 17. Summary log of the Byro Group, based on more detailed logs of Hocking et al. (1987), Keane (1999) and Haig (2003). Letters in brackets following species names are: A, ammonoid; C, conodont; F, foraminifer.

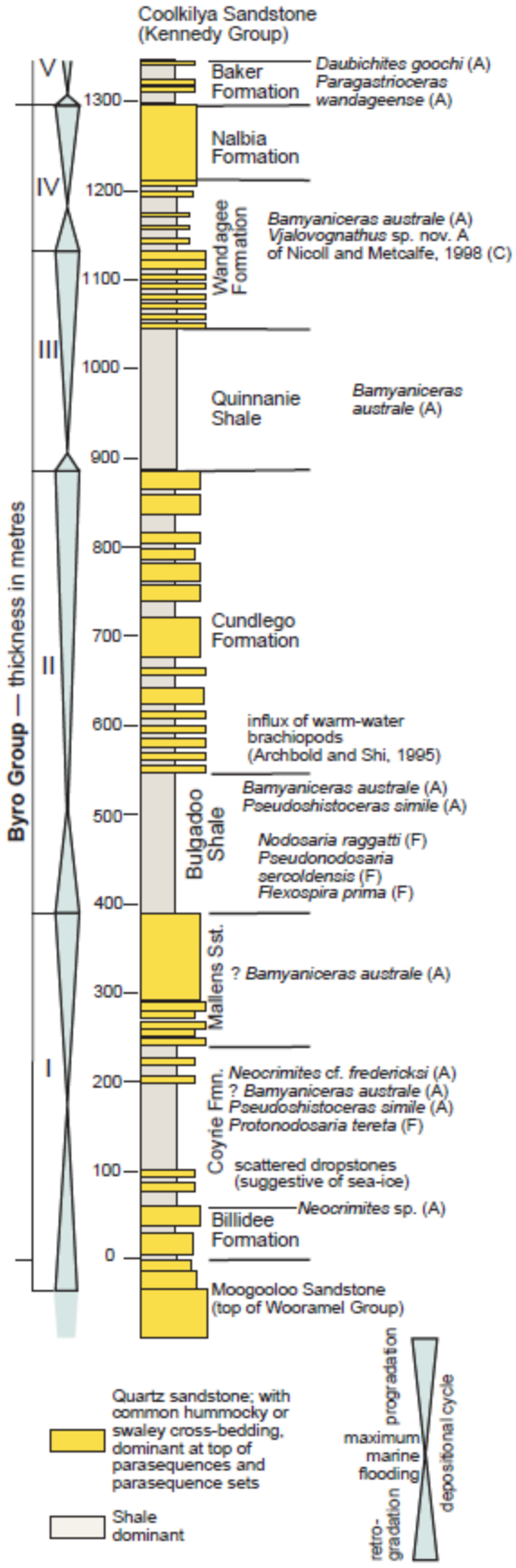

Fig. 18. Shale to sand shoaling upward cycles in Byro Group. Upper left diagram shows depositional model with the positions of fairweather wave base and storm wave base and the deeper zone of low dissolved oxygen in the shallow interior sea. The locations of illustrated facies against this model are indicated by letters A–G which refer to facies illustrated in the photographs designated by these letters. A, cliff section in part of Cundlego Formation showing two shoaling-up parasequences; B, cliff section in Bulgadoo Shale showing highly carbonaceous mudstone in maximum-marine flooding interval for Cycle II of the Byro Group and for the entire Cisuralian in the Southern Carnarvon Basin; C, bioturbated quartz sandstone with *Skolithos* burrows at the top of a parasequence in the Cundlego Formation (about 30 cm thick); D, E sections showing hummocking and swaley cross-bedding and interformational conglomerates in Cundlego Formation (sections about 2 m thick); F, quartz sandstone with large compacted *Zoophycos* burrows, Wandagee Formation; G, carbonaceous mudstone with calcareous mudstone nodules (partly ferruginized), Bulgadoo Shale (section about 1.5 m thick).

Figure 18

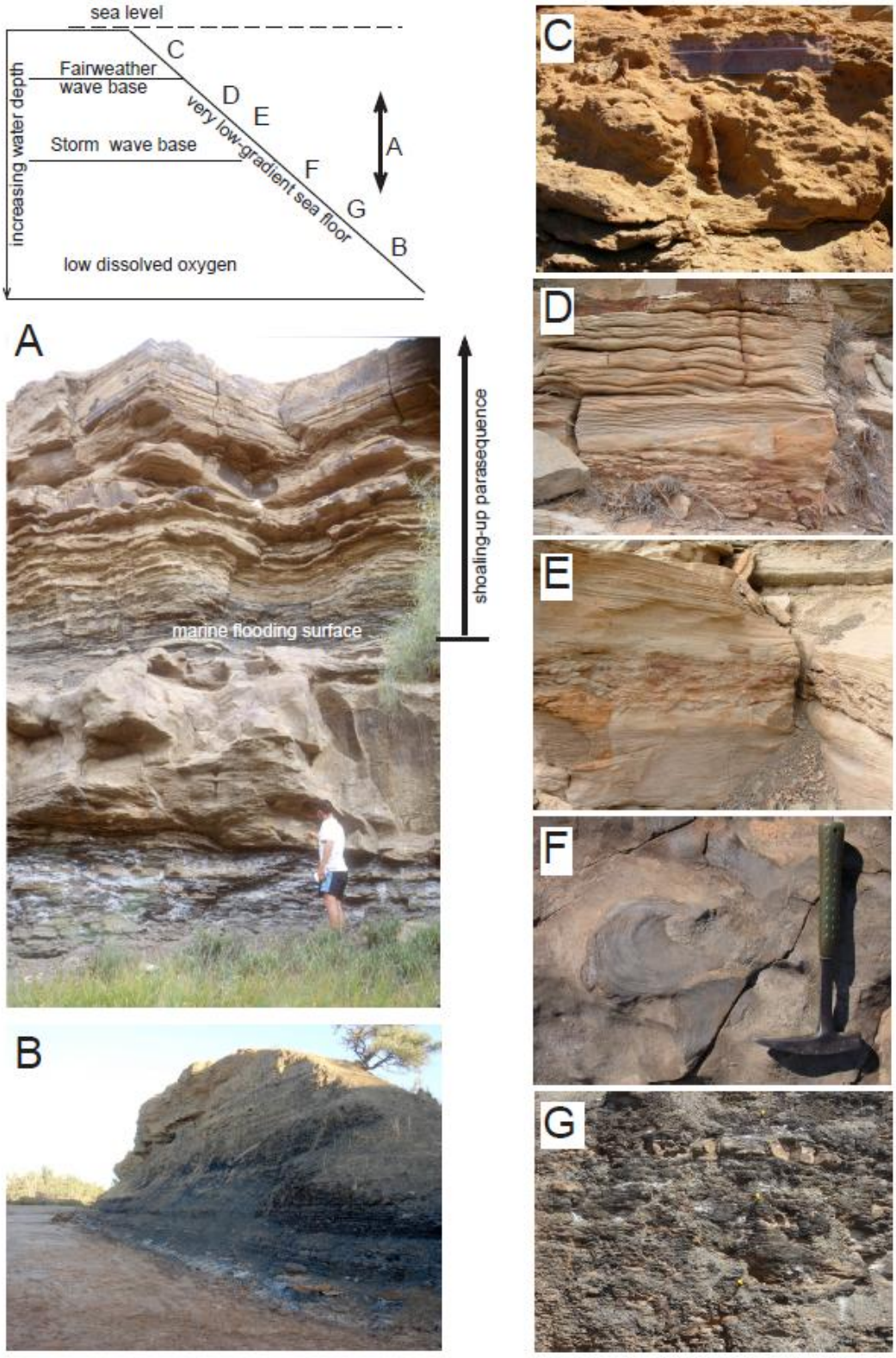

Fig. 19. Selected outcrops of the Billidee and Coyrie Formations (Cycle I) of the Byro Group in the Merlinleigh Sub-basin. A, outcrop in the upper Moogooloo Sandstone (Wooramel Group) in the Toby Bore region (see Mory and Haig, 2011, p. 44, 45) showing intensely bioturbated sandstone with *Skolithos* that lies near the base of a retrogradational succession leading to the Byro Group. B, pale-coloured weathered mudstone unit forming base of Billidee Formation (taken as base of Byro Group) in the Toby Bore region. C, major mudstone unit overlain by sandstone in the upper Billidee Formation in the Toby Bore region; D, granitic dropstone in very weathered middle Billidee Formation in the Toby Bore region. E, mainly fine sandstone succession above basal mudstone in the lower Coyrie Formation in the Toby Bore region. F, dropstone (?stromatolitic dolomite) weathered from mudstone in the lower Coyrie Formation.

1

Fig. 20. Map of northern Perth Basin showing distribution of Carynginia Formation (modified from Playford et al., 1976, and Mory and Iasky, 1996). 1 = Woodada Deep 1 well; 2 = IRCH 1 borehole; 3 = Irwin River outcrop area.

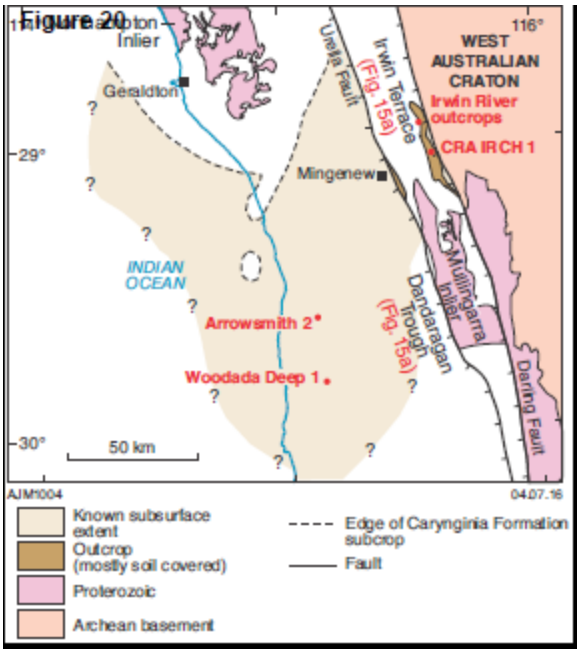

Fig. 21. Section at base of Carynginia Formation in South Branch of Irwin River.

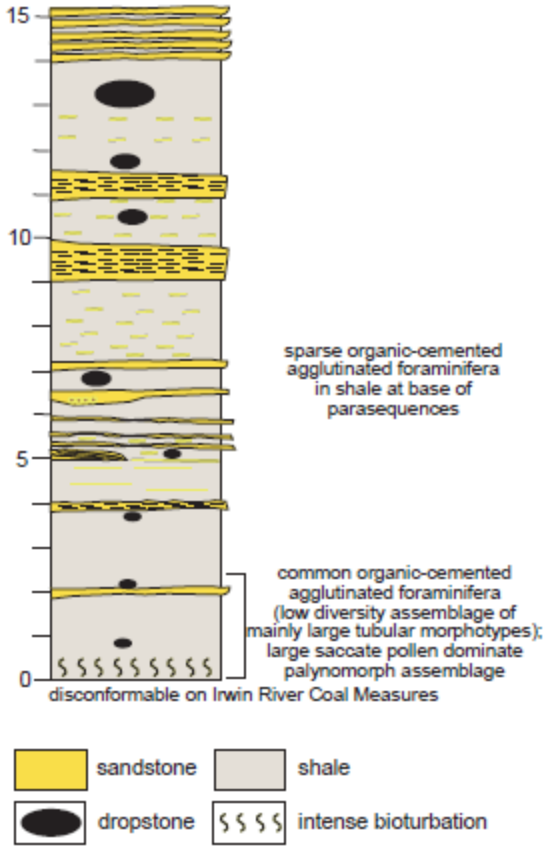

Fig. 22. Borehole sections of Carynginia Formation.

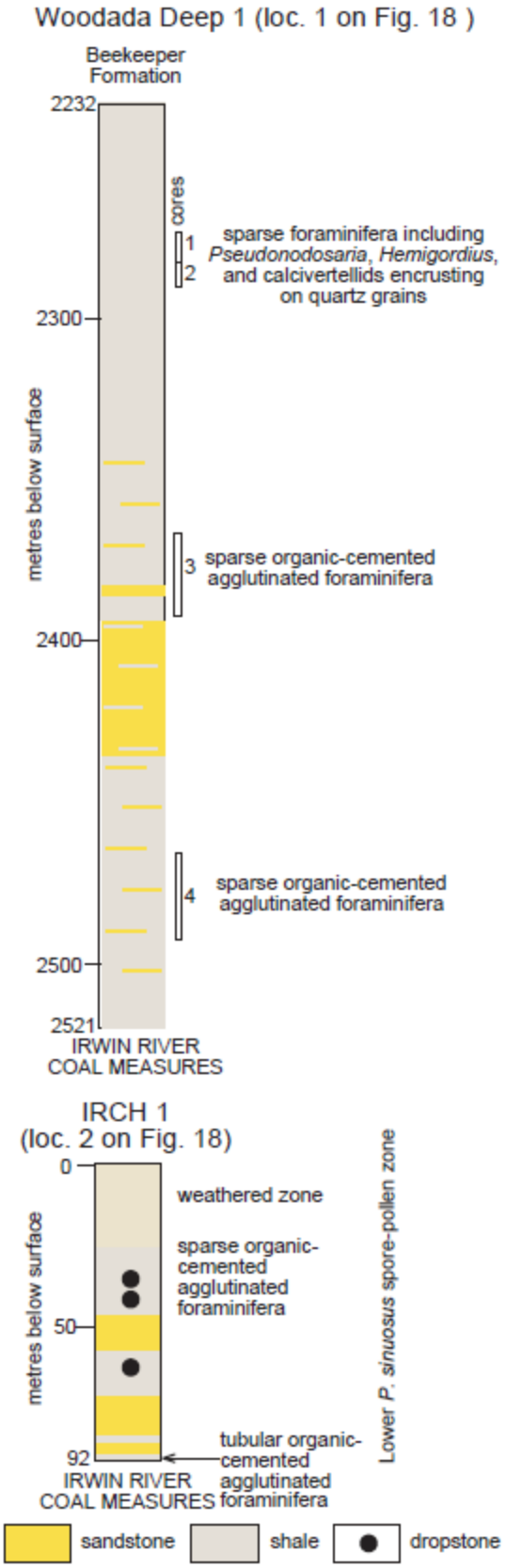

Fig. 23. Selected outcrops of Carynginia Formation. A, river cliff section in the South Branch of Irwin River showing the erosional unconformity, marked by arrow, between the Irwin River Coal Measures below, and the Carynginia Formation above; the basal 20 cm of the Carynginia Formation is intensely bioturbated; bar scale = 20 cm. B, river cliff section in the South Branch of the Irwin River showing the lower Carynginia Formation. C, sandstone from about 50 m above base of Carynginia Formation in the North Branch of the Irwin River with a stem from a *Glossopteris* tree showing terminal fructification and an attached leaf; D, river cliff section in South Branch of Irwin River showing a large dropstone 12–13 m above base of the Carynginia Formation.

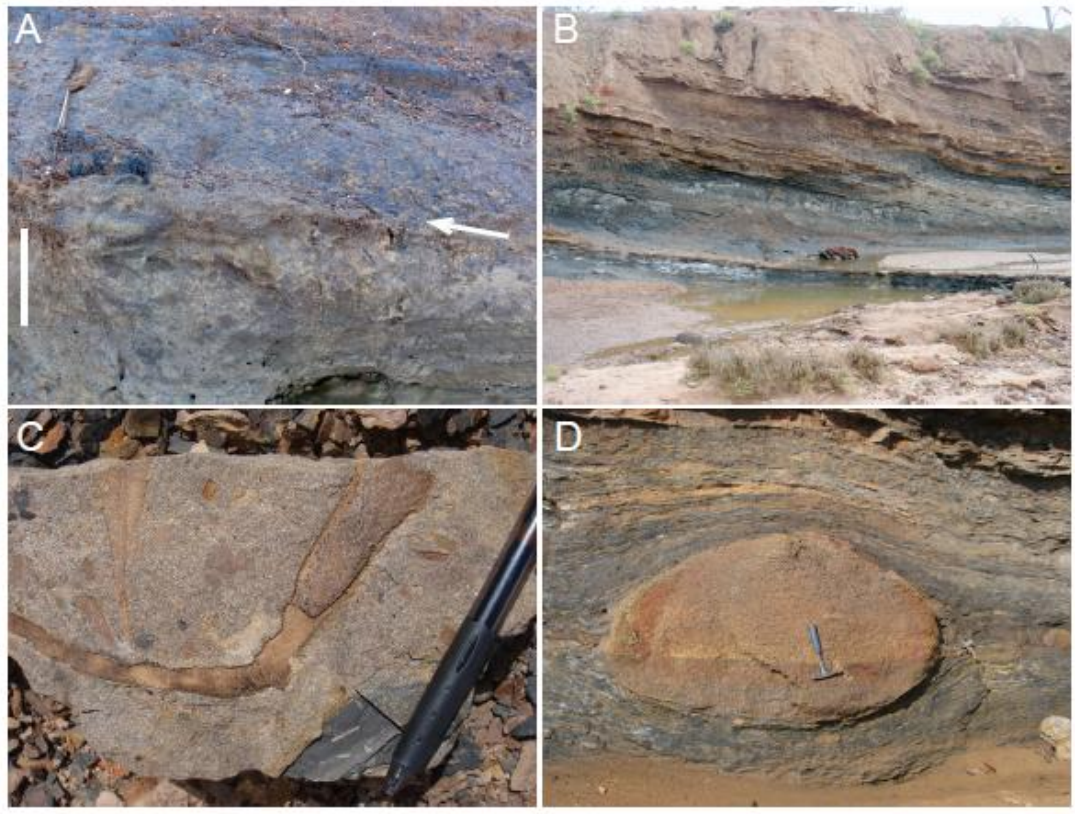

Fig. 24. Foraminifera from the Carynginia Formation in Woodada Deep 1 well. Thin-section images taken in transmitted light. Bar scale = 0.1 mm. A, Cross-section of tubular organic-cemented siliceous agglutinated foraminifera; compressed due to burial, from 2273.836 m. B, *Ammodiscus nitidus* Parr from 2489.35 m. C, ? *Digitina recurvata* Crespin and Parr, cross-section through basal stage of test, from 2283.90 m. D, *Tolypammina* sp. encrusted on quartz grain, from 2285.70 m. E, calcivertelline encrusted on quartz grain, from 2275.621 m. F, *Tolypammina* sp. encrusted on quartz grains, from 2285.70 m. G, *Hemigordius* sp. from 2280.345 m. H, ? *Digitina recurvata* Crespin and Parr, slightly oblique longitudinal section, from 2489.35 m. I, *Pseudonodosaria* sp., oblique section, from 2283.90 m.

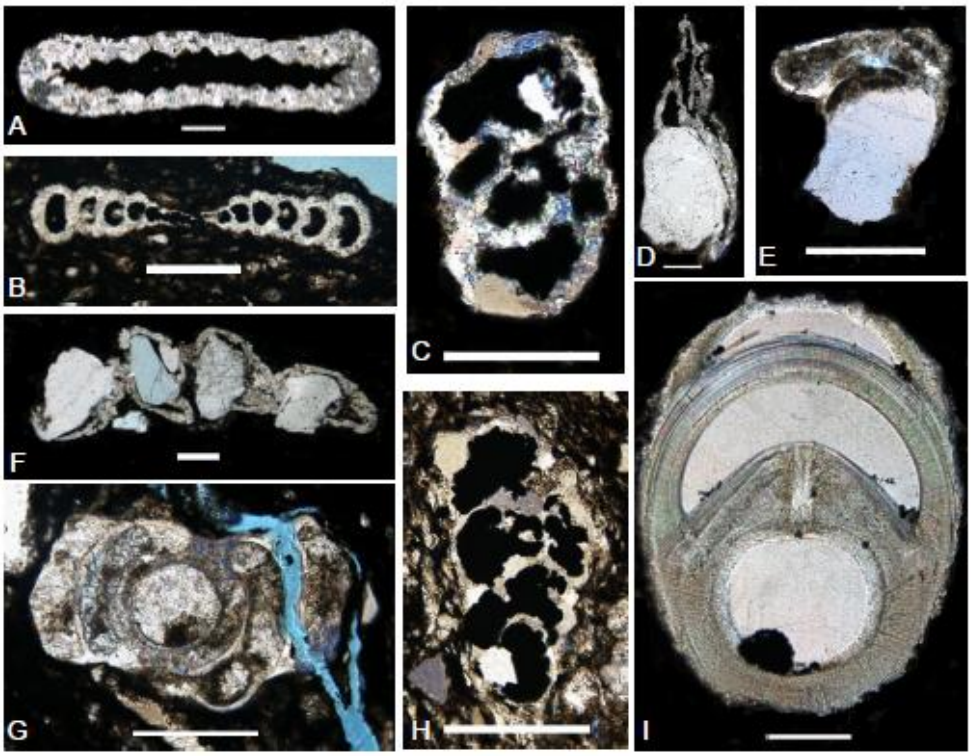

Fig. 25. Correlation of selected well sections in Western Australian marginal rift basins, showing the maximum marine flooding level close to the Artinskian–Kungurian boundary, and the major depositional (cycles I to V) of the late Artinskian to earliest Roadian.

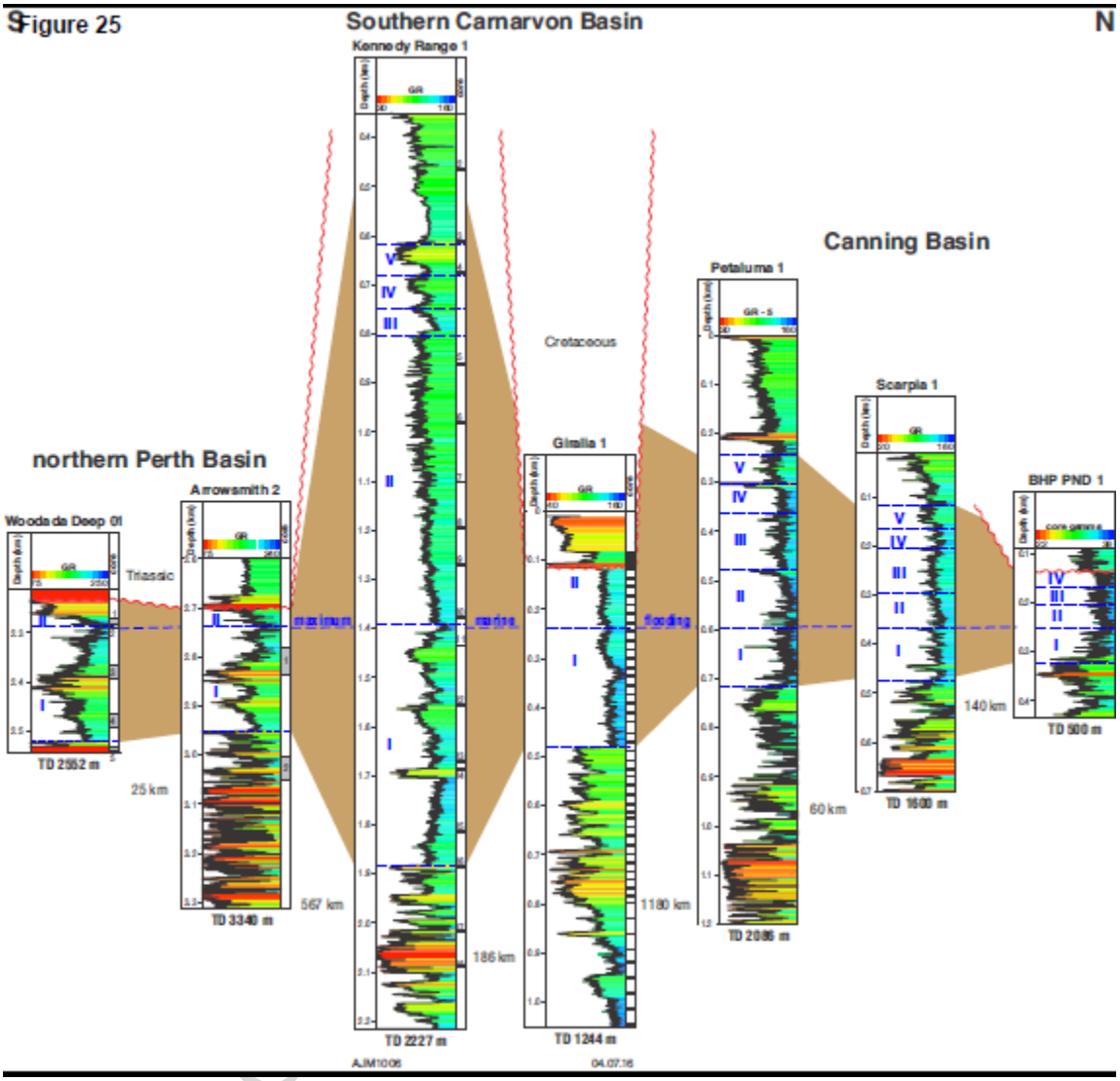

Fig. 26. Climate trends across the East Gondwana lowlands during the Mississippian to Cisuralian. A, East Gondwana interior rift; B, Lhasa terrane C, Sibumasu terrane (following Metcalfe 2013). Numbers beside the columns refer to evidence for climate conditions cited in section 7, Appendix 24.

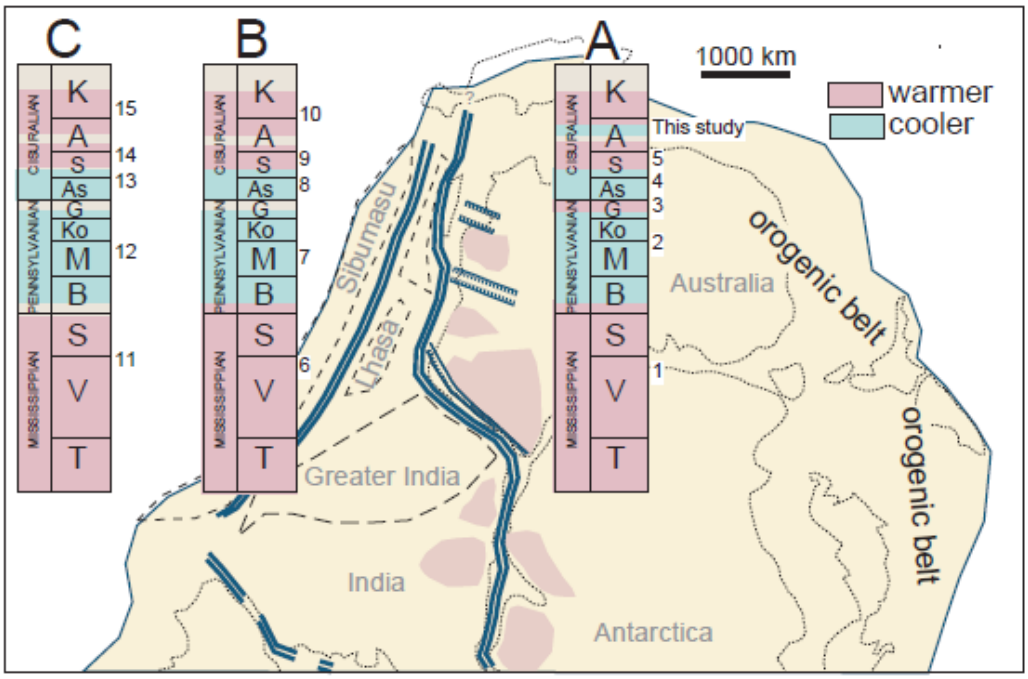

Fig. 27. Subsidence records for Permian successions in representative marginal rift basins: (A) Merlinleigh Sub-basin of the Southern Carnarvon Basin and (B) Canning Basin. The records are represented by cumulative stratigraphic thickness versus age plots. The units plotted are major depositional cycles. During the time intervals represented here, deposition almost kept pace with sediment accommodation created by subsidence. Thicknesses are taken from Hocking et al. (1987) and Mory (2010).

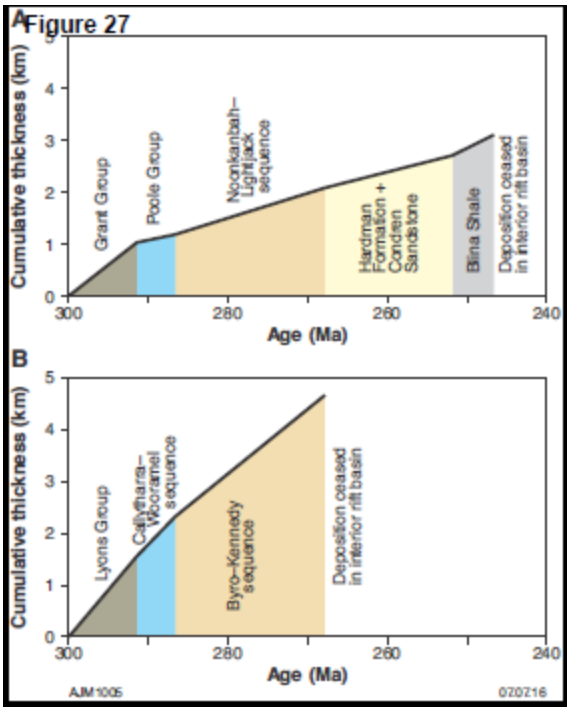

Figure 27

Table 1

Microfacies recognized in Bua-bai limestone at type locality (Loc. 1, Fig. 4A).

Microfacies	Lithology	Bedding and sedimentary structures	Biogenic grain com
1	Bryozoan-fusulinid-crinoidal floatstone to loose packstone; pale grey-brown to white in hand-specimen (referred to as *watubuti*, "white rock", by local people); bioclasts up to 2.5 cm in length; with variably recrystallized matrix generally in form of radial-fibrous calcite rims (~0.3 mm thick) around bioclasts. Matrix is micritic with minute scattered bioclasts. Matrix/cement forms 25-57% of total rock volume.	Bedding indistinct in hand specimen; massive in outcrop.	Bryozoans (34-60%) mainly fusulinids (1 plates (13-49%); bra *Tubiphytes* (2-8%); gastropods; soleno ostracods; trilobite fragments; tuberini rare dasycladacean (?*Epimastopora*). S cryptostome bryoz around cyclindrical degradable objects plant-like thalla of a fusulinids with oute corroded/abraded.

2	Bryozoan-crinoid-fusulinid-*Tubiphytes* floatstone to loose packstone; mottled pale grey to red-brown in hand specimen; bioclasts up to 8 mm in length; with variably recrystallized matrix generally in form of radial-fibrous calcite rims (~0.3 mm thick) around bioclasts. Matrix is micritic with some red-brown mud and minute scattered bioclasts. Matrix/cement forms 36% of total rock volume.	Bedding indistinct in hand specimen; massive in outcrop.	Bryozoans (39%); cr (20%); foraminifera fusulinids (18%); *Tu* brachiopods (5%); r spines; gastropods; tuberitinids.
3	Crinoidal-bryozoan closely-packed packstone; pale grey to white in hand specimen (*watibuti*); bioclasts to 1 cm length; matrix is micritic with scattered minute skeletal debris; in some places replaced by radial-fibrous cement rims around bioclasts. Matrix/cement forms 10% of total rock volume.	Bedding indistinct in hand specimen; massive in outcrop.	Crinoids (44%); bryo Tubiphyes (9%); for minor brachiopod d solenoporaceous al ostracods, recrystal indeterminant skele Some fusulinids wit corroded/abraded.
4	Crinoidal-bryozoan grainstone to rudstone; pale grey to white in hand specimen (*watibuti*); bioclasts to 1 cm; sparry calcite cement forms 1-14% of total rock volume.	In some places, alignment of large plate-like grains in crude bedding; massive in outcrop.	Crinoids (50-59%); b 35%); foraminifera *Tubiphytes*, brachio shell debris with pri microstructure, sole algae, gastropods, c tuberitinids. Some f outer walls corrode

Table 2

Larger Fusulinata assemblages illustrated from Timor.

Age	Fauna	Reference	Localities
late Capitanian (based on very close similarity between *L. weberi* and type species of genus as discussed	abundant *Lantschichites weberi* (Schubert)*;* abundant *Parafusulina nakazawae* (Nogami) [? = in part *Fusulina granum-avenae* of Schubert, 1915, pl. 39, fig. 1, pl. 41, fig. 5, but not pl. 41, fig. 6; = *Schwagerina* sp. of Thompson, 1949, p. 189, pl. 35, figs 7. 8]; rare *Parafusulina* sp. of Nogami, 1963.	Schubert, 1915 as *Fusulina weberi*; Thompson, 1949 as *Palaeofusulina weberi*; Tumanskaya, 1953 as *Codonofusiella* (*Lantschichites*) *weberi*; Nogami, 1963 as *Codonofusiella weberi* and *Schwagerina*	Schubert, 1915, Thompson, 1949, Timor-Leste, Block from Nai Neo, northern scree from Mt Aubeon, and stream east of Pualaca; Nogami, 1963, southeast foot of Mt Aubeon.

by Tumanskaya (1953).		*nakazawae.*	
late Artinskian–early Kungurian.	abundant *Praeskinnerella* sp. (associated with rare *Nankinella* sp., ?*Boultonia* sp., ? *Toriyamaia* sp., *Abadehella* sp.).	This study.	Bua-bai limestone, Locality 1.
late Artinskian–Kungurian.	common *Praeskinnerella* sp., rare *Monodiexodina wanneri* (Schubert).	This study.	Bua-bai limestone, locality 2 (see section 3.2.1. and section 7, Appendix 2).
late Artinskian–Kungurian (following Ueno, 2006).	abundant *Monodiexodina wanneri* (Schubert) + schwagerinid identified by Schubert, 1915 (but not illustrated from this assemblage) as *"Fusulina granum avenae"* = ? *Pseudofusulina brouweri* (Thompson) - see Thompson, 1949 (p. 187); and rare *Pseudofusulina brouweri* (Thompson).	Schubert, 1915; Thompson, 1949.	Schubert, 1915, Thompson, 1949, West Timor locality, Noil Boewan at Niki-Niki.
late Artinskian–Kungurian (following Ueno, 2006).	*Monodiexodina wanneri* (Schubert).	Schubert,1915 [as *Fusulina wanneri*]; Thompson, 1949 [as *Parafusulina wanneri*; selected Schubert's pl. 40, fig. 1 as "holotype" and refigured this pl. 35, fig. 1]; Ueno, 2006.	Schubert, 1915, West Timor localities 646, 653, 309, 195, 198, 244, 966; Timor-Leste locality, southeast of Mt Bissori; Thompson, 1949, additional material from West Timor, limestone blocks on Boenoe River east of Niki Niki; Ueno, 2006, West Timor, Oinlasi.
Sakmarian.	*Eoparafusulina molengraaffi* (Schubert).	Schubert, 1915 (as *Fusulina molengraaffi*); Thompson, 1949 (as *Schwagerina*? *Molengraaffi*).	Schubert, 1915, West Timor localities 110, 824, 458; Thompson 1949, on road between Kapan and Pene, Fusulina Mountain between Kapan and Akbidi-Hü.
Asselian or late Gzhelian.	?*Tricities* sp. of Nogami, 1963, p. 62, pl. 3, figs. 10-12.	Nogami, 1963.	Nogami, 1963, Timor-Leste, white bedded limestone north of Hato-Builico.
earliest Asselian - late Gzhelian	*Schellwienia klunnikovi* (Davydov); *Schellwienia malkovskyi* (Ketat); *Schellwiena porrecta* (Sjomina); *Schellwienia modesta* (Scherbovich); *Schwagerina gracilis* (Sjomina); *Schwagerina subrobusta* (Davydov); *Schwagerina vozhgalensis* (Rauser); *Schwagerina pomposa* (Sjomina); *Schwagerina biangpingensis* (Zhang and Dong); *Schwagerina timorensis* Davydov *Schwagerina maubissensis* Davydov.	Davydov et al., 2014.	Davydov et al., 2014; Timor-Leste, Kula limestone.

Table 3

Lithofacies observed in Noonkanbah Formation in the Liveringa Ridge outcrop section and in BHP PND-1. Biogenic grain composition is summarized from section 7 Appendix 10.

Lithofacies	Lithology	Bedding and sedimentary structures	Biogenic grain comp

1	Mudstone, grey, friable, poorly exposed in outcrop; minor very fine quartz sandstone.	Massive, in places laminated; in rare sections thinly rippled with rare examples of climbing ripples.	Abundant to rare fo common to rare ost asterozoan plates, b with prismatic micro conodonts, fish teet holothurian spicules
2	Gastropod-rich indurated mudstone.	Calcareous mudstone nodules within friable mudstone unit.	Gastropods form ~3 matrix = ~63%); min fragments with prism microstructure, brac ostracod valves, ind echinoderm plates, *Tubiphytes*.
3	Fine quartz sandstone.	Thin to medium bedded; interbedded with Lithofacies 1	
4	Fossiliferous coarse pebbly sandstone.	Thin bedded; interbedded with Lithofacies 1; associated with Lithofacies 8.	Brachiopod fragmen mollusc (?bivalve) fr
5	Fossiliferous quartz sandstone.	Medium to thick bedded; usually medium to coarse-grained; interbedded with Lithofacies 1; usually assocated with Lithofacies 3, 4, 6 and 7.	Brachiopods domina bryozoan fragments molluscs fragments, echinoderm debris.
6	Pebbly brachiopod-bryozoan packstone.	Thin beds usually associated with Lithofacies 3, 4 or 5; bioclasts rounded, clean without micritic envelopes or significant micro-borings.	Brachiopod fragmen bryozoan fragments indeterminant echin (including rare crino gastropods, ostraco recrystallized indete debris; *Tubiphytes.*
7	Pebbly bryozoan-brachiopod packstone.	Thin beds usually associated with Lithofacies 3, 4 or 5; bioclasts rounded, clean without micritic envelopes or significant micro-borings.	Bryozoan debris (74 brachiopod fragmen minor crinoid colum

8	Chamositic ooid packstone.	Irregular cm-scale irregular layers in Lithofacies 4; ooids are ellipsoidal in shape and aligned roughly parallel to bedding.	Brachiopod and thic ?bivalve fragments packstone.

Table 4. Similarity measurements between consecutive samples in Noonkanbah Formation sections. Two similarity measures are used: Similarity % (a) is based on the number of taxa in common between two consecutive samples, expressed as a percentage of the total number of taxa present in these samples. Similarity % (b) is based on percentage abundance data and is calculated by adding the percentage in common for each taxa between the two samples. Samples are designated by metres above base of outcrop section, or metres below surface in borehole section.

Foraminifera (marine mud facies)

Liveringa Ridge outcrop section (see Section 7, Appendix 11)

upper sample	2	46	186	265	405-439	450	481-482
lower sample	46	186	265	405-439	450	481-482	502
Total number of species	8	19	23	15	6	18	15
Similarity % (a) - total foram assemblage	**0**	**5**	**43**	**0**	**0**	**17**	**7**
Similarity % (a) - organic-cemented foram assemblage	**0**	**6**	**56**	**0**	**0**	**17**	**7**

Liveringa Ridge outcrop section - comparison of intervals with highest foraminiferal diversity (see Section 7, Appendix 11)

upper sample	186	265
lower sample	265	481-482
Total number of species	23	25
Similarity % (a) - total foram assemblage	**43**	**20**
Similarity % (a) - organic-cemented foram assemblage	**56**	**25**

BHP PND-1 boresection (see Section 7, Appendix 13)

upper sample	233 - 254	225	207
lower sample	225	207	158 - 186
Total number of species	26	14	24
Similarity % (a) - total foram assemblage	**23**	**14**	**25**
Similarity % (a) - organic-cemented foram assemblage	**50**	**29**	**15**

BHP PND-1 boresection - comparison of intervals with highest foraminiferal diversity (see Section 7, Appendix 13)

upper sample	233 - 254
lower sample	158 - 186
Total number of species	30

Similarity % (a) - total foram assemblage	63						
Similarity % (a) - organic-cemented foram assemblage	60						

Spore-Pollen (from marine mud facies, but reflecting terrestrial vegetation)

BHP PND-1 boresection (see Section 7, Appendix 14)

upper sample	272	254	233	207	176	158	139
lower sample	301	272	254	233	207	176	158
Total number of species	58	61	61	60	65	60	56
Similarity % (a)	**74**	**79**	**71**	**72**	**69**	**80**	**70**
Similarity % (b)	**65**	**75**	**61**	**68**	**76**	**74**	**69**

Acritarchs (phytoplankton from marine mud facies)

BHP PND-1 boresection (see Section 7, Appendix 14)

upper sample	272	254	233	207	176	158	139
lower sample	301	272	254	233	207	176	158
Total number of species	11	11	13	11	13	14	9
Similarity % (a)	**73**	**73**	**62**	**64**	**54**	**50**	**78**

Brachiopods (marine sand facies)

Type section of Noonkanbah Formation at Bruten Yard (see Section 7, Appendix 16)

upper sample	25-45	131-156	156-181	201-204	204	238	244
lower sample	131-156	156-181	201-204	204	238	244	270
Total number of species	8	7	2	8	13	7	5
Similarity % (a)	**0**	**0**	**0**	**0**	**0**	**29**	**20**

Type section of Noonkanbah Formation at Bruten Yard: continued

higher sample	297	303	320	335	347	357
lower sample	303	320	335	347	357	378
Total number of species	16	8	8	15	12	15
Similarity % (a)	**19**	**25**	**13**	**7**	**17**	**7**

Table 5

Similarity measurements between fossil assemblages from consecutive sequences in the Byro Group. The similarity is based on the number of taxa in common between two consecutive sequences, expressed as a percentage of the total number of taxa present in these sequences. Sequences are as designated on Fig. 17.

Mud-facies marine fauna

	I – II	**II – III**
Organic-cemented siliceous agglutinated foraminifera		
Total number of species	26	35

Similarity %	62	51

Sand-facies marine fauna

	I – II	II – III-IV	III-IV – V
Brachiopods			
Total number of species	34	43	47
Similarity %	9	14	9
Crinoids			
Total number of species	7	19	16
Similarity %	14	0	0
Corals			
Total number of species		10	
Similarity %		20	

Terrestrial flora (as reflected by spore-pollen assemblage in marine mud facies)

	11–III	III–IV	IV – V
Total number of species	48	33	32
Similarity %	40	55	53

Table 6

Distribution of major fossil groups in studied formations, based on information given in the appendices of this paper, and from Skwarko, 1993. Numbers are percentages based on grain counts (see section 7, Appendices 2, 9, 12).

	Axial Rift			Marginal Rift B			
	TIMOR		CANNING BASIN	SOUTHERN CARNARVO			
	Watabuti Limestone	Atahoc/Cribas Formations (type sections)	Noonkanbah Formation	Billidee Formation	Coyrie Formation	Mallens Sandstone	Bulgadoo Shale
Ammonoids		X		X	X	X	X
Annelids			X		X		X
Bivalves		2–100	X	X		X	X
Brachiopods	1–5	2–6	63–99		X		X
Bryozoa	35–37	1–7	<1–30		X		X

Calcareous algae – solenoporaceans	X						
Calcareous algae – dasycladaceans	X						
Calcareous algae – ? recrystallized phylloids	X						
Conodonts		X	X				
Conulariids					X	X	X
Corals – solitary Rugosa			X				
Corals – Tabulata			X				X
Echinodermata – Asterozoans			X				X
Echinodermata – Blastoids	?	?					
Echinodermata – Crinoids	13–49	2–4	X		X	X	X
Echinodermata – Echinoids		2–5					
Echinodermata – Holothurians			X				X
Echinodermata indeterminant debris		23–40	<1				
Fish debris			X		X		X
Foraminifera – organic-cemented agglutinates	X	X	X	X	X		X
Foraminifera – carbonate-cemented agglutinates	X						
Foraminifera – Fusulinata	~10						
Foraminifera – Miliolata	X	~5	X				X
Foraminifera – Nodosariata	X	~2	X		X		X
Gastropods	X	4–4	<1–100	X	X	X	X
Nautiloids					X		X
Ostracods	X	8–20	X		X		X
Plants – macrofossils			X		X	X	
Plants – spores + pollen			X				
Scaphopods					X		
Trilobites	X				X		X
Tuberitinids	X						
Tubiphytes	X		X				

Table 7

Summary of evidence for increasing bathymetry and warming climate close to Artinskian–Kungurian boundary in basins associated with the East Gondwana interior rift.

Timor	Canning Basin	Southern Carnarvon Basin	Northern Perth Basin

Bathymetric trends	Within the Cribas Group, interpretations are hampered by structural complexities. However the first appearance of atomodesmatinid laminites associated with *Glomospira* sp. analogous to modern *G. charoides* suggests an increase in water depth close to the Artinskian–Kungurian boundary - see section 3.2.2.	Within the Noonkanbah Formation, increase in faunal diversity (including a diverse nodosariid assemblage) suggests maximum marine flooding causing the most open-marine conditions close to the Artinskian–Kungurian boundary - see section 3.3.	Within the Byro Group, maximum marine flooding is recognized in the upper Bulgadoo Shale of depositional cycle II, close to the Artinskian–Kungurian boundary - see section 3.4.	Within the Carynginia Formation, the maximum marine flooding level is probably represented in the upper part of the formation, probably close to the Artinskian–Kungurian bounda - see section 3.5.
Climate trends	The fossil assemblage from the Bua-bai limestone, including larger fusulines, very rare dasycladacean algae, solenoporacean algae, and *Tubiphytes* indicates a warm shallow environment close to the Artinskian–Kungurian boundary - see section 3.2.1.	Within the Noonkanbah Formation, the appearances of *Tubiphytes* encrusting on brachiopod shells, the most diverse conodont assemblage of the Australian Cisuralian, and bryozoans and brachiopods with warm-water affinities suggest at least warm-temperate conditions close to the Artinskian–Kungurian boundary - see sections 3.3, 3.6.	Within the Byro Group, sea-ice was present during the early part of depositional cycle I (late Artinskian) and water-temperatures rose to enable an influx of brachiopods with "Tethyan" affinities during depositional cycle II, close to the Artinskian–Kungurian boundary - see section 3.4.	Within the Carynginia Formation, sea-ice was prese during early stages of deposit (probably late Artinskian), b disappeared with apparent warming (probably close to t Artinskian–Kungurian boundary) - see section 3.5.

Highlights

- Interior basins on main rift axis contrasted with marginal-rift splays.
- Timor lay close to main rift axis in an open-marine shelf-basin setting.
- Western Australian basins were marginal rifts in restricted shallow-marine settings.
- Similar patterns of warming and bathymetric change took place in all basins.
- Similar broad patterns of climate change are recognized across East Gondwana.